

博士論文

**Morphometric analyses of Danxia
landforms in China using GIS and DEMs**

(デジタル地形モデルと地理情報システムを用いた中国丹霞
地形の地形解析)

張 文

ABSTRACT

The “Danxia landform” is an erosional landform type originally defined in China. It is characterized by red-colored sandstones and steep cliffs, and developed via long-term erosion. In recent years, the landforms have been receiving international attention and recognized as World Natural Heritage in 2010. Research on Danxia landforms in China so far has focused on the definition, classification, qualitative description and discussion about the origin of Cretaceous strata. Considering the lack of quantitative morphometric research on Danxia landforms, this research aims to provide quantitative and objective characterization of Danxia landforms using a large number of morphometric parameters derived from digital elevation models (DEMs), which have seldom been made in previous studies. The approach permits an objective comparison among Danxia landforms at different stages of geomorphic evolution; the differences in such stages have been stressed in the past descriptions of Danxia landforms. This study also investigates the relationship between the topography and geology using digital geological maps and GIS to evaluate the effects of bedrock lithology and structure on landform development.

This study investigates Danxia landforms in three areas in subtropical southern China: Chishui, Mt. Danxia, and Mt. Longhu. They are the sites of the archetypal Danxia landforms with the World Heritage status, having a monsoon climate, and characterized by different stages of landform evolution: young, mature and old. The use of the ASTER GDEM permitted detailed geomorphometric analyses in the three areas. Stream-nets and watersheds were extracted from the DEM using the threshold drainage area method. Basic properties of the stream-nets including Horton’s parameters such as drainage density, stream orders, the bifurcation ratio and the stream-length ratio as well as the data of stream orientation were derived. Basic morphometric properties of the watersheds such as mean

slope and relative relief were also computed. The use of the MathWorks Matlab code allowed the derivation of the hypsometric curves and the hypsometric integral from the DEM. Longitudinal and transverse profiles of each watershed were also extracted. For a segment of a given river, the value of the stream length gradient (*SL*) index was obtained and for an entire reach the Hack profile was derived. Analysis was conducted on “anomalous points” where the height of a point along the river significantly differs from the height estimated from a power function fitted to the river longitudinal profile. Knickzones were also identified along the longitudinal profile of each stream by using the change rate of the stream gradient at different spatial scales. The transverse profiles were analyzed using parameters such as width, relief, slope, height, and their statistical moments (standard deviation, skewness, and kurtosis). The obtained data allowed the investigation of relationships among the morphometric properties and those between topography and geology.

The results of various geomorphometric analyses show distinct differences in landform characteristics among the three areas related to the landform evolutionary stages. The obtained *HI* values have confirmed previously inferred geomorphic stages. Other parameters related to slope, relief and drainage density were also found to change with the landform evolutionary stage. Correlations between morphometric parameters effectively indicate topographic differences among the three areas according to the evolutionary stage.

Analyses of stream networks indicate that fault systems are responsible for the stream direction in Mt. Danxia, where fault density is high and the effect of overall topographic gradient is relatively weak. Hypsometric curves and hypsometric integrals (*HI*) of the watersheds are significantly affected by lithology. The *SL* index and Hack profiles also reflect lithology and fault distribution. Lithology differences also show their effects on knickzone distribution and forms. More knickzones are found in the typical red terrestrial

sedimentary rocks. The locations of the anomalous points often correspond to those of the knickzones. In other words, the longitudinal profiles and the slope changes tend to change at the same points. In the Chishui area, difference in drainage density-slope angle relationship seems to reflect differing stages of channel development corresponding to relative watershed location. It was found that the watershed with the Type 4 drainage density-slope angle relationship in the Chishui area represent significantly different stages of evolution from those in Mt. Danxia and Mt. Longhu, in spite of some similarities in topographic characteristics.

The relationships between the representative shape parameters of longitudinal/transverse profiles and watersheds have revealed that the number of positive correlations increases in the following order: Chishui, Mt. Danxia, and Mt. Longhu. With the advance of erosion, topography of Danxia landforms tends to exhibit stronger correlations between various relief, slope, height and dimensional parameters. It can be said that more organized topography is formed in the later stages.

The analyses using a large number of morphometric parameters conducted in this research permitted the detailed evaluation on the independence and effectiveness of each parameter. For example, *HI* was found to be independent of other parameters for any stages of landform evolution so future studies using a lesser number of parameters should include *HI*.

The results of this study were compared with a previously proposed model on the evolution of Danxia landforms. It was found that the differences in slope and relief among the areas with different evolutionary stages and change in drainage density are not well represented in the model. The effects of geological differences within an area also need to be included. This result, along with the other results obtained through this research, provides a guideline for future studies on Danxia landforms widely distributed in China.

ABSTRACT	I
CONTENTS	IV
LIST OF FIGURES	VII
LIST OF TABLES	XI
1. CHAPTER 1 INTRODUCTION	1
1.1. Recognition and past studies of Danxia landforms	1
1.2. Review of general morphometric characteristics	4
1.2.1. General characteristics of watersheds	4
1.2.2. Stream networks	5
1.2.3. River longitudinal profiles	6
1.2.4. Transverse profiles	8
1.3. The objectives of this research	8
2. CHAPTER 2 STUDY AREAS	10
2.1. Chishui area	10
2.2. Mt. Danxia	13
2.3. Mt. Longhu	18
3. CHAPTER 3 DATA AND METHODS	23
3.1. Geomorphological and geological data	23
3.2. Stream network extraction	24
3.3. Watershed extraction	28
3.4. Morphometric properties of watersheds	30
3.4.1. Slope angle	30
3.4.2. Relative relief	31

3.4.3.	Hypsometry	31
3.5.	Characteristics of stream nets and their relation with slope	32
3.5.1.	Stream orientation	32
3.5.2.	Morphometric parameters of stream networks structure	32
3.5.3.	Slope angle and drainage density	32
3.6.	River longitudinal profiles and related analyses	35
3.6.1.	River longitudinal profiles	35
3.6.2.	Stream length gradient (<i>SL</i>) index and Hack's profile	36
3.6.3.	Identification of knickzones	37
3.7.	Transverse profiles of watersheds	38
4.	CHAPTER 4 RESULTS	41
4.1.	Watershed and stream net properties	41
4.1.1.	Overview of watershed properties in the three areas	41
4.1.2.	Stream orientations	43
4.1.3.	Drainage density – slope angle relationships and watershed classification	46
4.1.4.	Stream network structure and the watershed types	52
4.1.5.	Hypsometric curves and the hypsometric integral	53
4.2.	River longitudinal profiles	57
4.2.1.	Stream length gradient (<i>SL</i>) index and Hack profiles	57
4.2.2.	Distribution and characteristics of knickzones and the anomalous points	72
4.3.	Watershed transverse profiles	81
4.4.	Relations between longitudinal, transverse and overall watershed characteristics	85
5.	CHAPTER 5 DISCUSSION	88
5.1.	Evolutionary stages of Danxia landforms	88
5.2.	Effect of geology	92

5.2.1.	Stream network orientation	92
5.2.2.	Hypsometrical integral and curves.....	93
5.2.3.	<i>SL</i> and Hack profiles	95
5.2.4.	Knickzone generation and distribution	97
5.3.	Watersheds in the Chishui area.....	98
5.4.	Evaluation of morphometric parameters for efficient research	99
5.5.	Comparison with a previous model of Danxia landform evolution	100
6.	CHAPTER 6 CONCLUSIONS	103
	ACKNOWLEDGEMENTS.....	107
	REFERENCES	108

LIST OF FIGURES

Figure 1-1. Spatial distribution of six Danxia landform World Heritage sites in China.	9
Figure 2-1. Topography of the Chishui area. (A) Distribution of elevation and slope. (B) Representative topographic profile	11
Figure 2-2. Representative Danxia landforms and landscapes in Chishui area. (a) Steep cliff along the edge of a plateau. (b) Deep gorge.....	12
Figure 2-3. Geology of the Chishui area based on the 1:50,000 geological map published by the Institute of South China Karst, Guizhou Normal University.	13
Figure 2-4. Topography of Mt. Danxia. (A) Distribution of elevation and slope. (B) Representative topographic profiles	15
Figure 2-5. Representative Danxia landforms and landscapes in Mt. Danxia. (a) Peak forest landscape. (b) Red rock and red cliff. (c) Gorge of the Jinjiang river.	16
Figure 2-6. Geology of the Mt. Danxia.	17
Figure 2-7. Topography of Mt. Longhu. (A) Distribution of elevation and slope. (B) Representative topographic profiles.	20
Figure 2-8. Representative Danxia landforms and landscapes in Mt. Longhu. (a) Wide valley and peaks. (b) Butte in the periphery of Mt. Longhu.	21
Figure 2-9. Geology of the Mt. Longhu.	22
Figure 3-1 Change in drainage density with threshold contributing area for the Chishui area.	25
Figure 3-2. Change in drainage density with threshold contributing area for Mt. Danxia. .	26
Figure 3-3. Change in drainage density with threshold contributing area for Mt. Longhu. .	26
Figure 3-4. Distribution of stream-nets in (A) Chishui, (B) Mt. Danxia and (C) Mt. Longhu.	28

Figure 3-5. Distribution of third order watersheds in (A) Chishui, (B) Mt. Danxia and (C) Mt. Longhu.	30
Figure 3-6. Example of types of the drainage density–slope angle relationship in Chishui area.	35
Figure 3-7. Measurement of stream gradient (G_d) along the stream.	37
Figure 3-8. The example of the transverse profile in (A) Chishui area, (B) Mt. Danxia and (C) Mt. Longhu.	40
Figure 4-1. Diagram showing the distribution of stream flow direction for different Strahler orders in the Chishui area.	44
Figure 4-2. Diagram showing the distribution of stream flow direction for different Strahler orders in Mt. Danxia.	45
Figure 4-3. Diagram showing the distribution of stream flow direction for different Strahler orders in Mt. Longhu.	45
Figure 4-4. Trend lines of the drainage types for each watershed in Chishui area.	46
Figure 4-5. Trend lines of the drainage types for each watershed in Mt. Danxia.	47
Figure 4-6. Trend lines of the drainage types for each watershed in Mt. Longhu.	48
Figure 4-7. Spatial distribution of the types of slope angle - drainage density relationship in each study area.	51
Figure 4-8. Distribution of hypsometric integral (HI) values and a representative.	53
Figure 4-9. Map showing watersheds and streams in Mt. Danxia.	54
Figure 4-10. Box plots of HI for the two major rock types in Mt. Danxia.	55
Figure 4-11. Map showing spatial distribution of hypsometric integral (HI) values and the shape of a hypsometric curve in Mt. Longhu.	56
Figure 4-12. Box plots of HI for the five major rock types in Mt. Longhu.	57
Figure 4-13. Spatial distribution of SL along the main stream of each watershed in the	

Chishui area	58
Figure 4-14. Spatial distribution of K for each watershed in the Chishui area.	59
Figure 4-15. Relationships of SL and K with topographic indices for Chishui area.....	60
Figure 4-16. Spatial distribution of SL along the tributaries of the main stream (Jinjiang and Zhenjiang rivers) in Mt. Danxia and showing faults buffers along the faults and watershed divides.....	62
Figure 4-17. Box plots of logarithmic values of SL for the three major rock types in Mt. Danxia..	63
Figure 4-18. Spatial distribution of K for each watershed in Mt. Danxia.	64
Figure 4-19. Examples of Hack profiles (semi-log plot of distance versus elevation along a river) in the western side (A) and the eastern side (B) with step SL curves and overall K values.	65
Figure 4-20. Relationships of SL and K with topographic indices for Mt. Danxia	66
Figure 4-21. Distribution of SL along the main stream of each watershed in Mt. Longhu..	68
Figure 4-22 Box plots of logarithmic values of SL for the eleven major rock types in Mt. Longhu.....	69
Figure 4-23. Spatial distribution of K of each watershed in Mt. Longhu.	70
Figure 4-24 Relationships of SL and K with topographic indices for Mt. Longhu.....	71
Figure 4-25. Spatial distribution of knickzones and anomalous points in each study area. 74	
Figure 4-26. Relationships between form parameters of knickzones and drainage area in the Chishui area.	75
Figure 4-27. Relationships between form parameters of knickzones and normalized distance from the riverhead in the Chishui area.	75
Figure 4-28. Relationships between form parameters of knickzones and distance from the Chishui area	76

Figure 4-29. Relationships between form parameters of knickzones and drainage area in Mt. Danxia.	76
Figure 4-30. Relationships between form parameters of knickzones and distance from the riverhead in Mt. Danxia.	77
Figure 4-31. Relationships between form parameters of knickzones and normalized distance from the riverhead in Mt. Danxia.....	77
Figure 4-32. Relationships between form parameters of knickzones and drainage area in Mt.Longhu.	78
Figure 4-33. Relationships between form parameters of knickzones and distance from the riverhead in Mt. Longhu.....	78
Figure 4-34. Relationships between form parameters of knickzones and normalized distancefrom the riverhead in Mt. Longhu.....	79
Figure 5-1. Peng’s (2001) model of evolution of Danxia landforms.	101
Figure 5-2_Improved model of evolution of Danxia landforms.....	102

LIST OF TABLES

Table 4-1. Mean and range values of watershed properties for the three study areas.	42
Table 4-2. Horton’s parameters of streams in the three study areas	43
Table 4-3. Characteristics of watersheds of different types in the Chishui area	52
Table 4-4. Parameters of the stream-net structure in Chishui	52
Table 4-5. Statistical differences and Kolmogorov–Smirnov test for <i>HI</i> values in the western and eastern sides of Mt. Danxia.....	55
Table 4-6. General properties of knickzone forms in Chishui, Mt. Danxia and Mt. Longhu.	72
Table 4-7. Knickzone characteristics according to stream order.	80
Table 4-8. Knickpoint characteristics according to lithology.	80
Table 4-9. Correlation coefficients between average shape parameters of transverse profiles and their significance for the Chishui area.	82
Table 4-10. Correlation coefficients between average shape parameters of transverse profiles and their significance for Mt. Danxia.	83
Table 4-11. Correlation coefficient between average shape parameters of transverse profiles for Mt. Longhu.	84
Table 4-12. Average value of longitudinal/transverse profile for the whole watershed based on the types of slope angle - drainage density.	86

CHAPTER 1 INTRODUCTION

1.1. Recognition and past studies of Danxia landforms

The Chinese geologists discovered that there was a significant geomorphologic contrast between the red sandy conglomerate in Mt. Danxia and the surrounding pelitic red beds, and termed that kind of landform as “Danxia Landform” (e.g., Chen, 1935; Huang, 1992; Luo, 1999; Peng, 2001; Liu and Liu, 2003; Chen, 2005). Then the term “Danxia landform” is used for landforms in other areas underlain by red continental sandstones mainly of the Cretaceous period. They include such morphologic shapes as red cliffs, mesas, stone walls, stone peaks, stone pillars, narrow gorges, rock lanes, and rock caves. For example, Huang (1982, 1992, 1999) discovered nearly 800 sites of the Danxia landforms in China based mainly on field observations, and described their forms and characteristic features. The formation of Danxia landforms is considered to have begun with the tectonic uplift of red bed. The uplifted red beds are eroded under the influence of exogenic forces and processes such as fluvial erosion and mass movement.

Danxia landforms have been receiving international attention, and a group composed of six typical examples (Chishui, Taining, Mt. Lang, Mt. Danxia, Mt. Longhu, and Mt. Jianglang) became a UNESCO World Natural Heritage in 2010, designated as “China Danxia”. The six examples include landforms of different stages of geomorphic development (youth, mature and old) as described by UNESCO in the document of declaration of the World Heritage (<http://whc.unesco.org/en/list/1335>). The six examples represent Danxia landforms in the humid area of southeast China with different stages of landform evolution: young, mature and old (Huang, 2002; Li et al., 2009; Zhu et al., 2009;

Jiang et al., 2009; Li et al., 2013; Ouyang, 2013; Peng, 2013). In addition, the International Association of Geomorphologists (IAG) launched a new working group on Danxia landforms in 2009 and researchers from various countries joined the group. However, research on Danxia landforms so far generally focused on basic issues such as the formation of the Cretaceous strata as background information (e.g., Eschmeyer, 1998; Press and Siever, 1998), systems of qualitative classification of Danxia landforms (Peng, 2002; Huang et al., 1992; Luo, 1999) in relation to geologic material and structure, dominant landform features (Ouyang et al., 2009; Zhu et al., 2009, 2010; Jiang et al., 2011), and stages of development (Huang, 1992; Luo, 1999; Peng, 2001, 2002; Wu and Peng, 2005). Some researchers noted the diversity of Danxia landforms in different areas (Qi et al., 2005; Jiang et al., 2009) in relation to endogenetic and exogenetic forces but in a speculative way. Although base level lowering, tectonic, climate and bedrock lithological influences on the development of Danxia landforms have been suggested (Luo, 1993; Peng et al., 2001; Qi et al., 2005; Zhu et al., 2009, 2010, Kusky et al., 2010; Chen, 2010; Ouyang, 2011), how these factors affect landforms has seldom been described in a quantitative way, because landform characteristics are not represented numerically.

Huang (2004, 2006) dated fluvial landforms surrounded by bedrock slopes of Danxia landforms and used the obtained ages using the OSL dating method to estimate the rates of tectonic uplift and erosion. Zhu (2009) applied the K-Ar method to date an ophitic vein to estimate the uplift age of red bed. In spite of absolute dating records, these papers include uncertain assumptions about landform development and thus are speculative. Zeng et al. (1978), Chen (1935), Hao et al. (1986) and Peng (2000, 2001) related geomorphologic characteristics of the Danxia landforms to practical tourism development, but pure scientific aspects are weak.

As noted above, in spite of a relatively long research history of Danxia landforms,

geomorphological understandings of the landforms are still limited especially in terms of objective, less speculative, investigations. A serious problem is that the characteristics of Danxia landforms have not been well described in a quantitative way; most previous studies depend on qualitative descriptions of landforms such as illustrations of typical examples. One background of this is that Danxia landforms have often been regarded as unique and thus researchers did not try to apply established geomorphological methods used for more “normal” landforms. However, Danxia landforms can be considered as mountains and hilly lands dissected by fluvial and slope processes, and such landforms have been analyzed quantitatively based mainly on topographic maps until the 1980s (e.g., Strahler, 1964; Hooke, 1972; Hack, 1973; Hupp, 1986) but then on DEMs (digital elevation models) (e.g., Gratton et al., 1990; Burbank et al., 1996; Kühni and Pfiffner, 2001; Jaboyedoff et al., 2009; Lin and Oguchi, 2009; Pérez-Peña et al., 2010; Ferraris et al., 2012). Therefore, it is possible to apply the methods of morphometric analyses to Danxia landforms including the investigations of stream network, stream longitudinal profiles, valley transverse profiles and plan characteristics of watersheds. This paper presents such a first trial of morphometric analyses of Danxia landforms based on DEMs and GIS (Geographic Information Systems). In the next section some representative methods of geomorphometric analyses of watersheds are reviewed.

1.2. Review of general morphometric characteristics

1.2.1. General characteristics of watersheds

A watershed is defined as a collective surface area in which all the water flows down. It is a fundamental geomorphological unit in a fluvial landscape and a great amount of research has focused on their geometric characteristics (e.g., Horton, 1945; Langbein, 1947; Schumm, 1956; Strahler, 1952, 1964; Gregory and Walling, 1973; Chorley et al., 1984; Sorriso-Valvo et al., 1998; McAllister, 1999; Crosta and Frattini, 2004).

General characteristics of watersheds can be described using basin area, length, slope, and relief (e.g., Horton, 1932; Strahler, 1952, 1964; Morisawa, 1959). Such basic properties have been widely used in relation to geomorphic processes such as sediment yields and erosion rates (e.g., Baumgardner, 1987; Gardiner, 1990; Krishnamurthy et al., 1996; Barnes et al., 2006).

Hypsometric (area–altitude) curves (Strahler, 1952a, Pike and Wilson, 1971; Luo, 1998; Maroukian et al., 2008) provide a useful measure for characterizing the topographic relief of a watershed and comparing different watersheds. The hypsometric integral, defined as the area below the hypsometric curve (Strahler, 1952, Schumm, 1956), as well as the shape of the hypsometric curve has been related to the development stages of watershed topography (Strahler, 1952; Schumm, 1956; Ohmori, 1993; Willgoose and Hancock, 1998), hydrology (e.g., Howard, 1990; Masek et al. 1994; Montgomery et al., 2001; Bloomfield et al., 2011), lithology (e.g., Lifton and Chase, 1992; Hurtrez and Lucazeau, 1999; Walcott and Summerfield, 2008), tectonics (e.g., Ohmori, 1993, Hurtrez et al., 1999; Chen et al., 2003, Korup et al., 2005; PérezPeña et al., 2009), vertical and horizontal scales of basins (e.g., Azor et al., 2002; Hancock and Willgoose, 2001; Chen et al., 2003; Korup et al., 2005; Cheng et al., 2012), as well as the landscape genesis of Mars

(Luo, 2000, Luo, 2002, Sepinski and Coradetti, 2004; Ansan and Mangold, 2006). Because of such wide usage, this paper adopts hypsometric curves and their integrals as representing general forms of watersheds. The geomorphometric properties introduced in the following subsections are also adopted for similar reasons.

1.2.2. **Stream networks**

A stream network, i.e., the route of water flow within a watershed, is a fundamental component of watershed morphology. The classical study by Horton (1945) has developed one-dimensional laws of drainage in the form of stream variables such as the bifurcation ratio, stream length ratio and stream slopes. Further studies have been made to better characterize the morphology of stream networks (e.g., Abrahams, 1984; Shiman, 1992; Esper, 2008; Magesh et al., 2011; Bali et al., 2012).

Stream network structures are often influenced by tectonics, bedrock geology, and hydrology (Schumm, 1986; Leeder et al., 1991; Eliet and Gawthorpe, 1995; Burbank and Anderson, 2001). For example, stream direction is controlled by the distribution of joints and faults in bedrock (Judson and Andrews, 1955; Schumm et al., 2000; Burbank and Anderson, 2001; McCulloh, 2003; Vojtko et al., 2012), and lithological structures often affect other geometric patterns of stream networks (Howard, 1967; Chorley, 1984; Nag et al., 2003). Runoff characteristics also influence stream network structure (Hadley and Schumm, 1961; Rodríguez-Iturbe and Valdés, 1979; Gupta and Mesa, 1988; Zimpfer, 1982; Roe et al., 2002; Arp et al., 2012), and such structure with different water sources (e.g., glacial vs non-glacial) have been compared (Graf, 1970; Sharp et al., 1993; Brocklehurst et al., 2002; Willis et al., 2012)

Drainage density, the total stream length in a unit area (Horton, 1932), indicates the

degree of watershed dissection. It varies with soil and bedrock types (Toy and Hadley, 1987; Montgomery and Dietrich, 1988; Sameena et al., 2009), climate (Chorley, 1957; Melton, 1957; Gregory 1975; Moglen et al., 1998), vegetation (Melton, 1958; Istanbuluoglu et al., 2005; Luoto, 2007), and topographic relief or slope (Schumm, 1956; Montgomery and Dietrich, 1992; Oguchi, 1997). Drainage density is positively correlated with slope angle or relative relief in some regions in which the landform shaped by predominance of overland flow (Schumm, 1956; Smith, 1958; Montgomery and Dietrich, 1992; Tailing and Sowter, 1999), but negatively which the landscape shaped by of diffusive process (Mino, 1942; Yatsu, 1950; Montgomery and Dietrich, 1992; Tailing and Sowter, 1999). Oguchi (1997) has attributed the negative correlation to the decline of channel sidewalls on steep slopes related to slope failure. Lin and Oguchi (2004) have indicated that the correlation type does not depend on the type of erosion but mainly correspond more directly to the stages of channelization of the watershed.

1.2.3. River longitudinal profiles

A river longitudinal profile depicts the stream's elevation change over distance. Various geomorphological studies have looked into river longitudinal profiles to understand their evolution. River longitudinal profiles usually have concave-upward profiles and are considered to adjust to hydrological conditions (Mackin, 1948; Hack, 1957, 1973, 1975; Bishop et al. 1986; Howard et al., 1994; Goldrick and Bishop, 1995; Sinha and Parker, 1996; Whipple and Tucker, 1999; Rodoane, 2003). They are often approximated by exponential, logarithmic and power functions (Snow and Slingerland, 1987; Hovius, 2000; Rice and Church, 2001).

The shapes of longitudinal profiles have also been related to geology and environmental factors. Abrupt changes (discontinuities) in the gradient of a longitudinal

profile reflect lithological variations (Hack, 1973; McKeown et al., 1988; Duvall and Kirby, 2004), climate (Roe et al., 2002) and tectonics (Seeber and Gornitz, 1983; Merritts and Ellis, 1994; Snyder et al., 2003; Kirby and Whipple, 2000, Duvall and Kirby, 2004) especially neotectonics (Burnett and Schumm, 1983; Keller and Rockwell, 1984; Schumm, 1986; Merritts et al., 1994; Weissel and Seidl, 1998; Bishop et al., 2005.).

River longitudinal profiles have also been numerically analyzed in relation to erosional power of streams, particularly using the parameters of steepness (ks) and concavity (θ) (Flint, 1974; Whipple and Tucker, 1999; Snyder et al., 2000; Kirby et al., 2003; Clark et al., 2005). Numerous factors may influence steepness (ks) and concavity (θ) such as precipitation and runoff (Roe et al., 2003, Goswami et al., 2012), river bed sediment (Sklar and Dietrich 1998, 2004, 2006, 2008; Turowski et al. 2007), hydraulic geometry of channels (Duvall et al. 2004; Finnegan et al. 2005; Stark 2006; Wobus et al. 2006b, 2008; Whittaker et al. 2007a) and bedrock lithology (Moglen and Bras, 1995; Stock and Montgomery, 1999; Lavé and Avouac, 2001; Duvall et al., 2004).

Some other morphometric indices of river longitudinal profiles have been examined in relation to tectonics and bedrock lithology and structure (Keller, 1986, Douglas and Robert, 2001; Edward and Nicholas, 2002; El Hamdouni et al., 2008; Gao et al., 2013). Among such indices the stream length gradient (SL) index (Hack, 1957, 1973; Keller and Pinter, 1996; Goldrick and Bishop, 2007) describes the morphology of a river based on the longitudinal distribution of river gradient. SL is often used to indicate uplift zones (Merritts and Vincent, 1989; Chen et al., 2003; Harkins et al., 2005; Troiani and Della Seta, 2008), but lithology also affects it (Hack, 1973; Harkins et al., 2005). Brookfield (1998) and Štěpančíková et al., (2008) showed that sudden changes of SL values are caused by river capture or fault control. SL is sometimes analyzed with the Hack profile, which is defined as semi-logarithmic plot of distance versus elevation (Fried and Smith, 1992; Chen et al.,

2003; Singh and Tandon, 2008).

1.2.4. **Transverse profiles**

The transverse profiles of a valley or a watershed orthogonal to the main stream have some attracted attention in relation to dominant erosional processes, although the number of research so far is much smaller than that of longitudinal river profiles. One background of this is that a common method to extract transverse profiles has not been established. However, analysis of transverse profiles is important in relation to broadly used qualitative descriptions of topography such as V-shaped valleys and U-shaped valleys. One application example is to estimate whether a stream is actively incising to create a V-shaped valley or is primarily eroding laterally to creating a valley with a broad floor, in relation to tectonics and erosion (Wells et al., 1988; Bull and McFadden, 1977; Koukouvelas, 1998; Ramirez-Herrera, 1998; Zuchiewicz, 1998; Azor et al., 2002; Silva et al., 2003; Seong et al., 2008; Burbank and Anderson, 2011). Statistical analyses of watershed transverse profiles are also used to examine the stage of watershed evolution (Lin and Oguchi, 2006, 2009).

1.3. **The objectives of this research**

Considering the lack of quantitative morphometric research on Danxia landforms, this paper describes and analyzes the characteristics of Danxia landforms using parameters in relation to general watershed form, stream-net structure, stream longitudinal profiles and valley transverse profiles extracted from DEMs and GIS. This approach provides quantitative and objective characterization of Danxia landforms which have seldom been made in previous studies. Then this study investigates the relationship between the topography and geology including bedrock structure using digital geological maps and GIS

to evaluate the effects of lithology and structure on landform development. This is important because Danxia landforms has been defined and described in relation to red sandstone. This study also objectively compares Danxia landforms at different stages of geomorphic evolution since the difference in such stages have been stressed in the past descriptions of Danxia landforms including the declaration of its World Heritage status. Such approach is useful to discuss long-term development of Danxia landforms.

In relation to the final objective described above, we selected three areas from the six World Heritage sites of China Danxia as our study areas: Chishui, Mt. Danxia, Mt. Longhu (Fig. 1-1). They correspond to “young”, “mature” and “old” erosion stages, respectively.

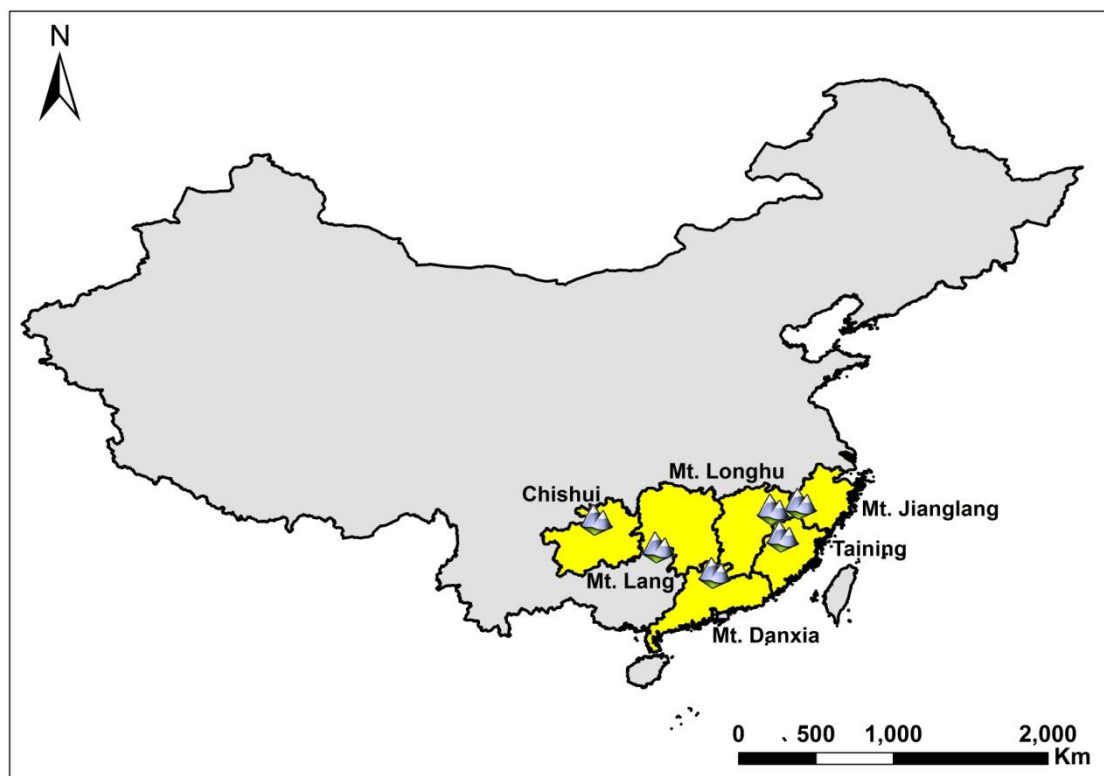


Figure 1-1. Spatial distribution of six Danxia landform World Heritage sites in China

CHAPTER 2 STUDY AREAS

The three study areas are all located in South China. During the Middle Jurassic to Early Cretaceous, tectonic extension along the southern part of the South China plate formed a series of grabens allowing deposition of thick continental sequences of alluvial, fluvial and lacustrine sediments. These sediments were consolidated to form sedimentary rocks mainly sandstone. They were then uplifted to be the basement of the Danxia landforms. The three areas have similar subtropical humid monsoon climates. Landforms in the three areas have been dissected by stream networks. The major rivers in Chishui and Mt. Longhu are tributaries of the Yangtze River and that in Mt. Danxia is the tributary of the Zhujiang River.

2.1. Chishui area

The Chishui area is located in the northeast of Zunyi City of Guizhou Province, China (28°20'11''–28°29'33''N, 105°57'20''–106°8'31''E). The Chishui River divides the site of World Heritage into eastern and western sides and we select the eastern side as our study area, because the area is characterized by gorges and waterfalls which represent complex young stage landscape compared to the western side. The mean annual temperature is 18.1°C and the mean annual precipitation is 1287 mm, mostly concentrated in the warmer period from April to October (Xiong et al., 2009; Weng and Chen, 2012).

The Chishui area corresponds to the transitional belt between the southern margin of the Sichuan Basin and the Guizhou Plateau. The altitude ranges from 410 to 1,664 m and the slope ranges from 0 to 78° (Figure 2-1). It is characterized by deep-gorges and relatively flat uplands, and regarded as the youth or early stages of landform development (Luo, 1999; Xiong et al., 2009; Li et al., 2013; Peng et al., 2013) (Figures 2-1B and 2-2).

Folds and faults are not densely distributed due to the influence of rigid rock formations along the Sichuan Basin. Instead, a few large-scale folds are observed including the Moziyan anticline and the Dabaitang syncline. The bedrock in the Chishui area is characterized by vertical joints and various kinds of bedding structure, which are considered responsible for the characteristic topographic features such as gullied surfaces marked by ravines, deep canyons and gorges and waterfalls (Li et al., 2013).

Figure 2-3 shows that the Chishui area is composed of only one rock type: the thick red quartz sandstone of the Cretaceous Jiaguan group (K_{2j}). The sandstone was originated from fluvial processes, combined with red mudstone indicative of cyclic discontinuities (Xiong et al., 2009; Li et al., 2013). The sandstone is rigid and resistant to weathering (Robinson and Williams, 1976; Labus and Bochen, 2012).

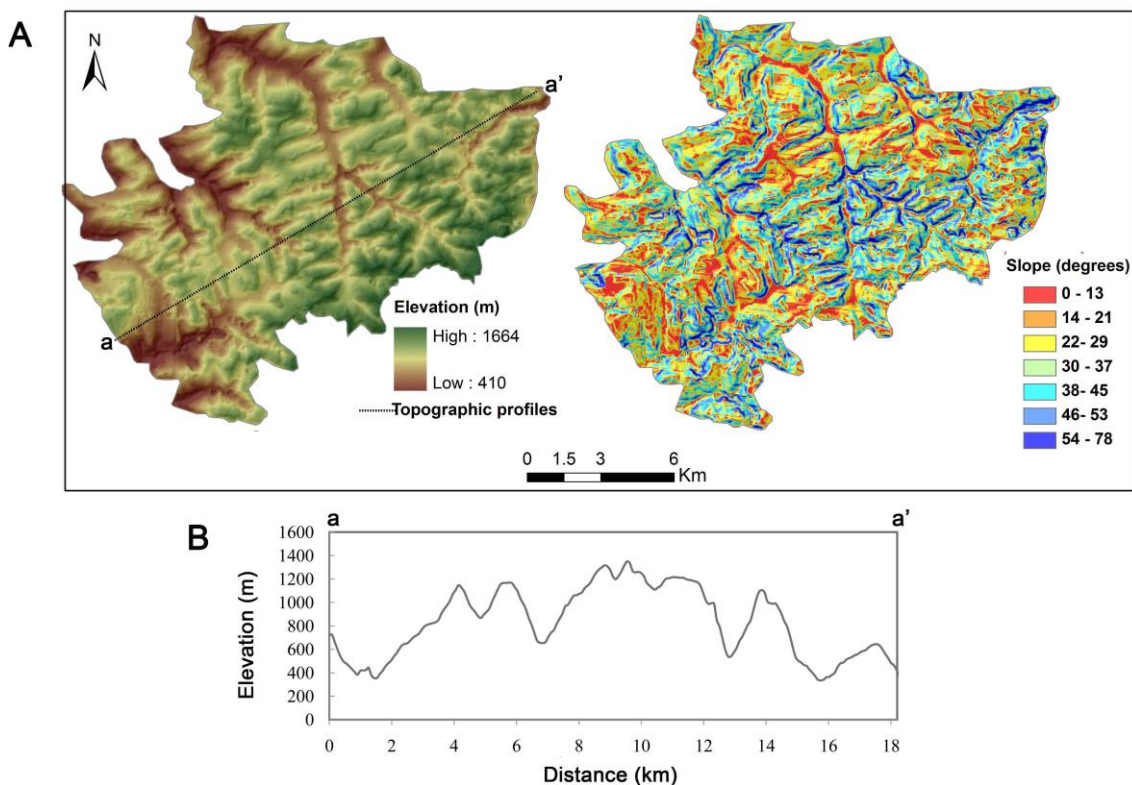


Figure 2-1. Topography of the Chishui area. (A) Distribution of elevation and slope. (B) Representative topographic profile.

Source: ASTER GDEM.

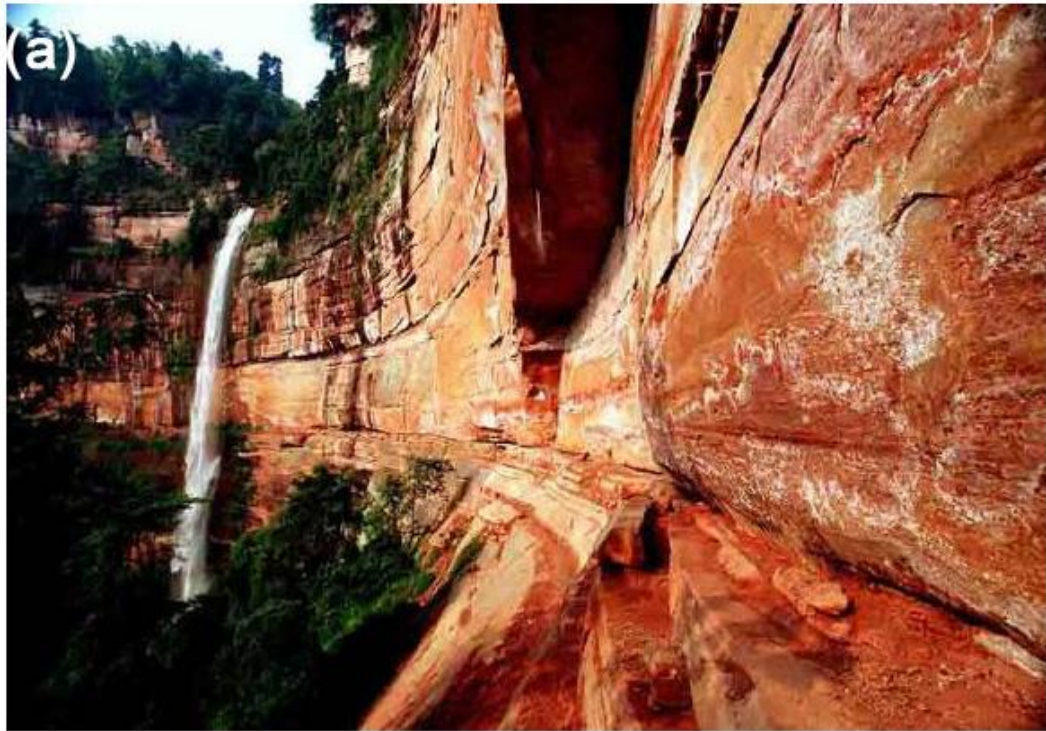


Figure 2-2. Representative Danxia landforms and landscapes in the Chishui area. (a) Steep cliff along the edge of a plateau. (b) Deep gorge.

Source: (a) <http://www.dxdm.com/EN/content/WH/2-5-2.html>;

(b) <http://www.dxdm.com/en/content/WH/chishui-6.html>

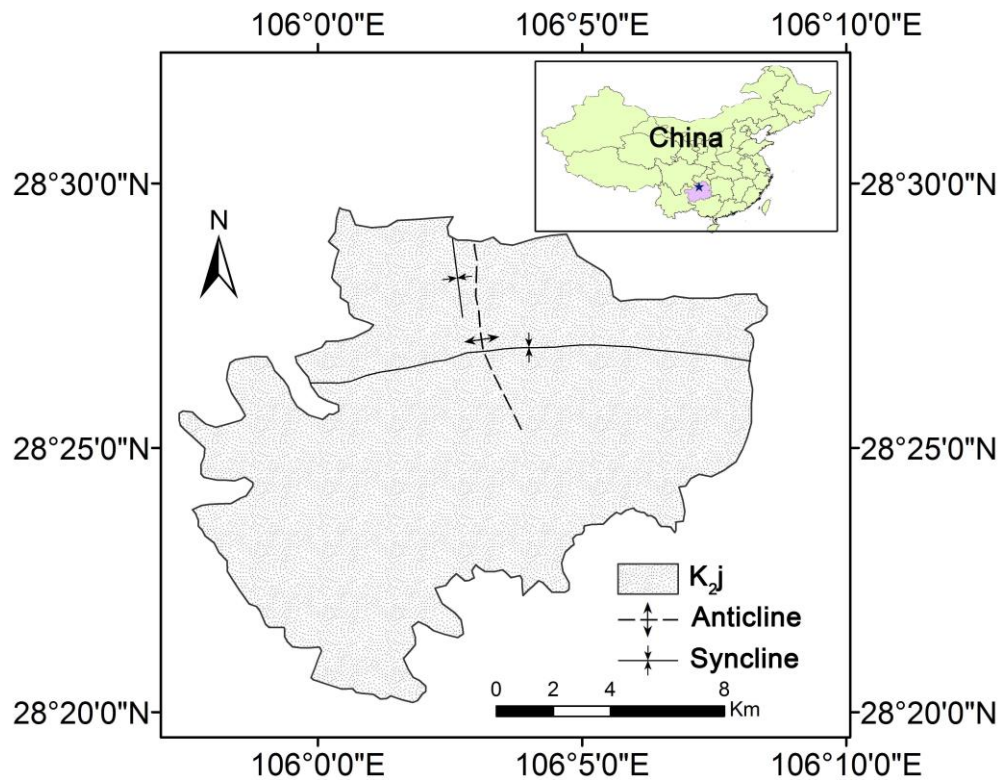


Figure 2-3. Geology of the Chishui area based on the 1:50,000 geological map published by the Institute of South China Karst, Guizhou Normal University.

K_{2j}: Jiaguan Group, upper Cretaceous.

2.2. Mt. Danxia

Mt. Danxia, the site of the archetypal Danxia landforms, is located in the northeast of Shaoguan City, Guangdong Province, China (24°51'48''–25°04'12''N, 113°36'25''–113°47'53''E). The elevation of Mt. Danxia ranges from 26 to 570 m a.s.l and the slope ranges from 0 to 61° (Figure 2-4A). The mean annual temperature is 19.7°C and the mean annual precipitation is 1,715 mm (Peng, 1992; Huang, 2010). The prominent landform types in Mt. Danxia include more than 600 stony peaks, fortresses, walls, pillars (hoodoos), and natural bridges of various sizes and heights (Peng, 2001) (Figure 2-5).

Topographic profile reveals the wide valley along the Jinjiang river (Figure 2-4B).

The area is mainly underlain by Cretaceous red sandstone. The Himalayan orogeny that started ca. 23 Ma resulted in the uplift of Mt. Danxia, and the red sandstone beds have since been eroded by fluvial processes and mass movement (Wu, 1994; Huang, 2004). Peng (2001) suggested that five planar surfaces of different levels formed in Mt. Danxia due to the intermittent uplift. Several levels of fluvial terraces occur along the Jinjiang and Zhenjiang rivers (Figure 2-6). Their relative height above the present river bed varies from ~11 to 43 m, and they have been dated as Late and Middle Pleistocene (ca. 29–518 ka) using the OSL dating method (Huang, 2010).

Fault lines are densely observed in this area (Figure 2-6). According to Peng (2000), the compressive early Yanshanian movement in the Middle Jurassic–Early Cretaceous resulted in two major structural components: 1) NNE and NE trending faults, including the Renhua Fault, belonging to the Wuchuan–Sihui thrust fault belt, which has created a gradually westward-rising structure and 2) numerous E–W to NE–SW vertical joints in the red beds formed during the crustal movement. The NNE-trending faults underwent a left-lateral strike slip during the Cenozoic, controlling the strike of mountain ranges and development of intermontane basins (Shu, et al., 2009). The two major geological formations in Mt. Danxia are the older Changba Formation (130–100 Ma) and the younger Danxia Formation (100–70 Ma) (Huang and Chen, 2003; Peng and Wu, 2003) (Figure 2-6). The Changba Formation ($K_1c^4-c^2$), with a total thickness of more than 2,400m, is composed of fluvial and lacustrine mud-siltstones, fine-grained sands and sporadic conglomerate, intercalated with marlite and gypsum beds. Except for some steep-faced slopes, the Changba Formation is mainly developed into low hills. The Danxia Formation ($K_2dx^3-x^1$) is a set of alluvial red beds, chiefly of fluvial phase with a total thickness of about 1,300 m. Conglomerate, gritstone and feldspar-quartz sandstone are gritty, with silicic and

ferruginous cementation. Archetypal Danxia landforms are found in red terrestrial sedimentary rocks of the Danxia Formation.

The evolutionary stage of Mt. Danxia is considered to be mature (Huang, 2010; Peng, 2013). We divided the study area into the western and eastern sides of the trunk streams of the Jinjiang and Zhenjiang rivers (Figure 2-6).

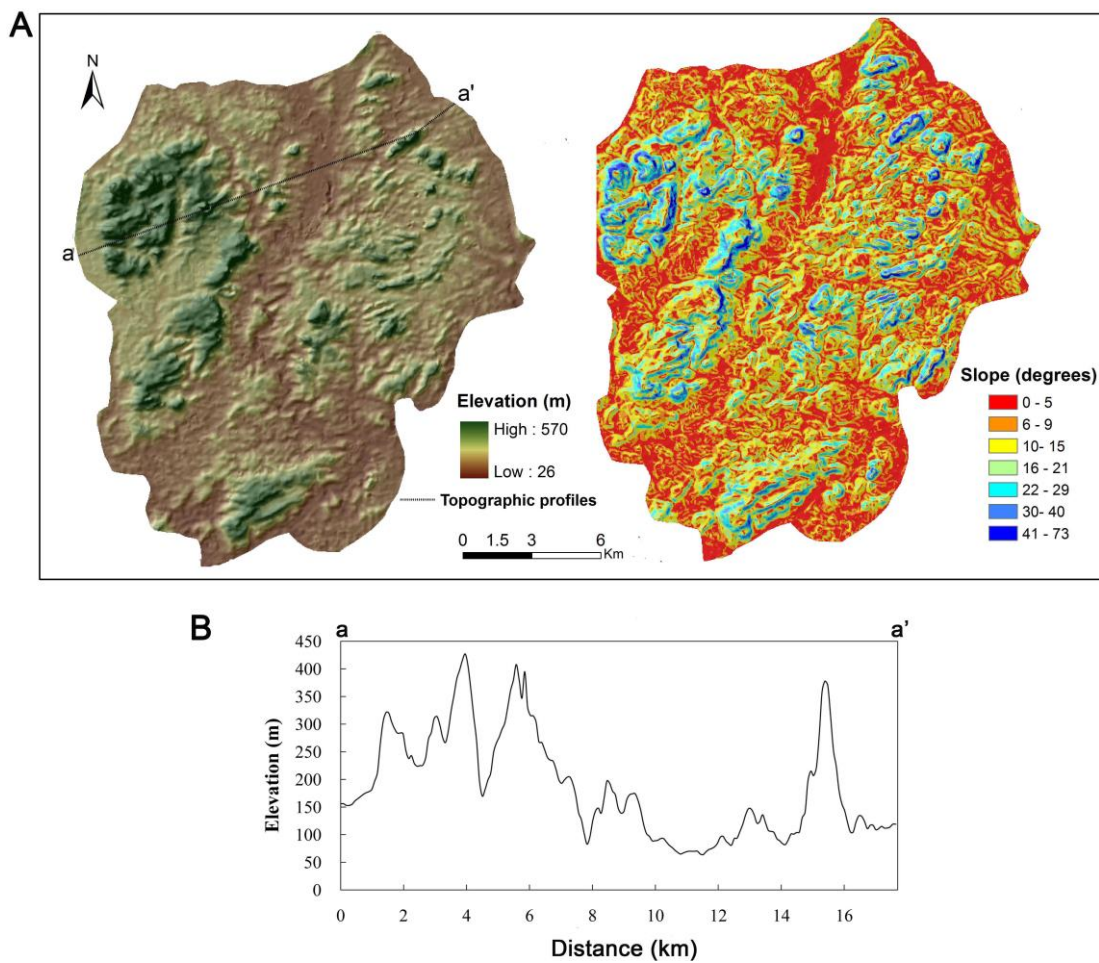


Figure 2-4. Topography of Mt. Danxia. (A) Distribution of elevation and slope. (B) Representative topographic profiles.

Source: ASTER GDEM

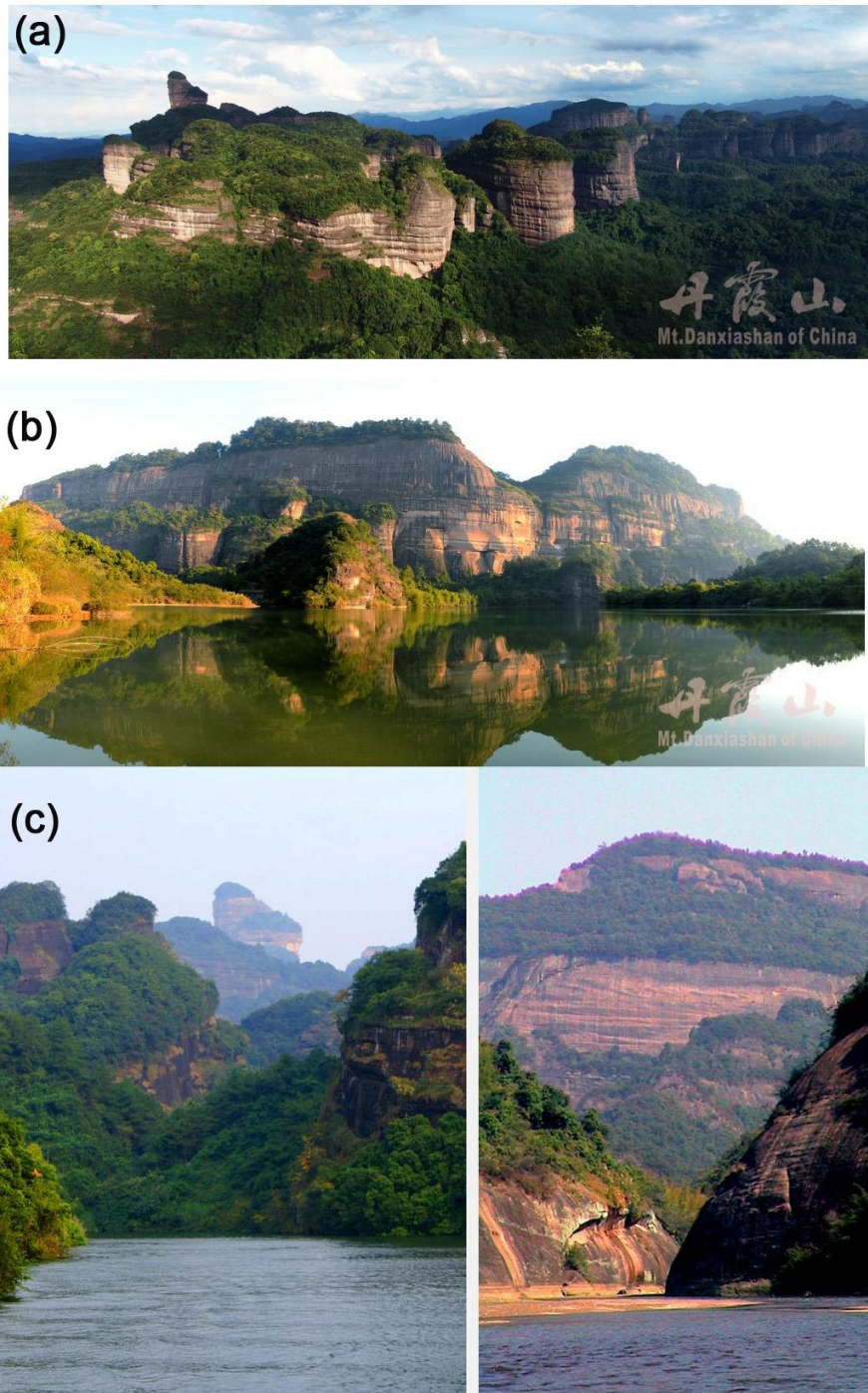


Figure 2-5. Representative Danxia landforms and landscapes in Mt. Danxia. (a) Peak forest landscape. (b) Red rock and red cliff. (c) Gorge of the Jinjiang river.

(a) and (b) Photos by Liu Jiaqing.

(c) Taken from <http://www.dxdm.com/en/content/WH/danxiashan-3.html>

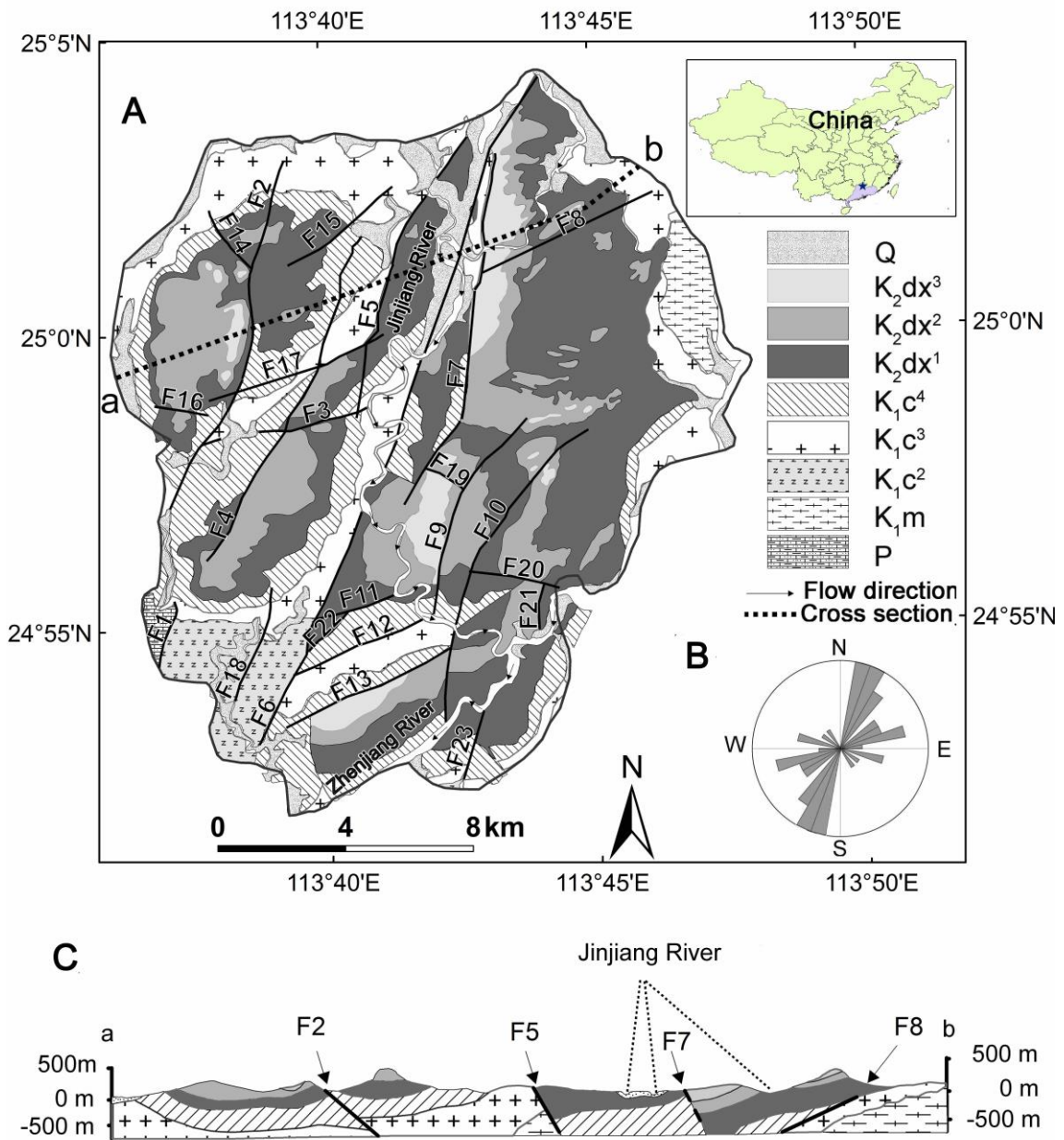


Figure 2-6. Geology of the Mt. Danxia.

(A) Geological map of the Mt. Danxia region showing main rock formations and faults, published by the Guangdong Institute of Geological Survey. (B) Rose diagram showing fault orientations, based on GIS analysis of digitized fault lines. (C) Geological cross-section (location shown in A) showing the stratigraphic-structural relationship of the units. Q: Quaternary sediments, sand, pebble, rock block, silty soil and loam; K_2dx^3 : 3rd member of the Danxia

Formation, brownish red interlaid conglomerate and medium arkose; K_2dx^2 : 2nd member of the Danxia Formation, arkose, thin bedded silty mudstone, siltstone and conglomerate; K_2dx^1 : 1st member of the Danxia Formation, brownish red conglomerate; K_1c^4 : 4th member of the Changba Formation, purplish red thin to medium bedded muddy sandstone and siltstone; K_1c^3 : 3rd member of the Changba Formation, purplish red complex conglomerate and sandy conglomerate; K_1c^2 : 2nd member of the Changba Formation, purplish red siltstone and intercalated sandstone; K_1m : Mazingping Formation, grayish white feldspathic quartz sandstone; P: Permian system, cherty limestone and mudstone.

2.3. Mt. Longhu

Mt. Longhu is located to the northeast of Yingtan City of Jiangxi Province, China ($27^{\circ}57'54''-28^{\circ}10'51''N$, $116^{\circ}54'46''-117^{\circ}6'23''E$). Its elevation ranges from 0 to 1,100 m and the slope ranges from 0 to 61° (Figure 2-7A). Topographic profile reveals a planar slope with U-shape valley in general and a steeper slope section representing the lithology transition (Figure 2-7B). The area is characterized by scattered dales and typical peak forest at the old stage of landform development (Jiang, 2009; Kusky et al, 2010; Guo et al., 2011; Peng, 2013). According to Guo et al., (2004), the prominent landform types in Mt. Longhu includes cliffs, mesas, stone walls, caves and valleys, peak-forests, peak-clusters, single-peaks and remnant-hills (Figure 2-8). The average annual precipitation is 1,878 mm, mostly concentrated from March to August and the mean annual temperature is $18^{\circ}C$ (Li et al., 2012).

Mt. Longhu is located at between the Beihai-Shaoxing rupture zone (extending EW) and the Ruyuan-Ningdu-Anyuan rupture zone (extending NNE) (Jiang et al., 2009; Kusky

et al., 2010; Guo et al., 2011). The area was uplifted during ca. 65 Ma-90 Ma with the formation of rupture and joint conformation, and incision tended to occur along the ruptures and joints (Kusky et al., 2010; Lv and Li, 2012). Figure 2-9 shows the fault lines and rock formations in the study area. Mt. Longhu presents a wide lithological variety: The main sequence of rock consists of a series of Jurassic and Cretaceous volcanic and sedimentary deposits (Ren, 2009; Kusky et al., 2010). The red clastic rock series of the Hekou Formation (K_2h) in the late Cretaceous is the basis of Danxia landscape development. The formation is a combination of ancient alluvial fan deposits and other rough aggradation of red clastic rock, with 687 m thick. Qingbaikou rocks, including the Wanyuan Formation, are composed of dark gray, brownish gray and gray garnetiferous biotite plagioclase granulite interbedded with biotite slate and two mica slate. The middle Jurassic rocks, including Zhangping Formation and Sanqiutian Formation, are composed of fine sandstone, siltstone and mudstone. Upper Jurassic rocks, including Ruyiting Formation, Wuxi Formation, Daguding Formation and Elinghu Formation, are composed of rhyolitic tuff, rhyolite, andesite, and dacite interbedded with pebbly siltstone. The Cretaceous rocks, including the Shixi Formation and Zhaixia Formation, are composed of rhyolitic tuffs and breccias interbedded with conglomerate and mudstone, overlain by purple and gray sandstone and conglomerate.

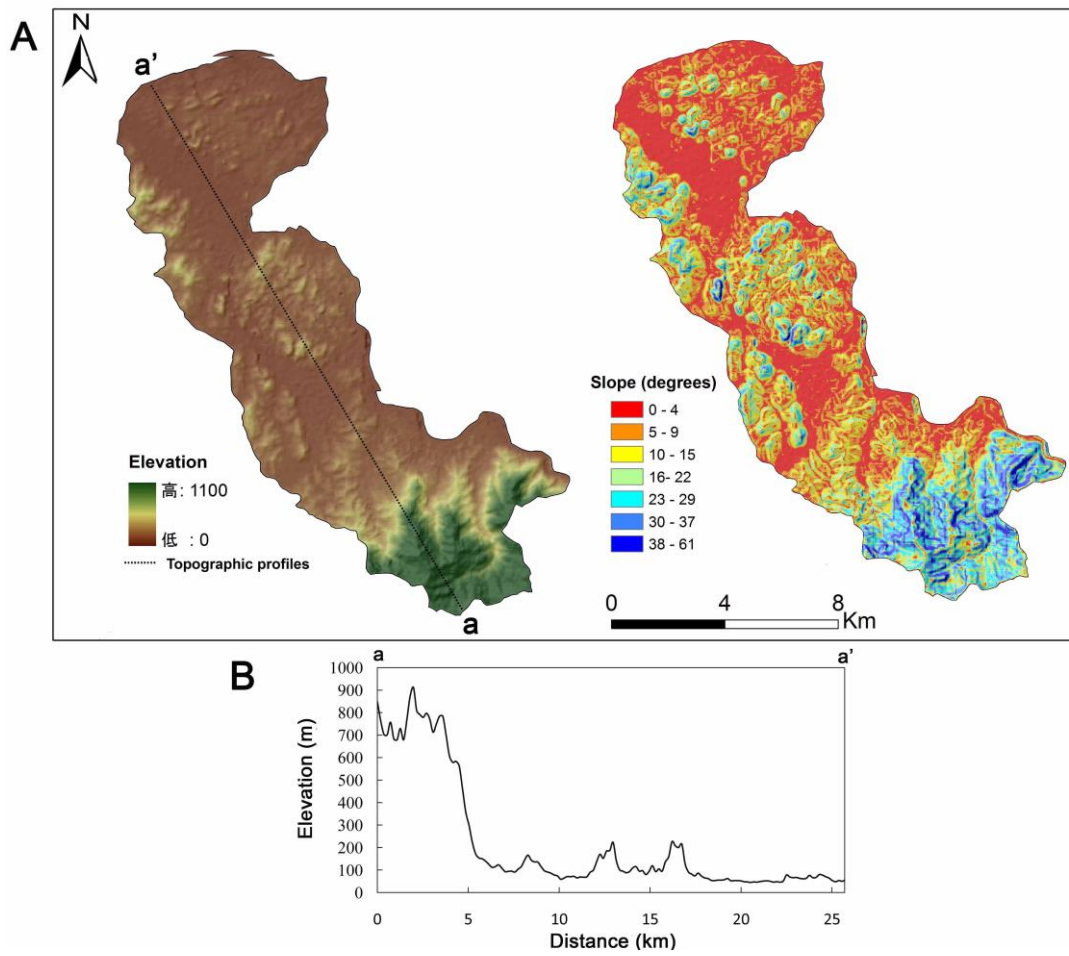


Figure 2-7. Topography of Mt. Longhu. (A) Distribution of elevation and slope. (B) Representative topographic profiles.



Figure 2-8. Representative Danxia landforms and landscapes in Mt. Longhu. (a) Wide valley and peaks. (b) Butte in the periphery of Mt. Longhu.

Sources: <http://www.dxdm.com/en/content/WH/2-3-3.html> and

<http://www.dxdm.com/EN/content/WH/2-5-2.html>

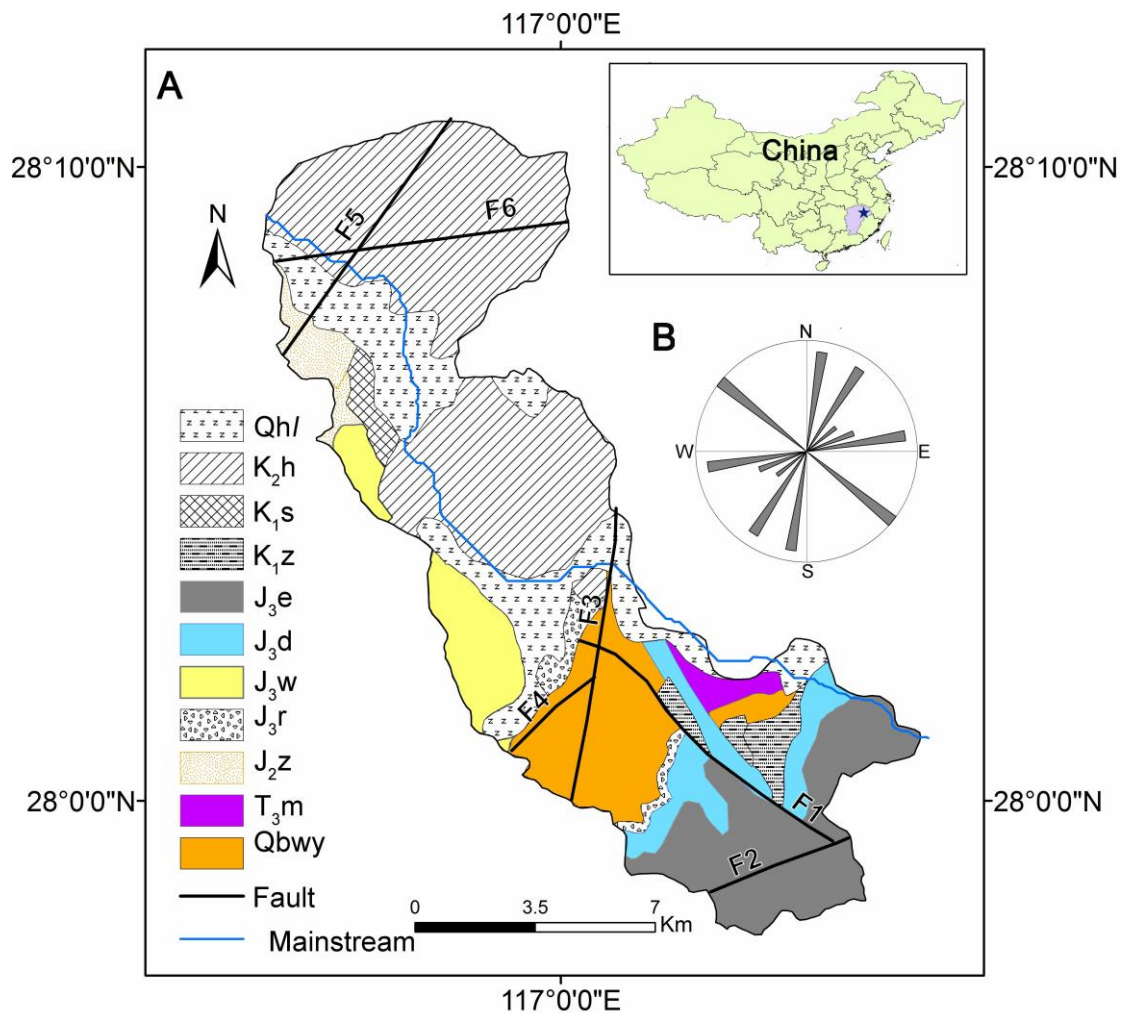


Figure 2-9. Geology of the Mt. Longhu.

(A) Geology of the Mt. Longhu based on the 1:100,000 map published by the Jiangzi Bureau of Geology and Mineral Resources. (B) Rose diagram showing fault orientations, based on GIS analysis of digitized fault lines. Qh/: Quaternary; K₂h: Hekou Formation; K₁s: Shixi Formation; K₁z: Zhaixia Formation; J₃e: Elinghu Formation; J₃d: Daguding Formation; J₃w: Wuxi Formation; J₃r: Ruyiting Formation; J₂z: Zhangping Formation; T₃m: Sanqiutian Formation; Qbwy: Wanyuan Formation.

CHAPTER 3 DATA AND METHODS

3.1. Geomorphological and geological data

A Digital Elevation Model (DEM) is a digital representation of the Earth's topographic surface. Since numerous previous studies have effectively used DEMs and GIS for morphometric analyses. This research also uses a DEM and digital geological data.

The data for the Chishui area are a 1:50,000 topographic map, a 1:50,000 geologic map, and the ASTER GDEM. The ASTER GDEM was provided by the Ministry of Economy, Trade, and Industry (METI) of Japan and the United States National Aeronautics and Space Administration (NASA). We downloaded the DEM for the study areas from the NASA web site and rectified it from its original WGS84 coordinates (1 arc-second resolution) into the UTM projection by bilinear interpolation to ensure a uniform cell size (30 × 30 m). The topographic and geologic maps were published by the Institute of South China Karst, Guizhou Normal University, China, in 2008.

The data for Mt. Danxia are also a 1:50,000 topographic map, a 1:50,000 geologic map, and the ASTER GDEM. The topographic map was published by the Sun Yat-Sen University, China, in 2008. The geologic map was published by the Guangdong Institute of Geological Survey, China, in 2000.

The data for Mt. Longhu are a 1:100,000 geologic map and the ASTER GDEM. The geologic map was published by the Jiangxi Bureau of Geology and Mineral Resource, China, in 1984.

Computer processing of data including the georeferencing and digitization of scanned maps was carried out. The original geological and topographic maps were scanned as tiff files. The scanned maps were georeferenced to the same projection as the DEM data using

the Georeferencing Toolbar in ArcGIS. Then the polygons of geological units and features were digitized from the georeferenced maps.

3.2. **Stream network extraction**

Stream-nets for the study areas were delineated using the DEMs. DEMs permit the automatic extraction of stream-nets via different algorithms (e.g., Mark, 1984; Martz and Garbrecht, 1992; Giannoni et al., 2005; Hancock and Evans, 2006; Tarolli and Fontana, 2009). The most common method, which is often implemented in major commercial GIS software, assumes a minimum contributing area to determine channel-head locations. However, the minimum contributing area should vary even within a small watershed according to local factors such as topography and lithology (e.g., Tucker et al., 2001; Vogt et al., 2003).

Stream-nets were automatically extracted from the DEMs based on the threshold contributing-area method of Jenson and Domingue (1988) embedded in the ArcHydro Tools of ESRI ArcGIS. ArcHydro is an extension of water resource applications developed for ArcGIS by the University of Texas (Maidment, 2002). This tool can be used for efficient delineation of watersheds and stream networks generation by means of the D8 algorithm (O'Callaghan and Mark, 1984; Jenson and Domingue, 1988). The DEM data were first loaded into ArcHydro and the sink filling function was applied to create a seamless elevation dataset with no sink. Then the Flowdirection function is employed to determine the steepest downstream slope among the eight slopes and assign the direction of flow from each grid cell; and the Flowaccumulation function calculates the accumulated

number of cells upstream which corresponds to the catchments area. In this research, change in drainage density with change in the threshold contributing area was firstly investigated (Figs. 3-1, 3-2 and 3-3). The result shows that drainage density decreases with an increasing contributing drainage area and it tends to be more constant if the contributing area is 100 grid cells ($\approx 0.1 \text{ km}^2$). This indicates that if the contribution drainage area is smaller than 100 grid cells, extracted stream nets tend to include depressions on hill slopes. Therefore, stream-nets were automatically extracted using the threshold contributing area of 100 grid cells. The extracted stream networks correspond well to the actual stream networks shown in the topographic maps. The streams were ordered based on the method of Strahler (1952) (Figure 3-4).

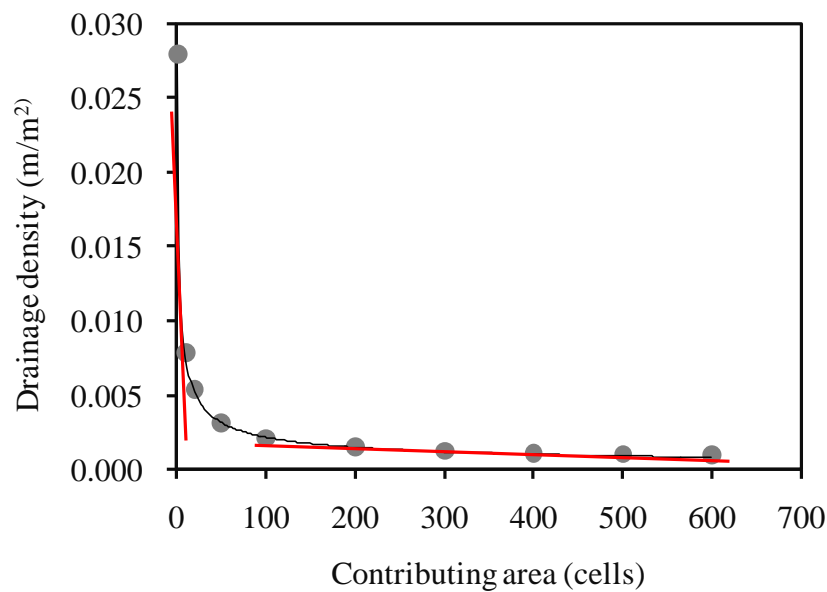


Figure 3-1 Change in drainage density with threshold contributing area for the Chishui area.

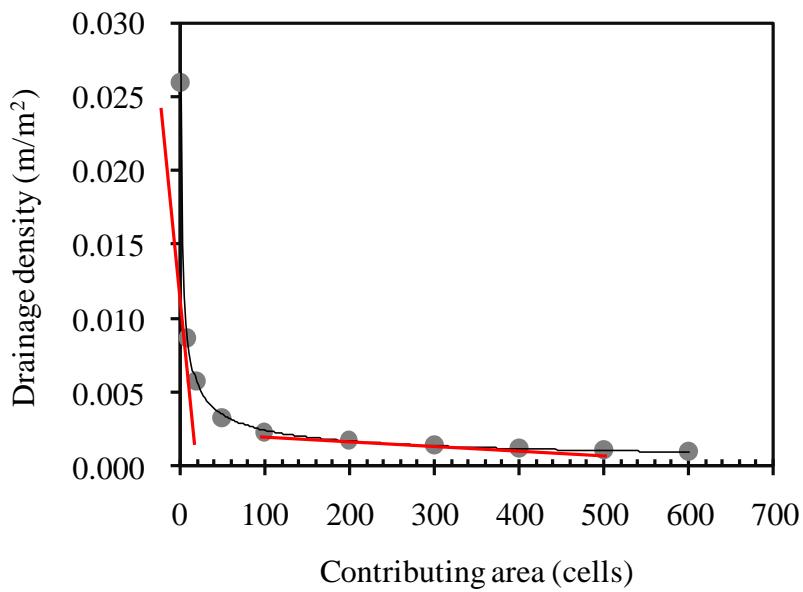


Figure 3-2. Change in drainage density with threshold contributing area for Mt. Danxia.

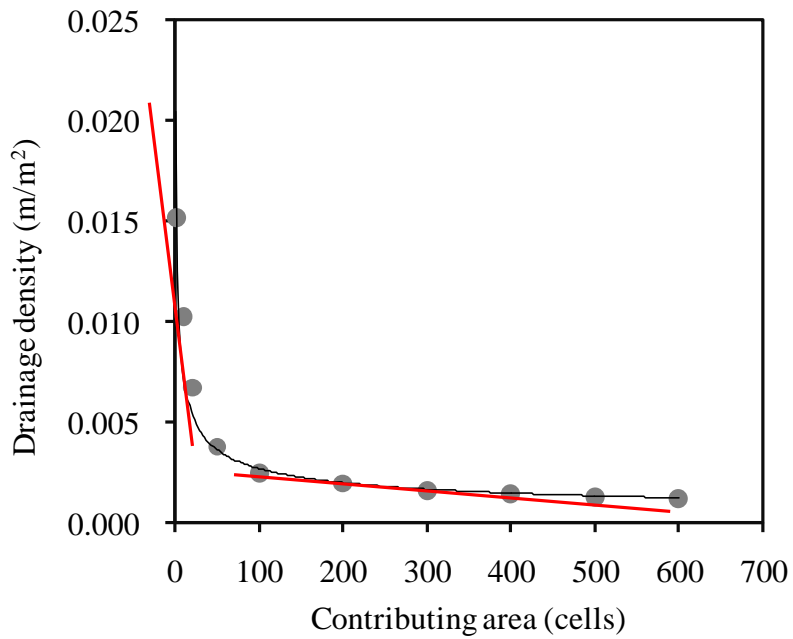
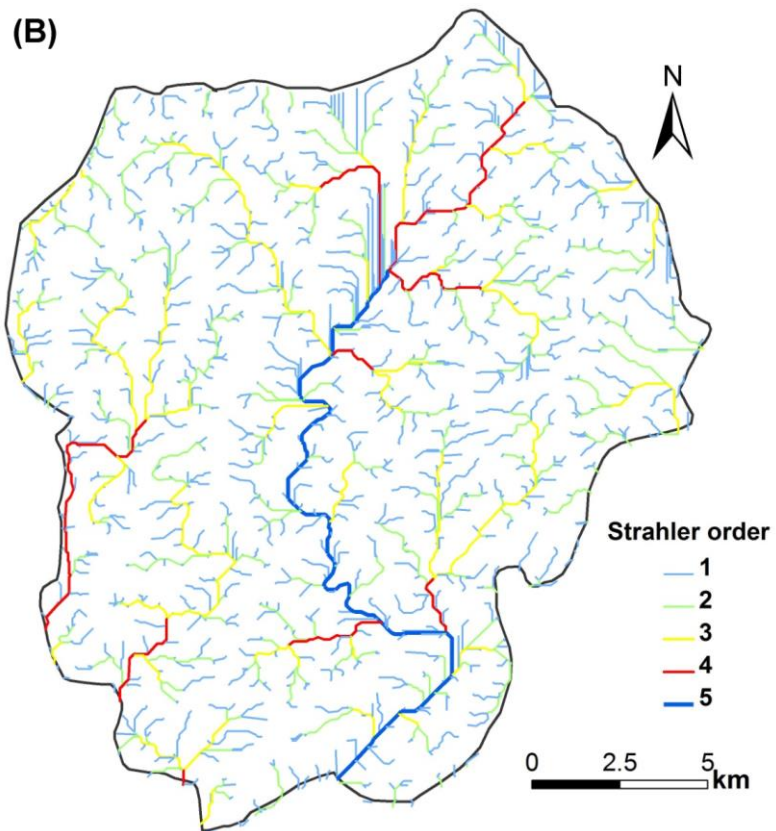
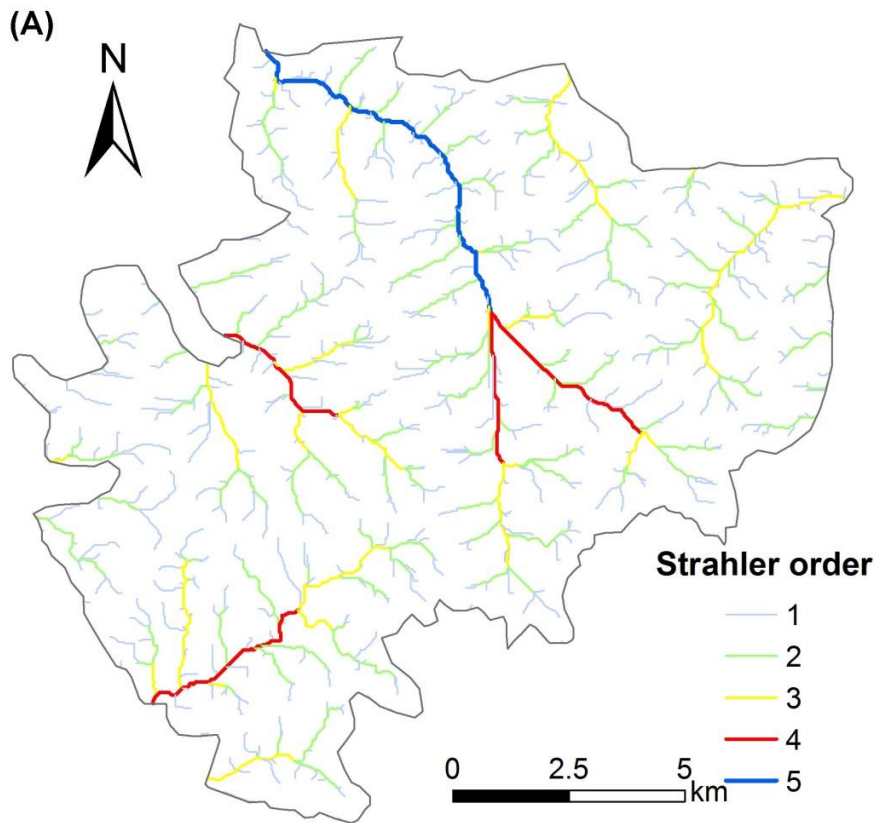


Figure 3-3. Change in drainage density with threshold contributing area for Mt. Longhu.



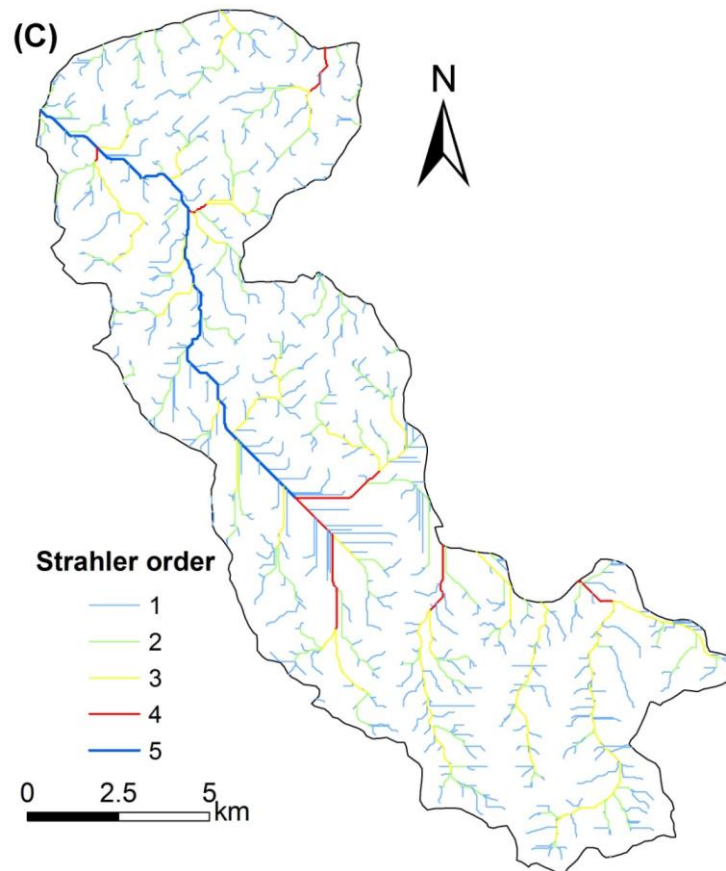
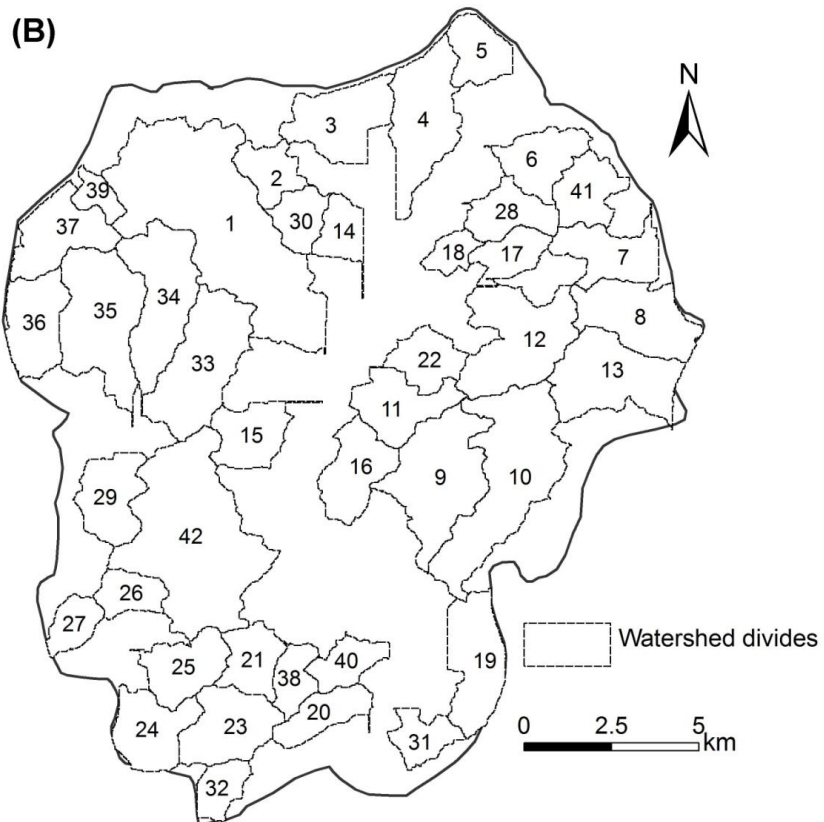
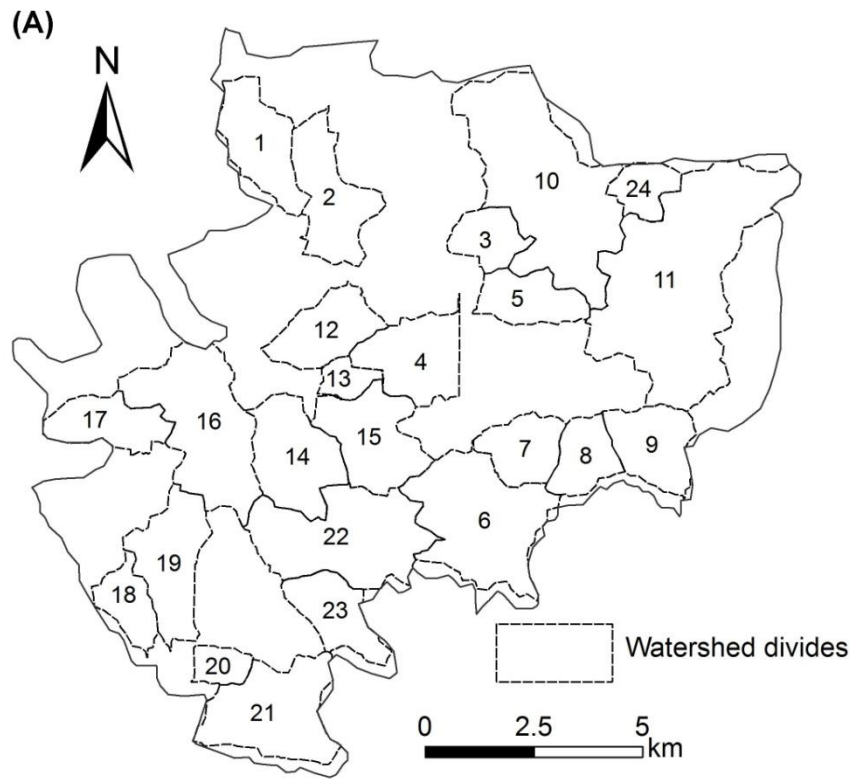


Figure 3-4. Distribution of stream-nets in (A) Chishui, (B) Mt. Danxia and (C) Mt. Longhu.

3.3. Watershed extraction

Third order watersheds within each study area were delineated using the DEMs and the Watershed function of the ArcHydro Tools of ESRI ArcGIS. The number and size of each stream order watershed can be measured and compared. Both the area of each watershed and the total number of the watersheds should be adequately large for statistically meaningful analyses but it is tedious to analyze too many watersheds. Therefore, the third order was selected to obtain some 20 to 40 watersheds for each area. The number of the extracted watersheds is 24 for the Chishui area, 42 for Mt. Danxia, and 26 for Mt. Longhu (Figure 3-5).



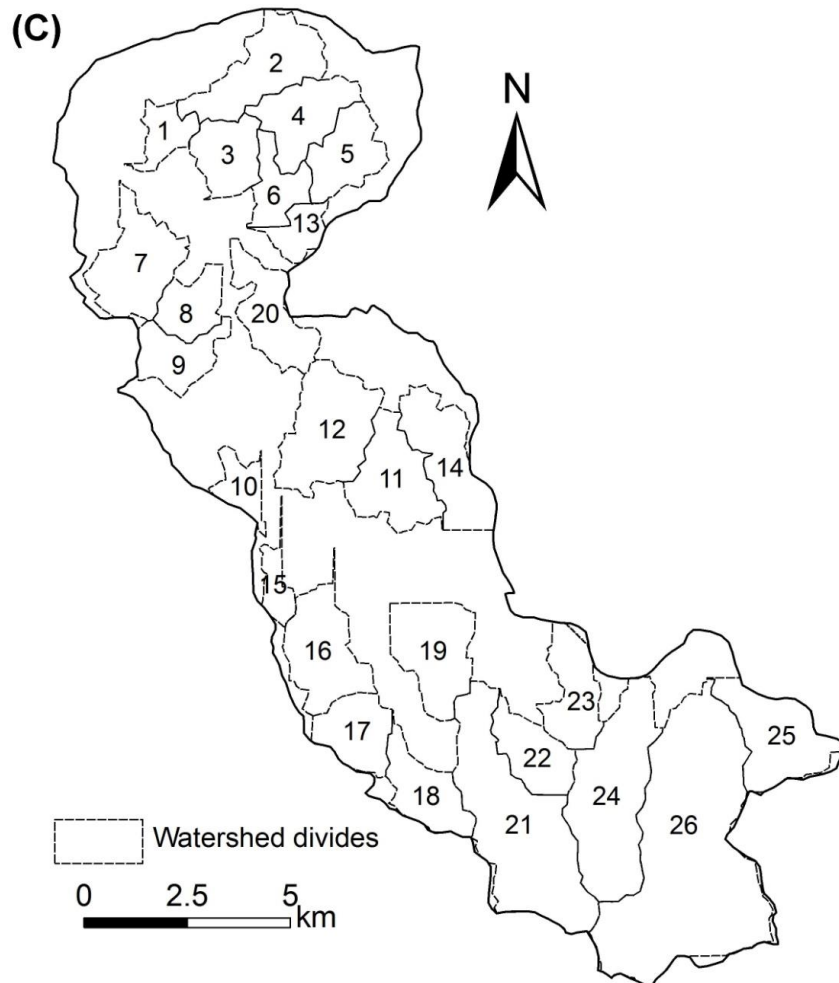


Figure 3-5. Distribution of third order watersheds in (A) Chishui, (B) Mt. Danxia and (C) Mt. Longhu.

3.4. Morphometric properties of watersheds

3.4.1. Slope angle

Slope angle, one of the most basic terrain properties, was calculated for each cell on the basis of the elevations of the eight nearest neighbors as proposed by Jenson and Domingue (1988). Then the mean of the calculated slope for a 300×300 m area was calculated. The mean slope for each watershed was also calculated.

3.4.2. Relative relief

Relative relief of each watershed was obtained. The parameter is defined here as the maximum elevation difference between the lowest and the highest points in a watershed (Hadley and Schumm, 1961). It expresses the overall magnitude of river incision.

3.4.3. Hypsometry

The hypsometric curve is a plot of the relative height (h/H) against the relative area (a/A), where H is the highest elevation of the watershed, A is the total area of the watershed, and a is the area of the watershed above a given elevation h (Strahler, 1952). The hypsometric integral (HI) is a measure of the overall proportion of high and low areas inside a watershed:

$$HI = \int_{\min\ elevation}^{\max\ elevation} \frac{a}{A} \times \Delta\left(\frac{h}{H}\right) \quad (3-1)$$

The shape of the hypsometric curve and the HI provide valuable information not only on the erosional stage of the watershed, but also on the tectonic and lithological factors controlling it (e.g. Moglen and Bras, 1995; Willgoose and Hancock, 1998; Huang and Niemann, 2006). For example, convex-up hypsometric curves indicate relatively young watersheds; S-shaped curves characterize moderately eroded watersheds; and concave curves indicate relatively old watersheds (Keller and Pinter, 2002; Strahler, 1957; Delcaillau et al., 1998). The hypsometric curves and the HI for each watershed were obtained from the DEM using MathWorks Matlab. Strahler (1952) assumed three stages of landform evolution based on the values of HI : “youthful, non-equilibrium” stage ($HI = 0.6$ to 1.0), “mature equilibrium” stage ($HI = 0.35$ to 0.6), and “old age” ($HI = 0.0$ to 0.35).

3.5. Characteristics of stream nets and their relation with slope

3.5.1. Stream orientation

The data of the flow direction of each cell of the DEM, obtained using the method of Jenson and Domingue (1988), were summarized in the form of rose diagrams to describe the frequency distribution of the orientation of streams.

3.5.2. Morphometric parameters of stream networks structure

The basic parameters related to Horton's (1945) "law of stream numbers" and Horton's (1932) "law of stream length" were obtained from the stream network data, including the total stream number, total and mean stream lengths, the bifurcation ratio, the stream length ratio and drainage density (Horton, 1932, 1945; Vijith and Sathesh, 2006) were derived for each watershed.

The stream length ratio is the ratio of the mean length of streams of a given order (n) to that of streams of the next lower order ($n - 1$) (Horton, 1945). The bifurcation ratio was introduced by Horton (1932) to express the ratio of the number of streams of a given order (n) to the number in the next higher order ($n + 1$).

Drainage density was calculated for each of $300 \times 300 \text{ m}^2$ areas within a watershed. The results were used to analyze the relationship between drainage density and slope as noted below. The mean drainage density for each watershed was also calculated.

3.5.3. Slope angle and drainage density

The relationship between slope angle and drainage density was examined for each watershed, based on the method of Lin and Oguchi (2006). For the $300 \times 300 \text{ m}^2$ areas in a

watershed, mean slope was computed, and mean drainage density for each 2° slope bin was obtained and plotted against slope angle. Then the quadratic equation was fitted to approximate the relationship between slope angle and drainage density for each watershed,

$$y = ax^2 + bx + c \quad (3-2)$$

where x is slope angle, y is drainage density, and a , b , and c are constants.

Visual observations indicate that the relationships between the slope angle and drainage density can be classified into five types: Type 1 is concave upward showing that drainage density tends to decrease with increasing slope angle for smaller slope angle but increase for larger slope angle, Type 2 is convex upward showing that drainage density tends to increase with slope angle for smaller slope angles but decrease for larger slope angles, Type 3 is positive upward that showing the drainage density increase with increasing slope angles, Type 4 is negative showing that drainage density tends to decrease with increasing slope angle, and Type 5 is constant. When the quadratic function of Eq. (3-2) is written as $y = f(x)$, and the curve type for a watershed can be judged based on a decision-tree procedure as follows (Lin and Oguchi, 1996):

(1) If $|\max (f'(x)) - f'(x)| < T$ holds true for any x , $f(x)$ is Type 5

where $f'(x)$ is first order derivative for any a point in the curve $f(x)$; $\max (f'(x))$ is the maximum value of $f'(x)$; and T is a threshold value. The value of T was set to be 0.1 based on the visual investigation of some sample data plots with fitting curves, and the values of $|\max (f'(x)) - f'(x)|$ for the curves.

(2) If there is a value of x which fulfills $|\max (f'(x)) - |f'(x)|| \geq T$, then,

- [1] If $f'(x) > 0$ for any x , $f(x)$ is Type 3;
- [2] If $f'(x) < 0$ for any x , $f(x)$ is Type 4;
- [3] If a value of x_i fulfills $f'(x_i) = 0$, then,

- (a) if $0.2 < \frac{x_t - x_{\min}}{x_{\max} - x_{\min}} < 0.8$ and $f'(x_{\min}) > 0$, $f(x)$ is Type 2;
- (b) if $0.2 < \frac{x_t - x_{\min}}{x_{\max} - x_{\min}} < 0.8$ and $f'(x_{\min}) < 0$, $f(x)$ is Type 1;
- (c) if $\frac{x_t - x_{\min}}{x_{\max} - x_{\min}} < 0.2$ and $f'(x_{\max}) > 0$, $f(x)$ is Type 3;
- (d) if $\frac{x_t - x_{\min}}{x_{\max} - x_{\min}} < 0.2$ and $f'(x_{\max}) < 0$, $f(x)$ is Type 4;
- (e) if $\frac{x_t - x_{\min}}{x_{\max} - x_{\min}} > 0.8$ and $f'(x_{\min}) > 0$, $f(x)$ is Type 3;
- (f) if $\frac{x_t - x_{\min}}{x_{\max} - x_{\min}} > 0.8$ and $f'(x_{\min}) < 0$, $f(x)$ is Type 4;

The classification results show that most of the drainage density–slope angle relationships belong to Type1, Type 2, Type 3 and Type 4 (Figure 3-6). Figure 3-6 shows the example of the plots of the four types with the fitted trend lines.

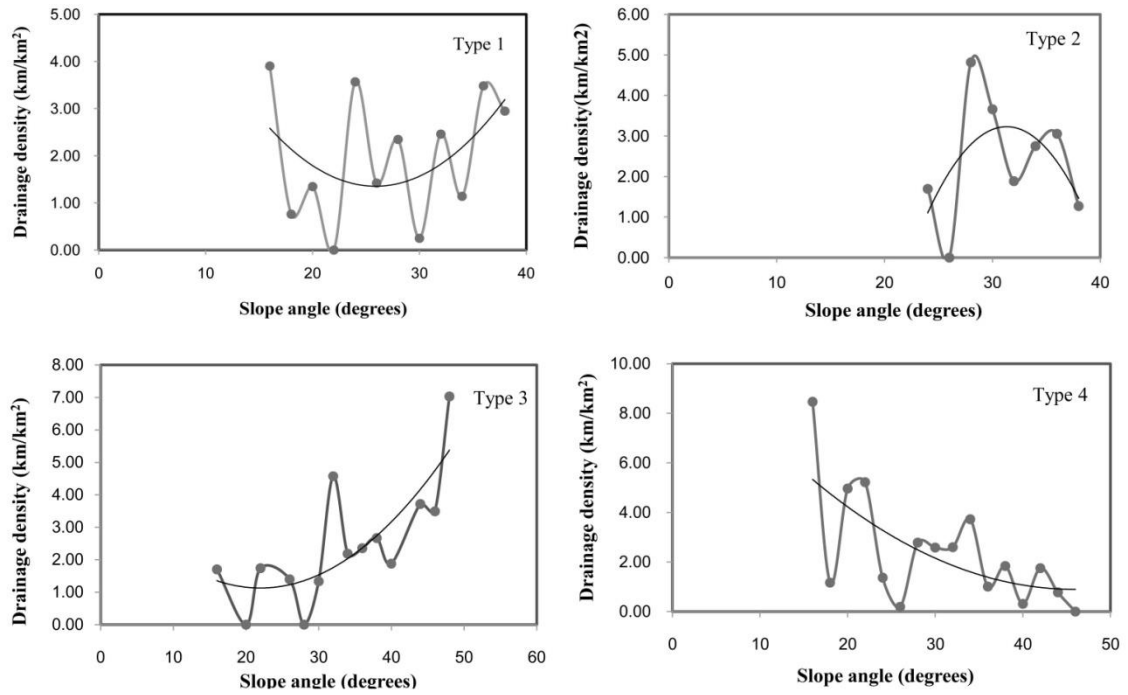


Figure 3-6. Example of types of the drainage density–slope angle relationship in Chishui area. The thick line is the quadratic approximation.

3.6. River longitudinal profiles and related analyses

3.6.1. River longitudinal profiles

The stream route between the summit of the watershed divide (the highest point) and the mouth of the watershed (the lowest point) is regarded as the master stream. The longitudinal profile of the master stream was investigated as a representative topographic property of a watershed. After the normalization of x (distance) and y (height) values for each profile into a range of 0 to 1, a power function was fitted to the profile data based on the least square method.

$$y = A x^B \tag{3-3}$$

where, A and B are constants.

The simple and basic power function was selected because of the various profile forms including knickzones, and the fitting of the power function yielded good results in almost all the cases. Therefore, the form characteristics of the longitudinal profile were expressed using two simple parameters following Lin and Oguchi (2006): the exponent of the power function fitted to a profile (B), which represents the curvature characteristics of the profile, and overall slope (β) calculated from the position of the two end points of a long profile.

We also extracted “anomalous points” along a river where the height of the river bed significantly differs from the height estimated from Eq. (3-3) as proposed by Lin and Oguchi (2006). The threshold value for identifying the anomalous point was set to be 0.07 based on the average values of sampled data for the study areas.

3.6.2. Stream length gradient (SL) index and Hack’s profile

The SL index (Hack, 1973), a parameter related to river longitudinal profiles, is defined as:

$$SL = (\Delta E / \Delta L)L \quad (3-4)$$

where, ΔE is the difference in elevation (E) between the ends of the reach of interest, ΔL is the length of the reach, and L is the horizontal length from the watershed divide to the midpoint of the reach. We calculated SL at 120-m intervals, yielding 1240 points for the calculation. We also followed the methodology proposed by Chen et al. (2003) and produced the Hack profiles and computed the idealized gradient index (K) (Hack, 1973) for the entire profile of each main stream of the 3rd watershed. K can be deemed as the proxy of stream power and is computed as:

$$K = \frac{E_i - E_j}{\ln L_i - \ln L_j} \quad (3-5)$$

where, i and j refer to two points along the river profile.

A convex Hack profile suggests a river adjusting to fault movements and/or increasing

rock resistance downstream, and a concave profile suggests a river adjusting to decreasing bedrock resistance downstream or significantly increasing discharge downstream (DeGraff,1981; Harkins et al., 2005). The theoretical equilibrium Hack profile is straight if a river is flowing across uniform bedrock (Hack, 1973; Hack, 1982; Merritts and Vincent, 1989; Brookfield, 1998; Hadley and Schumm, 1961).

3.6.3. Identification of knickzones

A knickzone is a locally high-gradient reach between lower gradient reaches (Seidl and Dietrich, 1992; Crosby and Whipple, 2006; Hayakawa and Oguchi, 2006, 2009). This study includes identification and analyses of knickzones. Following the method proposed by Hayakawa and Oguchi (2006), stream gradients of the rivers are first computed with varying measurement lengths, and an index of relative steepness was derived from the stream gradients. A threshold value of the relative steepness index was then established for determining knickzones.

Stream profiles were first smoothed using the built-in smoothing algorithm in ArcGIS tools and a 60-m smoothing window. This smoothing eliminates the minor “stair-step” features seen in a longitudinal profile from a DEM. Stream gradient (G_d) was calculated at each of 60-m interval point, which gradient is defined as below:

$$G_d = H/L = (E_1 - E_2)/L \quad (3-6)$$

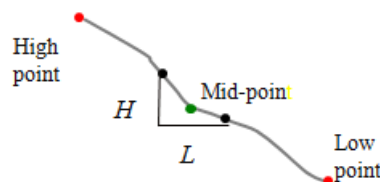


Figure 3-7. Measurement of stream gradient (G_d) along the stream.

where, L is the length of the reach used for the gradient calculation (m), H is the change in elevation. and E_1 and E_2 are the elevation at the 1/2 upstream reach and

downstream reach of the sampled point. For each sampling point, different G_d values were obtained by changing L at a 120 m interval.

For each sampling point a linear regression line was fitted to the relationship between L and G_d .

$$G_d = -R_d L + b \quad (3-7)$$

where, R_d and b are constants, and the value of R_d was used to identify knickzones. The value of R_d for each river was examined and its average for all the rivers was calculated for three study areas. We determined the threshold value of for knickzone extraction to be $3.52 \times 10^{-5} \text{ m}^{-1}$ based on one standard deviation away from the average for the entire dataset; if a point is larger than this value, then the point is identified as a part of a knickzone.

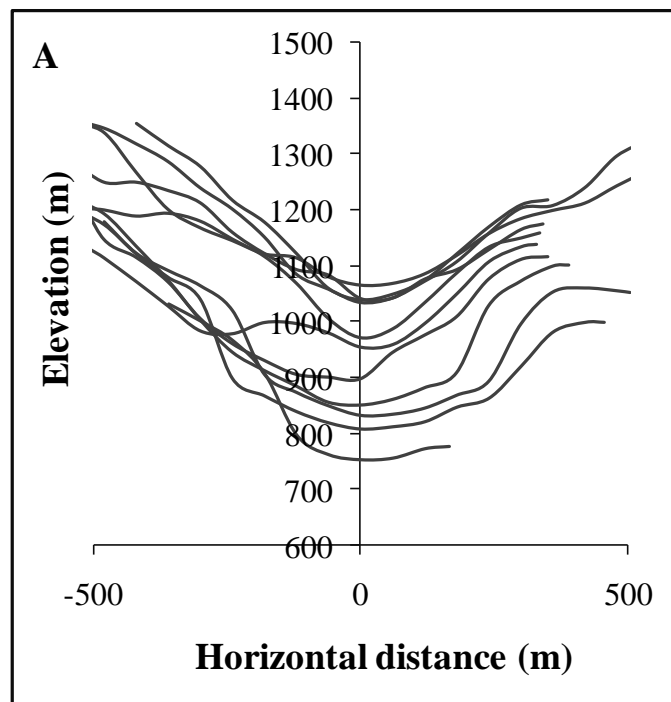
3.7. Transverse profiles of watersheds

Along the master stream, a series of transverse profiles of a watershed were extracted from the DEMs at a 120 m interval. Each transverse profile is perpendicular to the orientation of the master stream. Figure 3-3 shows examples of the obtained transverse profiles for watersheds of the three study areas.

Basic morphometric parameters of the transverse profiles such as width (W), relief (R), slope (α), height (H), and the statistical moments (standard deviation, skewness, and kurtosis) of their slope and height were acquired to examine the form of the watershed as proposed by Lin and Oguchi (2006). Slope angle at the t -th point along the transverse profile ($0 \leq \alpha_t \leq 90^\circ$) was obtained:

$$\alpha_t = \arctan \left| \frac{H_{t-1} - H_t}{D_{t-1} - D_t} \right| \quad (3-8)$$

Then, using all the height data for each profile, the most basic statistical measures of frequency distribution of height, the first to fourth moments, were calculated: mean (*AVH*), standard deviation (*SDH*), skewness (*SKH*), and kurtosis (*KUH*). The same moments of the slope α were also calculated for each profile: mean (*AV α*), standard deviation (*SD α*), skewness (*SK α*), and kurtosis (*KU α*).



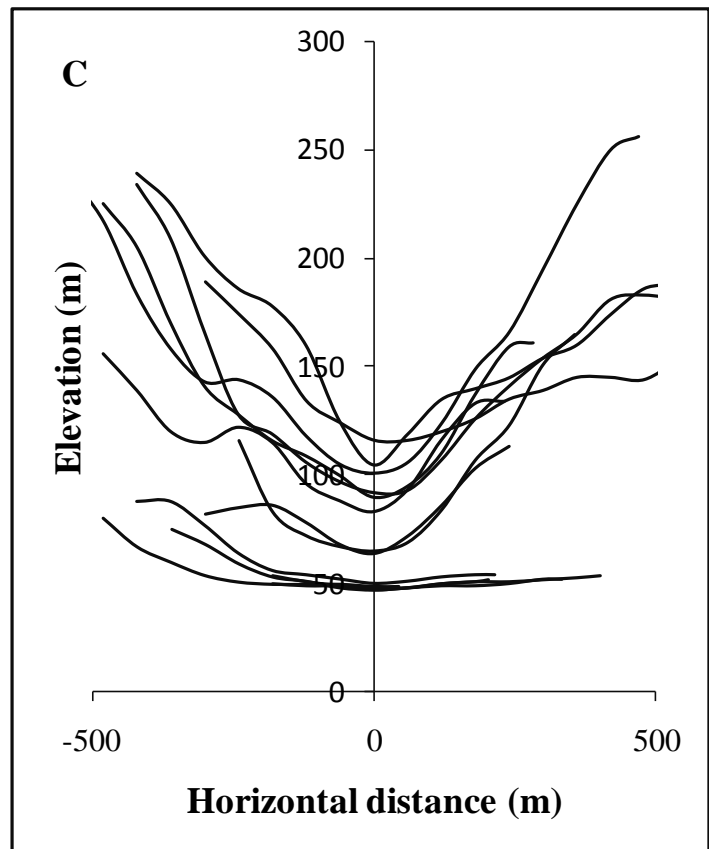
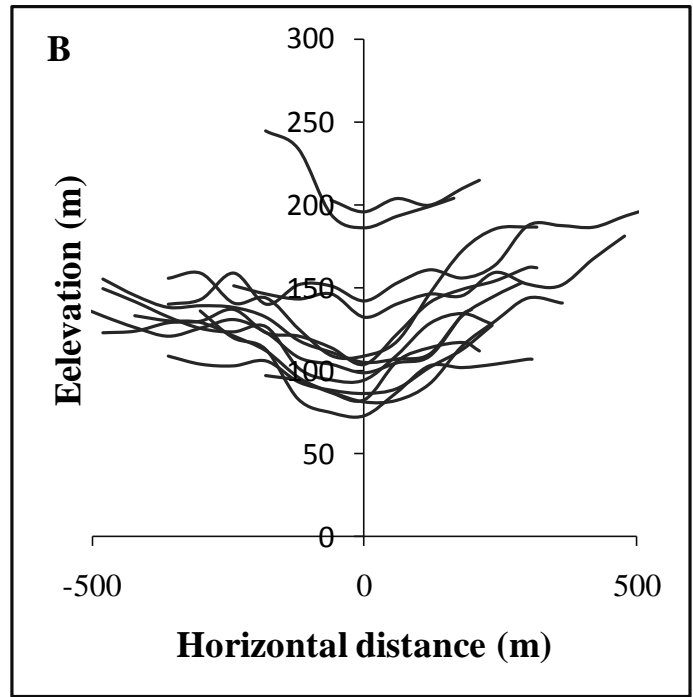


Figure 3-8. The example of the transverse profile in (A) Chishui area, (B) Mt. Danxia and (C) Mt. Longhu.

CHAPTER 4 RESULTS

4.1. Watershed and stream net properties

4.1.1. Overview of watershed properties in the three areas

Table 4-1 shows the mean and range of each morphometric property for each study area. The properties expressing slope or relief, i.e., mean watershed slope, relative relief, β , SL , K , $Av\alpha$, and R are larger for the Chishui area but smaller for Mt. Danxia and Mt. Longhu. Curvature of longitudinal profiles (B) and HI also show higher values for the Chishui area and smaller values for the other two areas. In contrast, drainage density is the lowest in the Chishui area, intermediate in Mt. Danxia, and the highest in Mt. Longhu. W tends to be similar for the three areas. In general, the mean values of a parameter for Mt. Danxia and Mt. Longhu are similar, whereas the Chishui tends to take more unique values.

The properties of the stream network structure for the three areas are summarized in Table 4-2. For the same stream order, the mean stream length tends to increase in the following order: Chishui, Mt. Danxia, and Mt. Longhu, which corresponds to the difference in drainage density. The bifurcation ratio between the 1st and 2nd order streams is consistently larger than that between the 2nd and 3rd order streams.

Table 4-1. Mean and range values of watershed properties for the three study areas.

Area	Slope (degrees)	Relative relief (m)	Drainage density (km ² /km ²)	θ	B	SL (m)	K	HI	Av α (degrees)	W (m)	R (m)
Chishui	29.9; 23.4–36.4	713; 423–936	2.03; 1.54–2.54	12.1; 5.1–21.5	0.42; 0.24–0.68	274.0; 138.8–396.2	81; 56–106	0.56; 0.45–0.65	23.8; 16.4–30.6	13111.9; 723.7–2065.8	313.0; 213.8–445.7
Mt. Daxia	11.0; 6.2–16.8	273; 124–516	2.22; 1.68–2.82	3.5; 1.2–9.2	0.25; 0.13–0.45	58.0; 22.1–136.7	27; 11–47	0.32; 0.21–0.57	10.3; 6.3–17.9	1360.2; 492.0–2417.1	107.7; 35.9–228.6
Mt. Longhu	10.1; 3.5–23.6	299; 56–1018	2.53; 1.98–3.59	2.4; 0.6–7.0	0.26; 0.11–0.66	52.9; 9.7–277.9	24; 3–103	0.29; 0.17–0.45	7.1; 2.2–17.6	1144.1; 557.9–2299.9	89.1; 6.7–401.8

Table 4-2. Horton's parameters of streams in the three study areas

Area	Stream order	Stream number	Bifurcation ratio	Mean stream length (m)	Stream length ratio
Chishui	1	320	4.57	351.69	2.52
	2	70	2.92	885.07	1.79
	3	24		1580.38	
Mt. Danxia	1	590	4.84	393.45	2.49
	2	122	2.90	980.06	2.17
	3	42		2127.67	
Mt. Longhu	1	361	4.57	411.02	1.62
	2	79	3.04	667.71	3.47
	3	26		2319.90	

4.1.2. Stream orientations

Stream orientation data for the Chishui area (Figure 4-1) show that the 1st and 2nd order streams tend to have flow directions of W, NW, and N, whereas the higher order streams tend to flow toward N to NW. Overall, flow directions from N to W are dominant; this simply reflects the flow of water toward the downstream areas (Figure 2-1). Other than that, stream orientations in the Chishui area tend to distribute more evenly than those of the other two areas.

In Mt. Danxia, the 1st and 2nd order streams tend to have flow directions of E, W, and S, whereas the higher order streams tend to flow toward S to SW (Figure 4-2). These approximately correspond to the fault orientation data in Figure 2-6B; the larger higher-order streams follow the most distinct fault orientation (N–S to NE–SW), whereas the smaller lower-order streams additionally follow the second most distinct fault orientation (E-NE to SW-W).

In Mt. Longhu, the 1st and 2nd order streams tend to have flow directions of N and E, whereas the higher order streams tend to flow toward N to NW (Figure 4-3). The most

dominant orientation is N, which corresponds to the general water flow direction toward the downstream area (Figure 2-7). The correspondence of the stream directions and the fault orientation data shown in Figure 2-9B is unclear, partly because unlike Mt. Danxia, the fault directions do not show strong anisotropy.

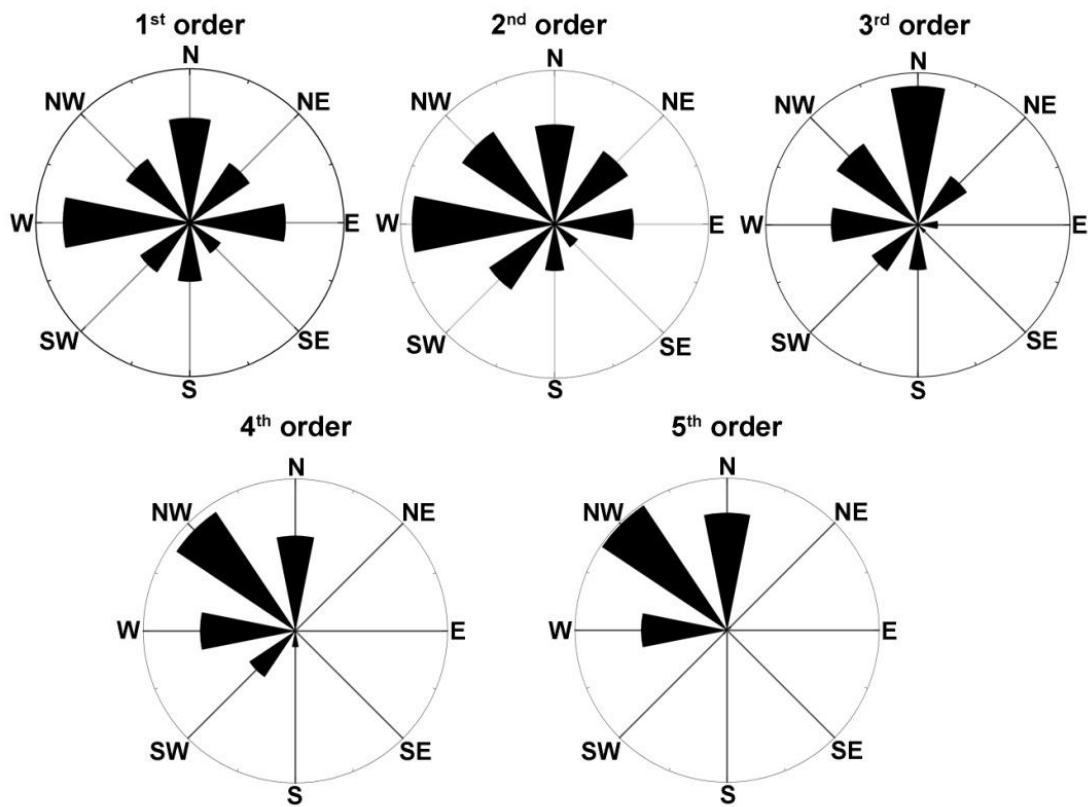


Figure 4-1. Diagram showing the distribution of stream flow direction for different Strahler orders in the Chishui area. Flow direction is shown for each DEM cell.

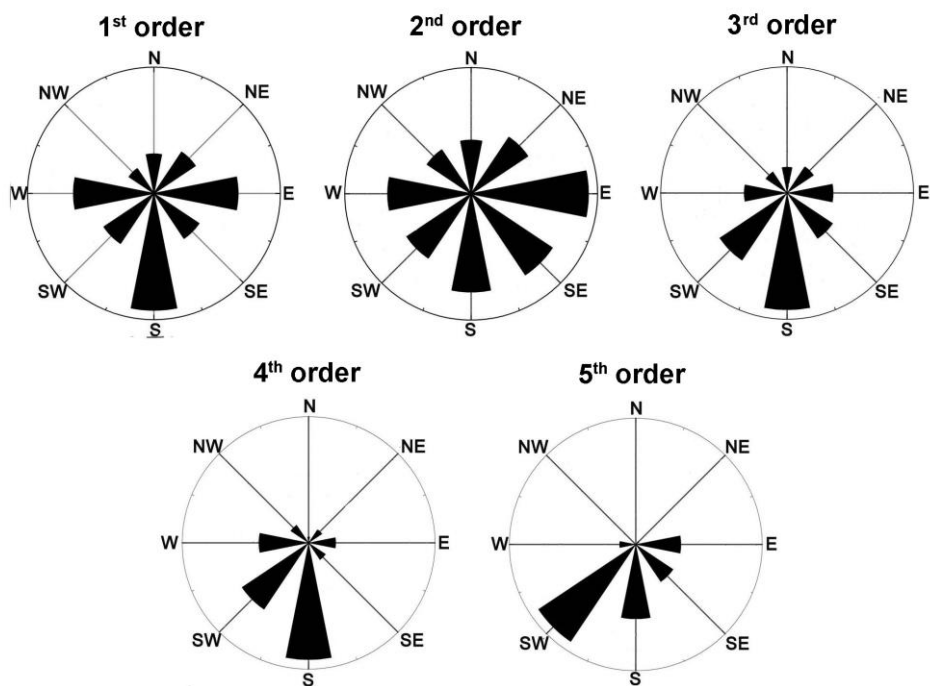


Figure 4-2. Diagram showing the distribution of stream flow direction for different Strahler orders in Mt. Danxia. Flow direction is shown for each DEM cell.

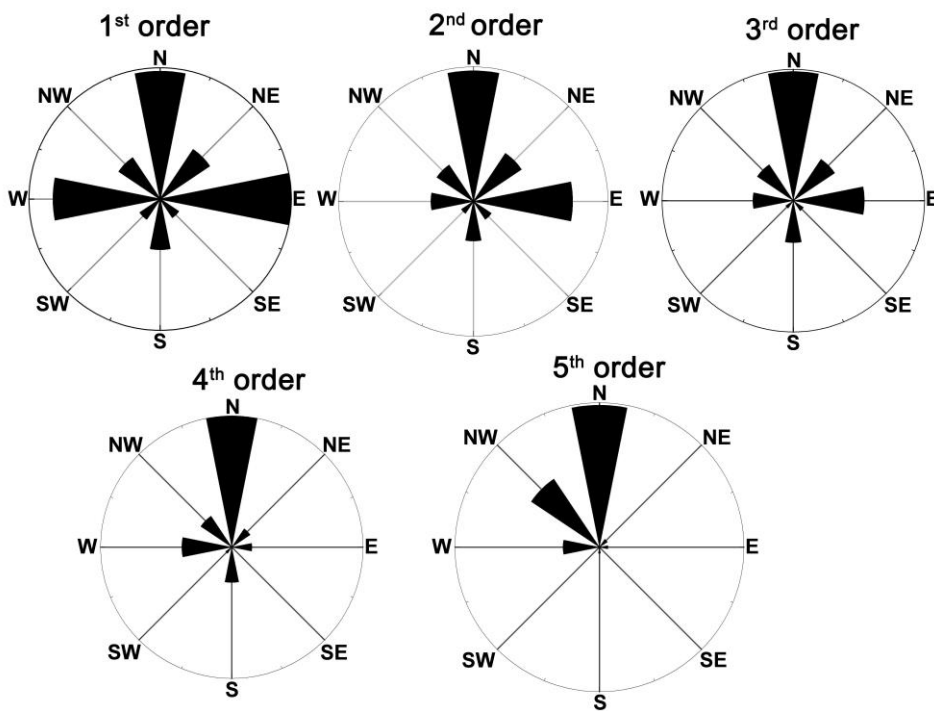


Figure 4-3. Diagram showing the distribution of stream flow direction for different Strahler orders in Mt. Longhu. Flow direction is shown for each DEM cell.

4.1.3. Drainage density – slope angle relationships and watershed classification

The relationship between slope angle and drainage density was examined for each watershed in each study area. Figure 4-4 shows the example of the plots with the fitted trend lines in the Chishui area. Four watersheds belong to Type 1, seven watersheds belong to Type2, seven watersheds belong to Type 3, and six watersheds belong to Type4. In other words, the four types occur with relatively similar frequencies. By contrast, only Type 4 is dominant in Mt. Danxia and Mt. Longhu (Figures 4-5 and 4-6).

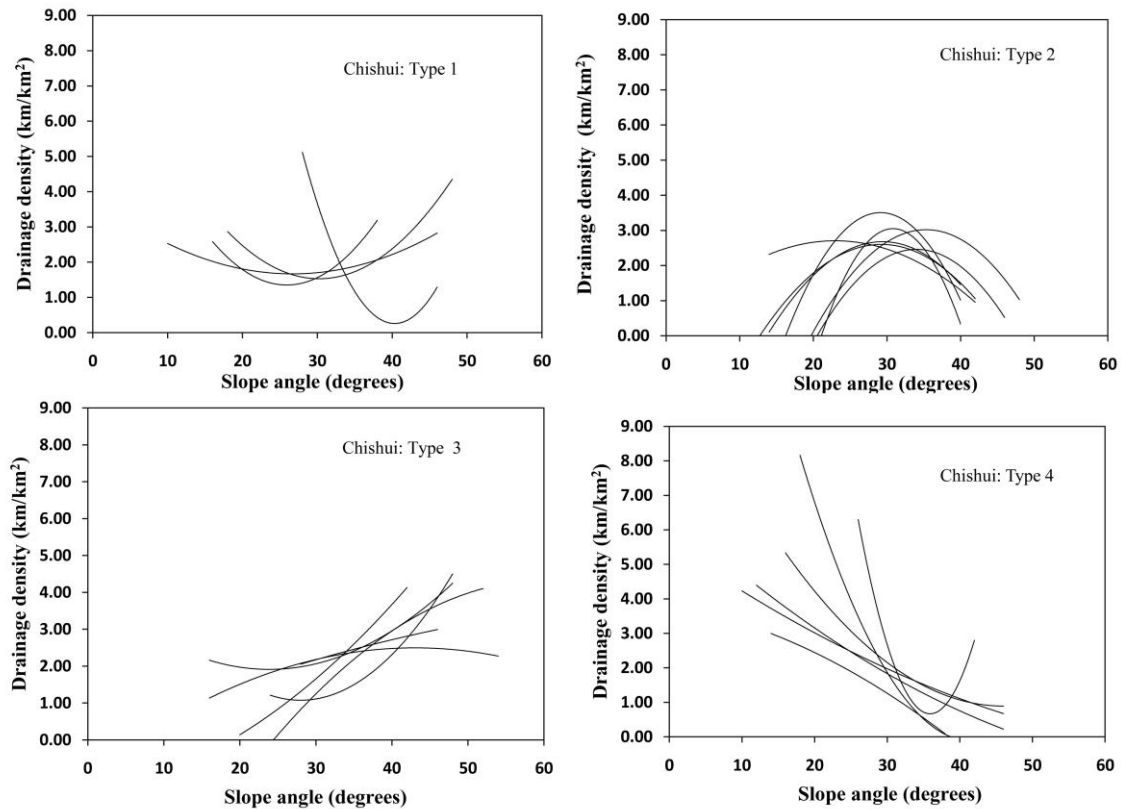


Figure 4-4. Trend lines of the drainage types for each watershed in Chishui area.

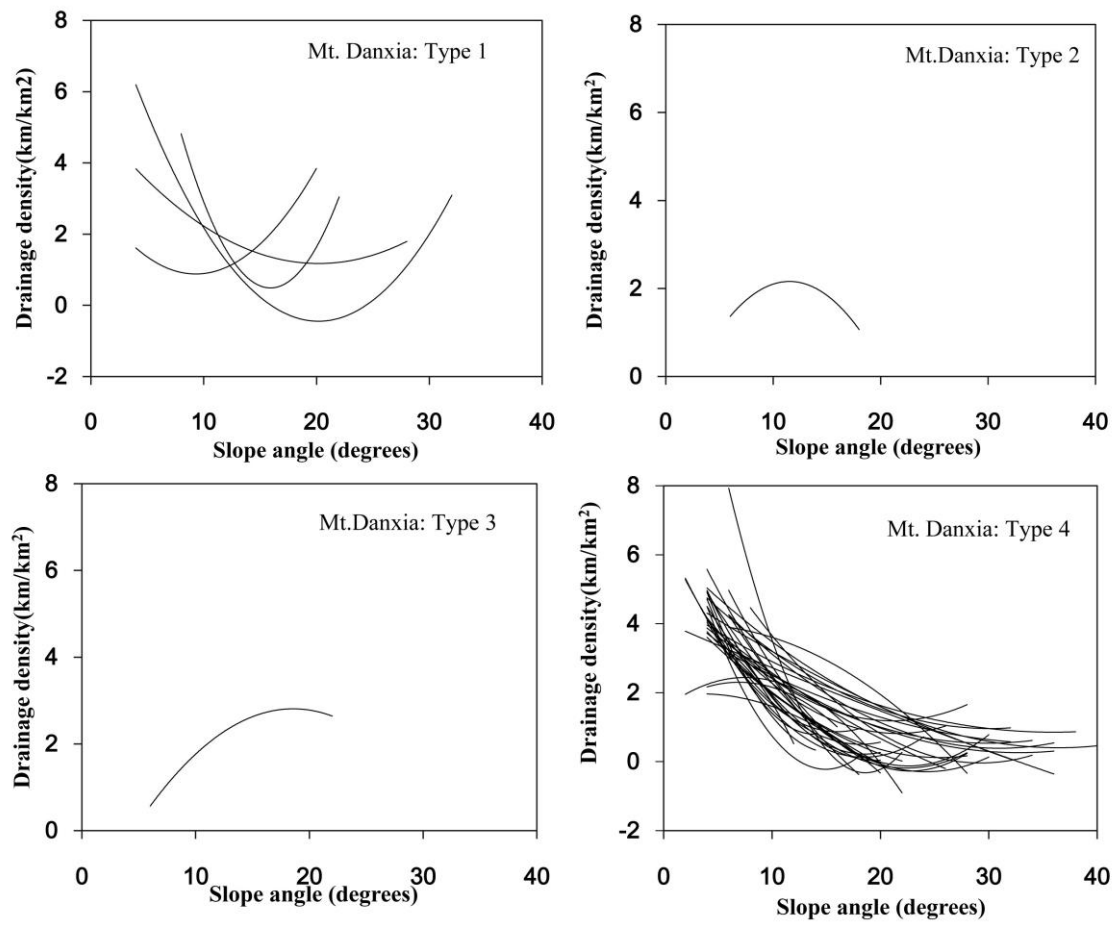


Figure 4-5. Trend lines of the drainage types for each watershed in Mt. Danxia.

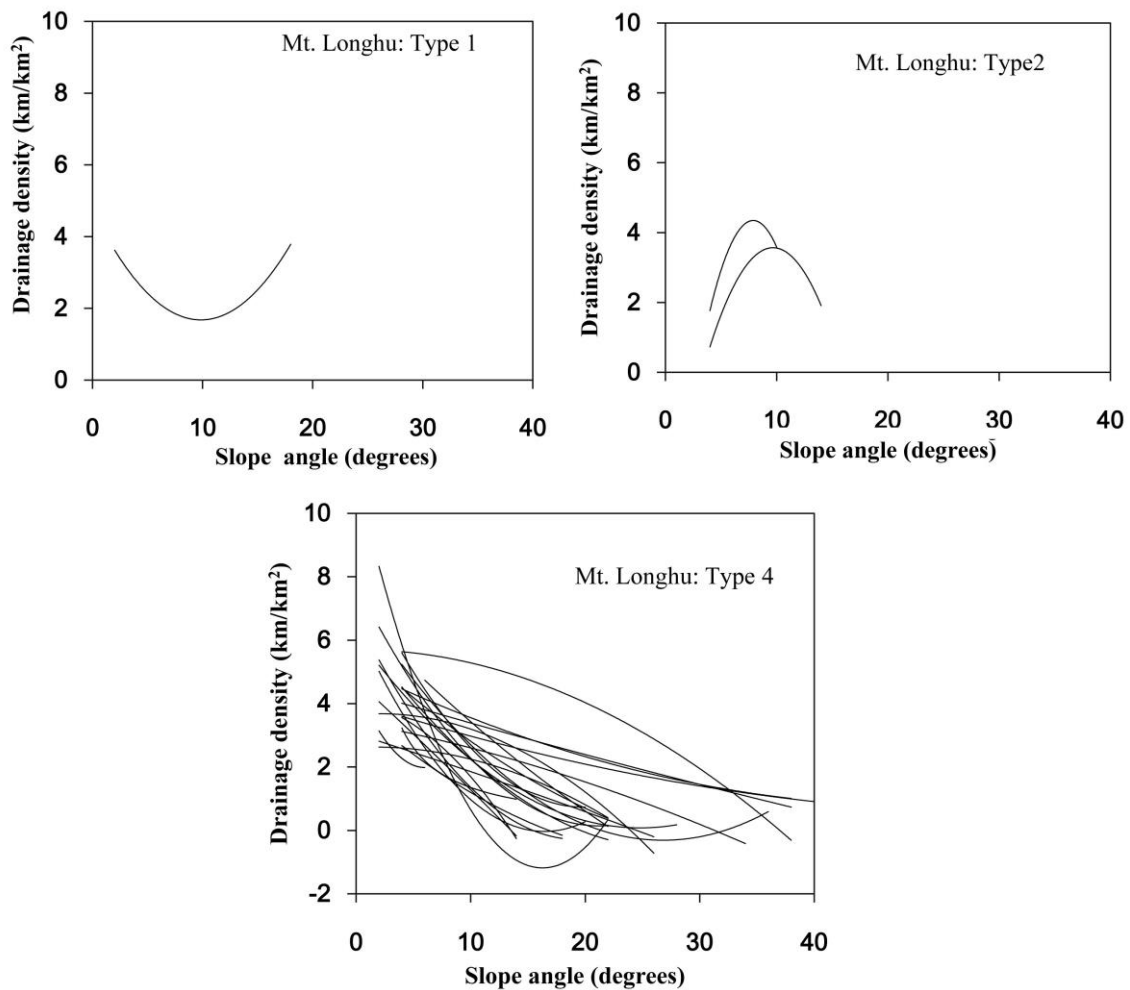
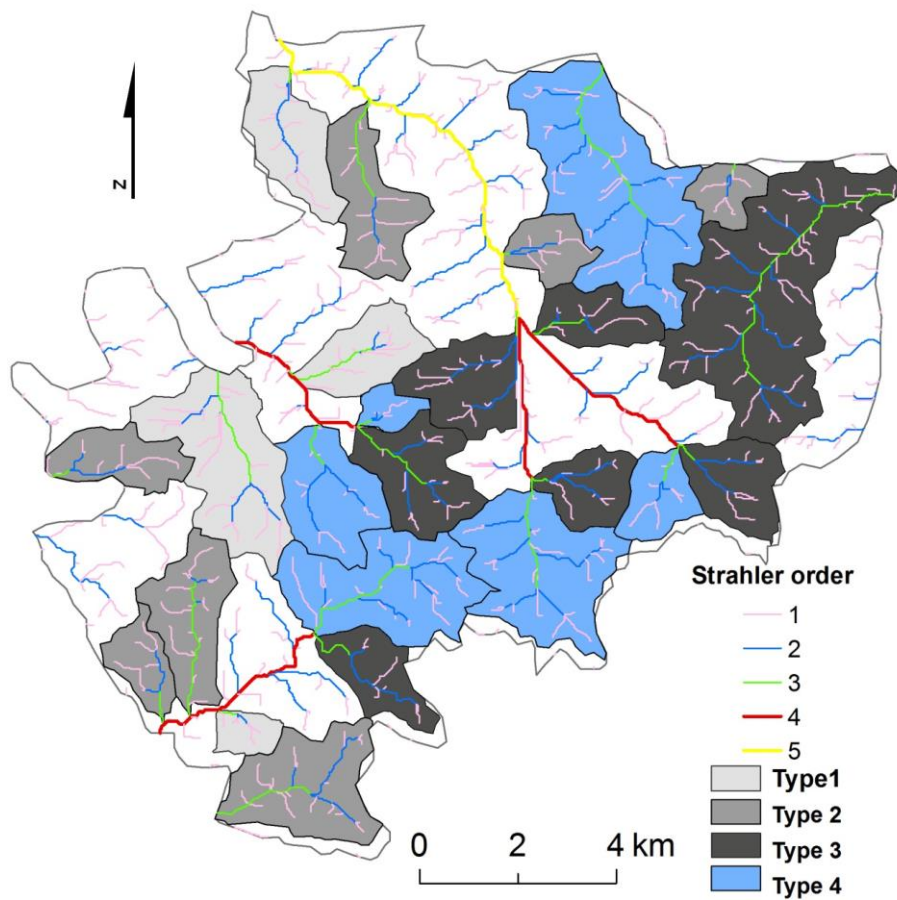
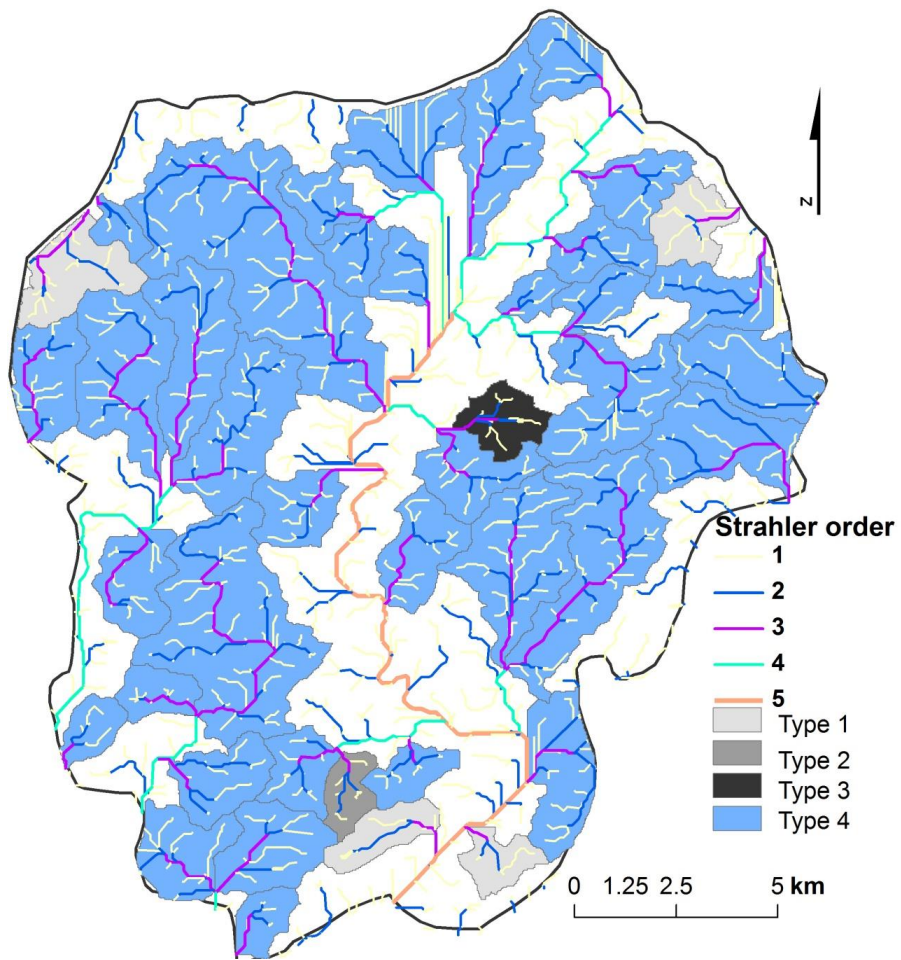


Figure 4-6. Trend lines of the drainage types for each watershed in Mt. Longhu.

Figure 4-7 shows the spatial distribution of the watersheds with the four types of drainage density – slope angle relationship. For the Chishui area, Type 1 tends to occur in downstream areas. Types 2, 3 and 4 tend to concentrate in the SW, SE, and NE parts, respectively. The watersheds of the four types do not show distinct differences in terms of mean slope, mean drainage density, and mean height (Table 4-3).

In Mt. Danxia and Mt. Longhu, Types 1 to 3 seem to occur in smaller watersheds near the master streams. However, the number of these watersheds is too small to discuss the details.





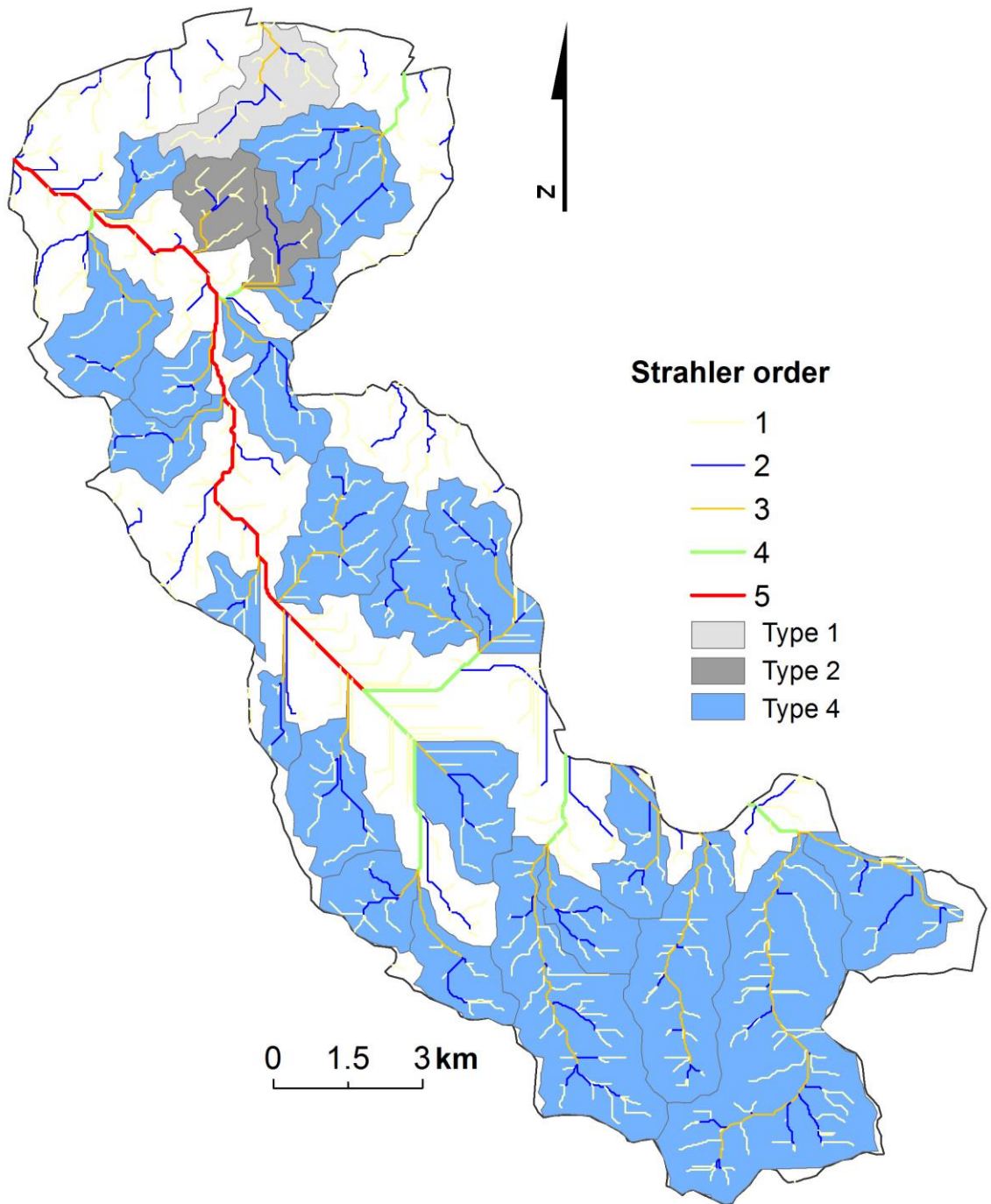


Figure 4-7. Spatial distribution of the types of slope angle - drainage density relationship in each study area.

Table 4-3. Characteristics of watersheds of different types in the Chishui area

Type	Mean slope (degrees)	Mean drainage density (km/km ²)	Mean height (m)
Type1	30.29	2.20	988.53
Type2	27.98	2.07	1019.74
Type3	33.13	2.11	1192.26
Type4	29.40	1.90	1184.19

4.1.4. Stream network structure and the watershed types

Basic Horton's parameters of stream-net structure were calculated for each watershed type in the Chishui area (Tables 4-4). The results of such calculation for Mt. Danxia and Mt. Longhu are not presented here because these areas almost completely consist of Type 4 watersheds, which eventually gave results very similar to all watersheds shown in Table 4-4. In the Chishui area, the Type 3 and Type 4 watersheds have larger values of the bifurcation ratio between the 2nd and 3rd order streams and larger values of the stream length ratio between the 1st and 2nd order streams than the Type 1 and Type 2 watersheds.

Table 4-4. Parameters of the stream-net structure in Chishui

Type	Stream order	Stream number	Bifurcation ratio	Total stream length (m)	Mean stream length (m)	Stream length ratio
1	1	51	5.10	20067.56	393.48	1.70
	2	10	2.50	6687.98	668.80	1.96
	3	4		5242.95	1310.74	
2	1	67	4.47	26070.14	389.11	1.80
	2	15	2.14	10478.96	698.60	1.87
	3	7		9141.28	1305.90	
3	1	104	4.33	34295.06	329.76	2.97
	2	24	3.43	23503.49	979.31	1.71
	3	7		11743.11	1677.59	
4	1	98	4.67	32107.46	327.63	3.09
	2	21	3.50	21285.47	1013.59	1.94
	3	6		11802.49	1967.082	

4.1.5. Hypsometric curves and the hypsometric integral

The distribution of HI values for the 24 watersheds in the Chishui area and the representative hypsometric curves are shown in Figure 4-8. The values were grouped into three classes according to the natural breaks method. HI ranges between 0.45 and 0.65 with a mean of 0.56. Approximately 90% of the watersheds have $HI > 0.5$. The distribution of HI looks complex but watersheds with $HI > 0.59$ tend to occur in the downstream areas.

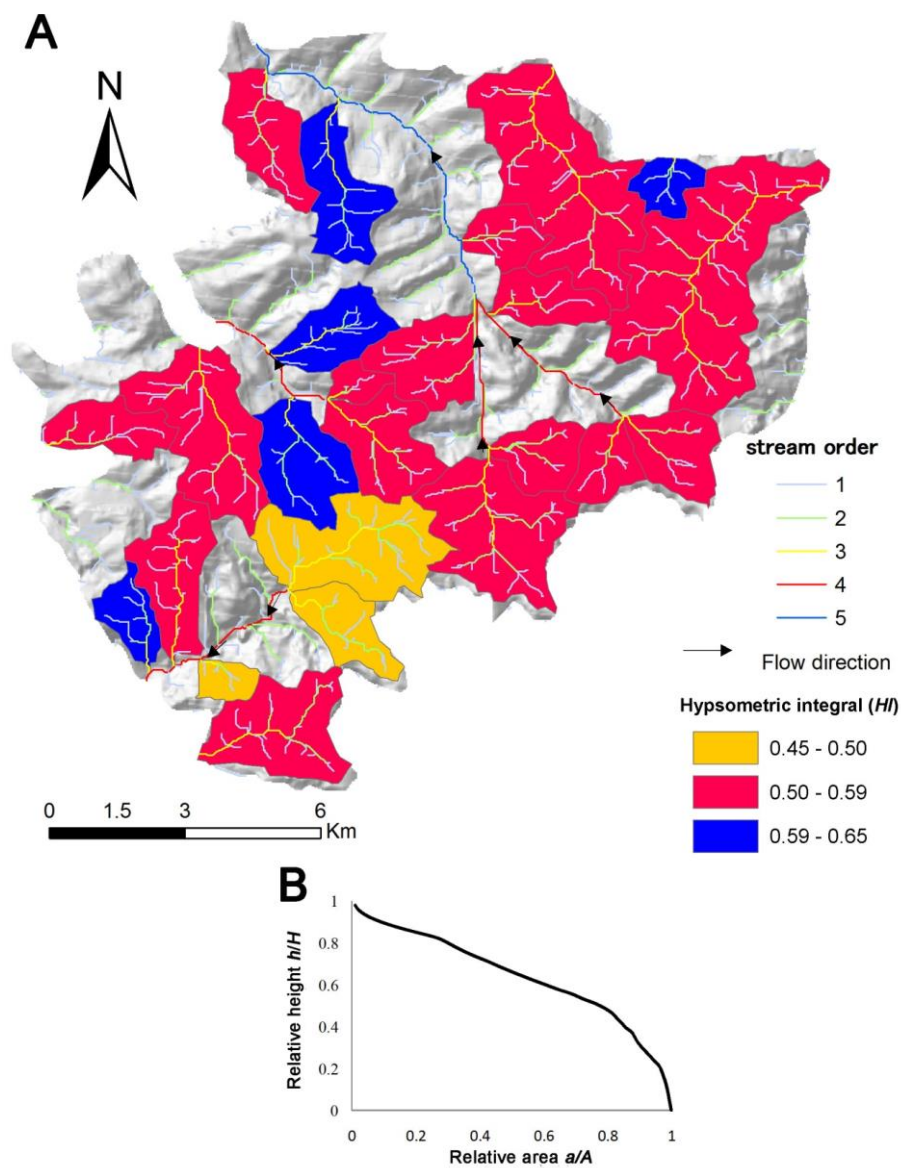


Figure 4-8. Distribution of hypsometric integral (HI) values and a representative hypsometric curve in the Chishui area.

The HI values obtained for the 42 watersheds in Mt. Danxia and some representative hypsometric curves are shown in Figure 4-9. HI ranges between 0.21 and 0.57 with a mean of 0.32. HI values can be grouped into three classes with respect to the convexity or concavity of the hypsometric curve: class 1 with concave curves ($HI < 0.3$), class 2 with S-shaped curves ($0.3 \leq HI < 0.4$), and class 3 with S-shaped curves ($HI \geq 0.4$). The hypsometric curves and HI values for the western and eastern sides of Mt. Danxia display a marked difference. Watersheds with concave hypsometric curves and lower HI , representing a more mature topography, are located mostly on the western side, whereas watersheds with S-shaped curves and higher HI with a less mature topography are mostly located on the eastern side. Because the population of HI values is not normally distributed, we used the Kolmogorov–Smirnov nonparametric test method to evaluate the difference between the HI values of the western and eastern sides (Davis, 1986; Snyder et al. 2003). The result shows that the difference is statistically significant ($D = 0.7778$, $p = 0.008$) (Table 4-5).

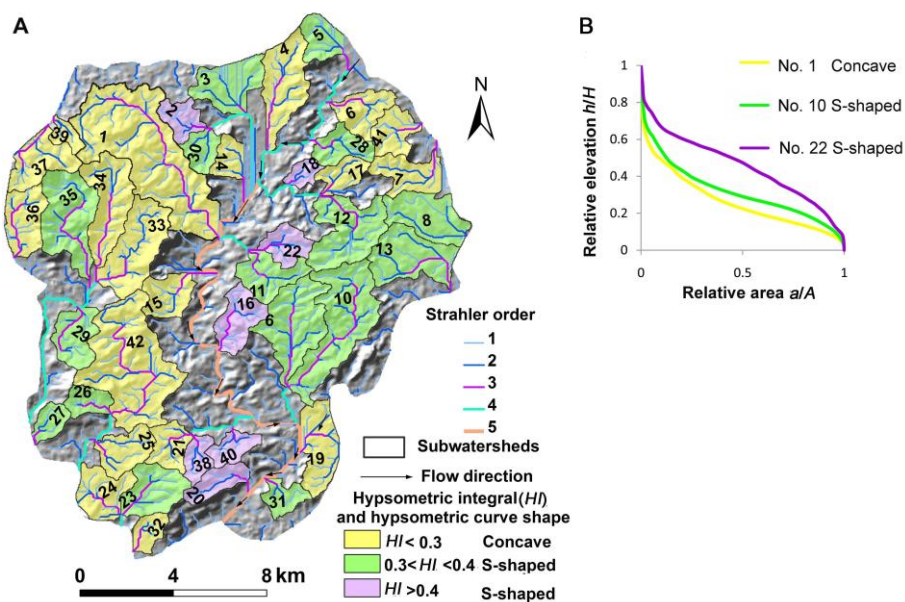


Figure 4-9. Map showing watersheds and streams in Mt. Danxia. Watersheds are numbered and classified according to their hypsometric integral (HI) values.

Table 4-5. Statistical differences and Kolmogorov–Smirnov test for *HI* values in the western and eastern sides of Mt. Danxia

	Western Side	Eastern Side
Number	26	16
Mean	0.29	0.38
Standard Deviation	0.082	0.092
Minimum	0.21	0.28
Maximum	0.50	0.57
Standard Error of Mean	0.016	0.023
Skewness	1.12	0.93
Kurtosis	1.04	0.21
<i>p</i> -Value	0.008	
<i>D</i>	0.7778	

Figure 4-10. shows the distribution of *HI* values for the two rock types, each of which occupies the largest area in each watershed. *HI* for the Danxia Formation is significantly larger than that for the Changba Formation (Kruskal–Wallis test; $p < 0.05$).

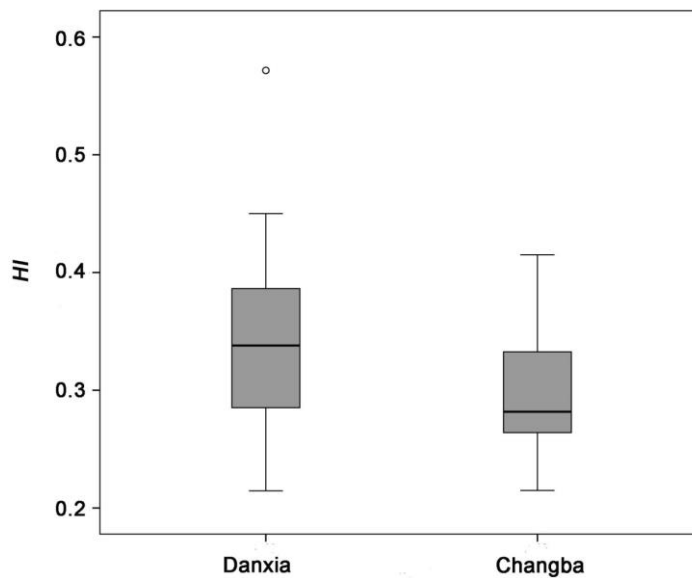


Figure 4-10. Box plots of *HI* for the two major rock types in Mt. Danxia.

The difference between the rock types is significant based on the Kruskal–Wallis test ($p < 0.05$).

The HI values for the 26 watersheds in Mt. Longhu and a representative hypsometric curve is shown in Figure 4-11. The values were grouped into three classes according to the natural breaks method. HI ranges between 0.17 and 0.45 with a mean of 0.29. Approximately 80% of the watersheds have $HI < 0.3$. Mt. Longhu is underlain by various units of rock formation. HI differs according to lithology. Figure 4-12 shows HI for the five rock types, each of which occupies the largest area in each watershed. The highest HI values correspond to the Elinghu Formation (J_3e) and the lowest values correspond to Quaternary sediments (Qh) (Figure 4-12). The Kruskal-Wallis test has shown that the difference shown in Figure 4-12 is statistically significant ($p < 0.001$).

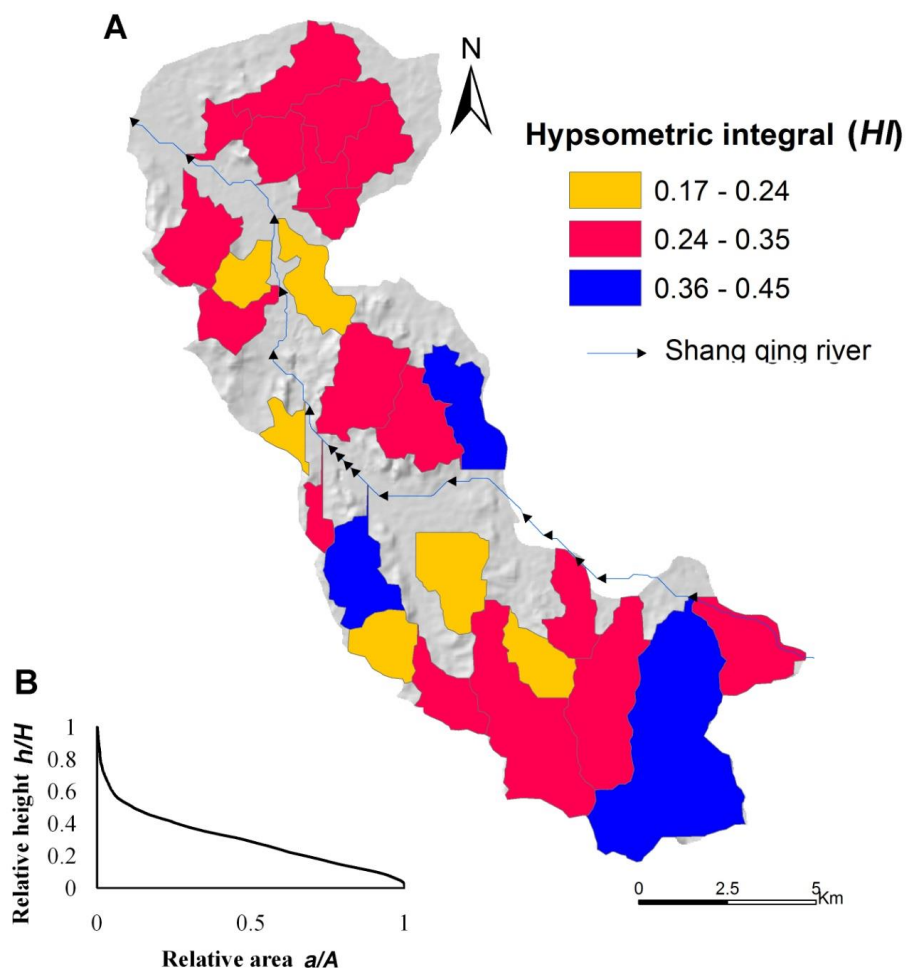


Figure 4-11. Map showing spatial distribution of hypsometric integral (HI) values and the shape of a hypsometric curve in Mt. Longhu.

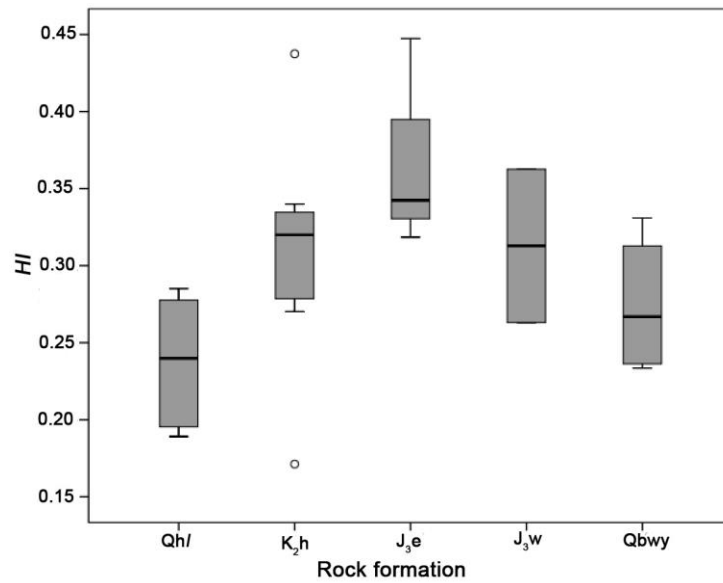


Figure 4-12. Box plots of *HI* for the five major rock types in Mt. Longhu. The difference between the rock types is significant based on the Kruskal–Wallis test ($p < 0.001$).

4.2. River longitudinal profiles

4.2.1. Stream length gradient (*SL*) index and Hack profiles

The *SL* values for the Chishui area range from 0 to 2895.1 m, with a mean of 288.4 m and a standard deviation of 316.9 m. The majority of the study reaches (80%) show *SL* smaller than 700 m. The values were grouped into four classes according to the size of the standard deviation: 0–129, 129–446, 447–764, 765–1083 and >1083 m (Figure 4-13). The classes of *SL* >1083 m can be regarded as anomalously high because they only appear in 6.7% of all reaches. They are often found in the lowermost reaches in a watershed. As shown in Figure 4-13, distinct waterfall-type knickpoints are often observed, and they correspond to the locally high *SL* values.

The *K* values for the Chishui area are from 56 to 106 with a mean of 80.6. Figure 4-14 shows the distribution of *K* for each watershed. Watersheds with the highest *K* values occur in downstream areas of two major rivers, at the northwestern and southwestern parts of the

Chishui area. Watersheds with lower K values tend to occur in the central part.

We also investigated the relationships between the watershed slope gradient, relative relief, HI , mean SL and K computed for each watershed (Figure 4-15). SL and K have significant positive linear correlations with relative relief and a weak negative linear correlation with slope gradient (Figures 4-15 A, B, D, E), but not with HI (Figures 4-15 C, F).

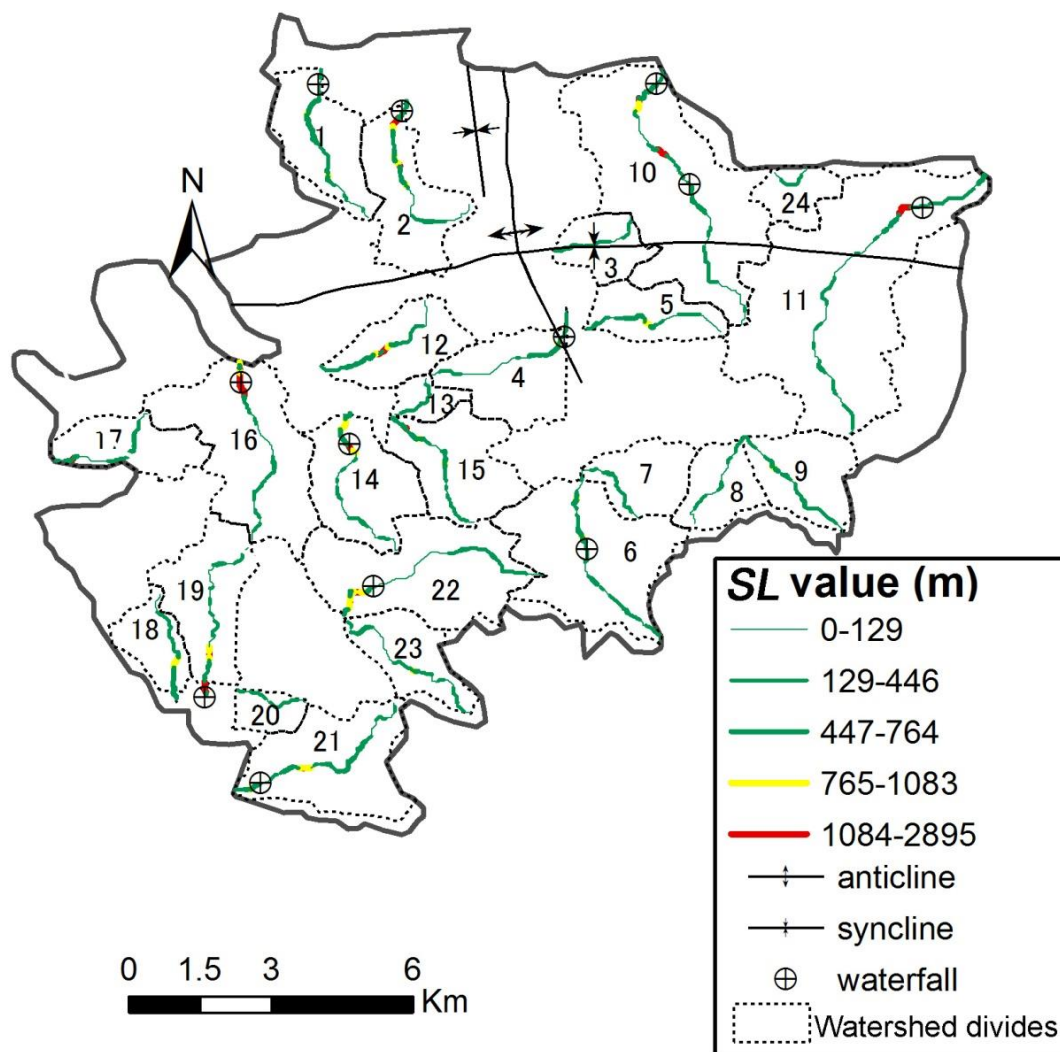


Figure 4-13. Spatial distribution of SL along the main stream of each watershed in the Chishui area.

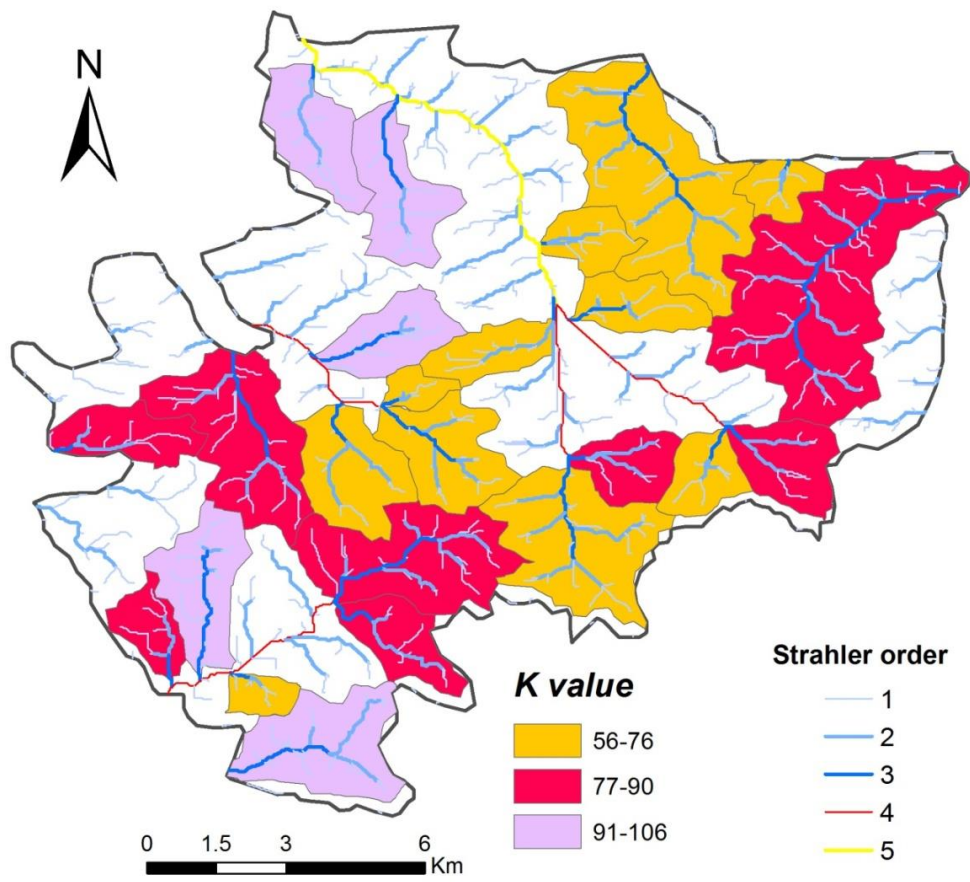


Figure 4-14. Spatial distribution of K for each watershed in the Chishui area.

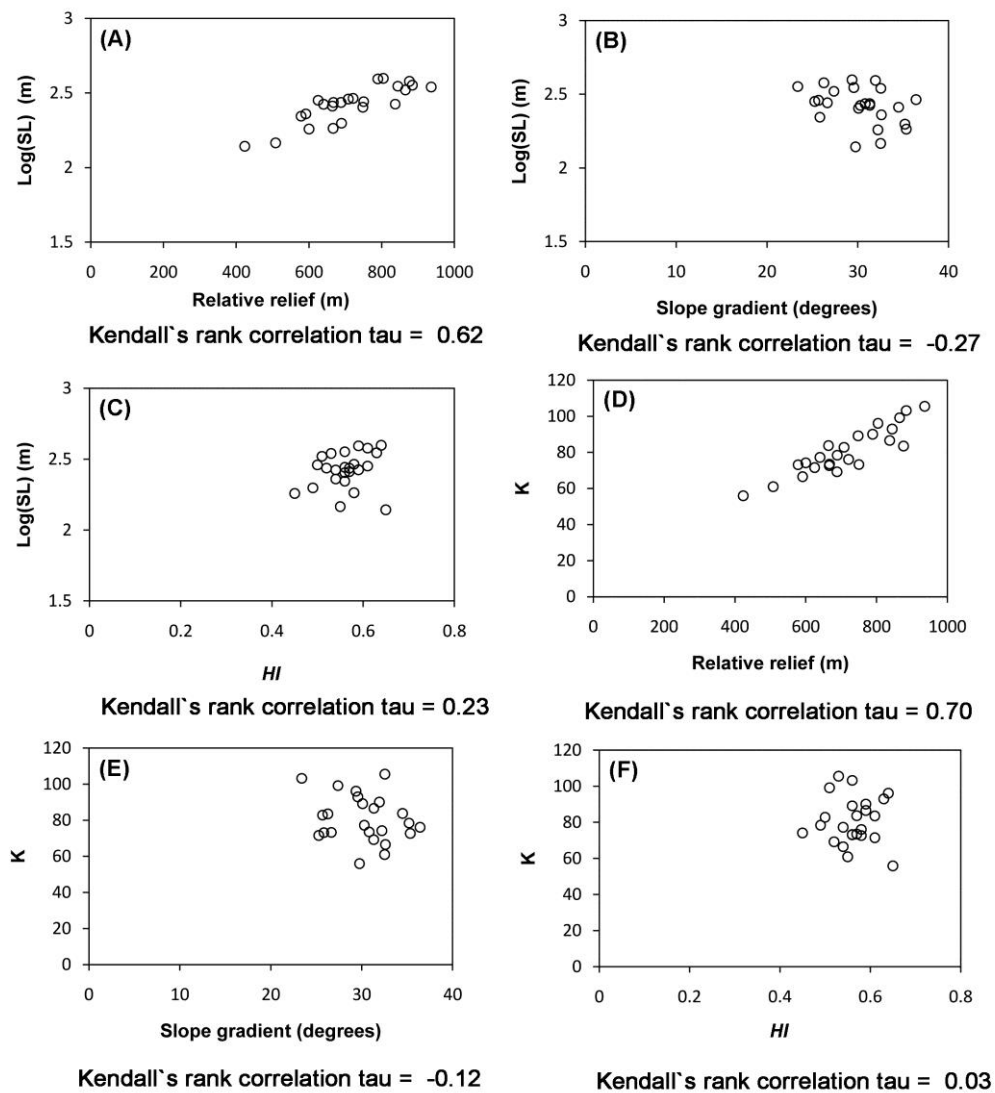


Figure 4-15. Relationships of SL and K with topographic indices for Chishui area.

- (A) SL versus relative relief, (B) SL versus slope gradient, (C) SL versus HI ,
 (D) K versus relative relief, (E) K versus slope gradient, (F) K versus HI .

The measured SL values for the watersheds in Mt. Danxia range from 0.2 to 992.7 m, with a mean of 66.7 m and a standard deviation of 94.9 m. The majority of the study reaches (80%) show SL smaller than 100 m. The values were grouped into four classes according to the size of the standard deviation: 0–100, 101–250, 251–350, and >351 m

(Figure 4-16). The classes of $SL > 250$ m can be regarded as anomalously high because they only appear in 3.1% of all reaches. They are often found in the lowermost reaches in a watershed (Figure 4-16). A Kruskal-Wallis test confirmed differences in SL according to the types of lithology found along the rivers: the Danxia Formation has the highest SL values and the Quaternary sediments have the lowest values (Figure 4-17).

However, the average SL value for the western side (70.7 m) is slightly larger than that for the eastern side (52.7 m), although the areal ratio of the Changba Formation to the Danxia Formation is apparently higher on the western side (Figure 2-6). The difference in the average SL between the western and eastern sides is statistically significant according to the Kolmogorov–Smirnov test ($D = 0.1128$, $p = 0.001$).

The K values for Mt. Danxia are between 11 and 47 with a mean of 27.0. Figure 4-18 shows the distribution of K for each watershed. Watersheds with the higher K values occur more in the western side.

Most major rivers in the eastern side show less convex Hack profiles with average K value (25.0) than western side with average K value (28.3) (Figure 4-19). In addition, some locally high SL values correspond to faults, rather than rock boundaries, e.g., Watersheds 4 (F6), 23 (F13), 26 (F18), and 33 (F4 and F17) of the western side (Figures. 4-16 and 4-19).

The average values of relative relief and slope gradient for the western side (303.9 m, 11.03°) are slightly larger than those for the eastern side (265.2 m, 10.7°), which corresponds to the higher SL and K values in the western side. To examine such correspondences, we investigated the relationship between the slope gradient, relative relief, HI , SL and K (Figure 4-20). SL and K have significant linear correlations with relative relief and slope gradient (Figures 4-20A, B, D, E), but not with HI (Figures 4-20C, F).

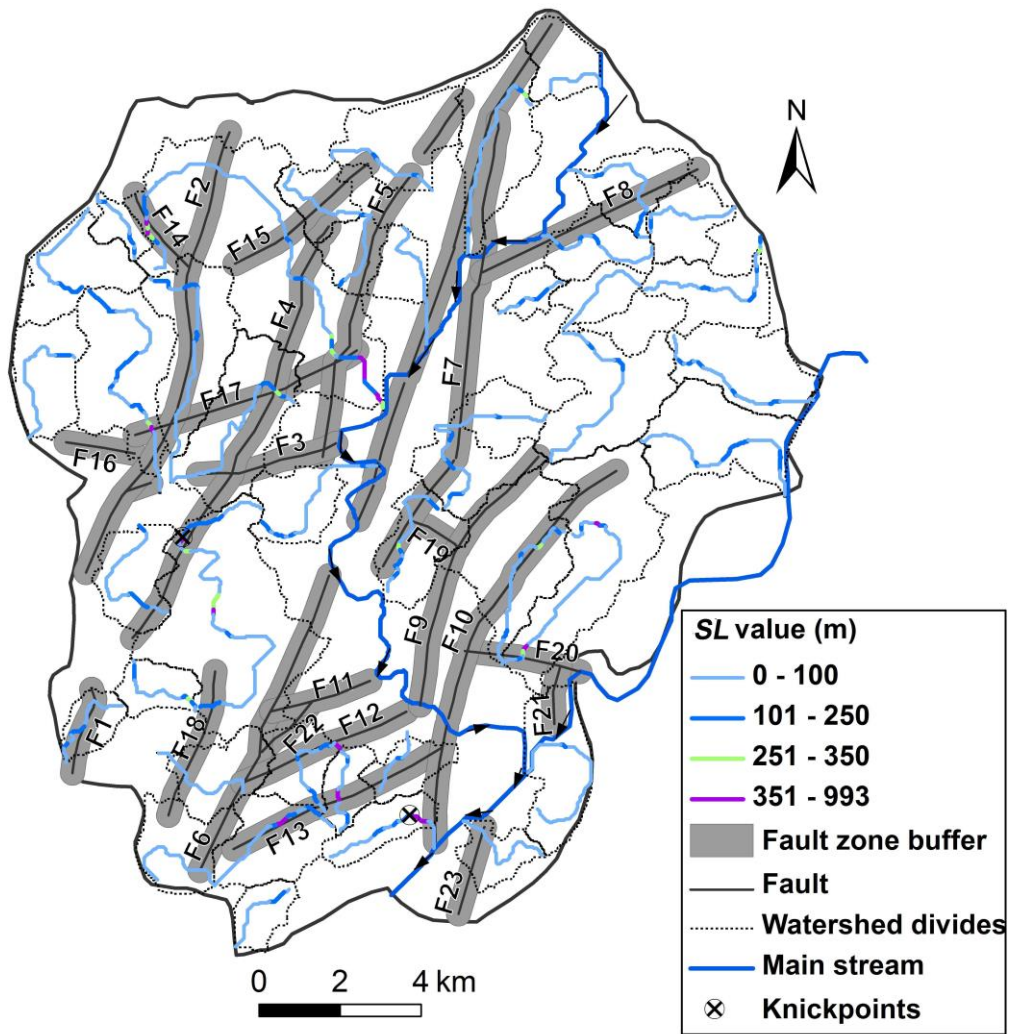


Figure 4-16. Spatial distribution of *SL* along the tributaries of the main stream (Jinjiang and Zhenjiang rivers) in Mt. Danxia and showing faults buffers along the faults and watershed divides.

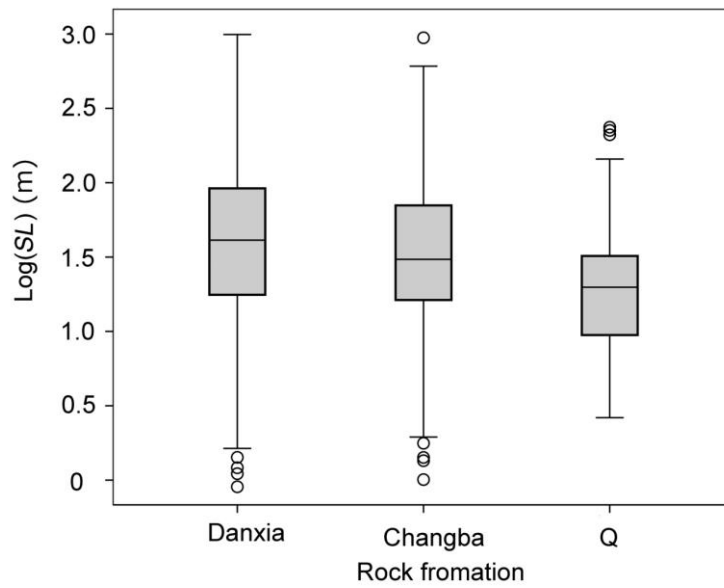


Figure 4-17. Box plots of logarithmic values of SL for the three major rock types in Mt. Danxia. The difference between the rock types is significant based on the Kruskal-Wallis test ($p < 0.001$).

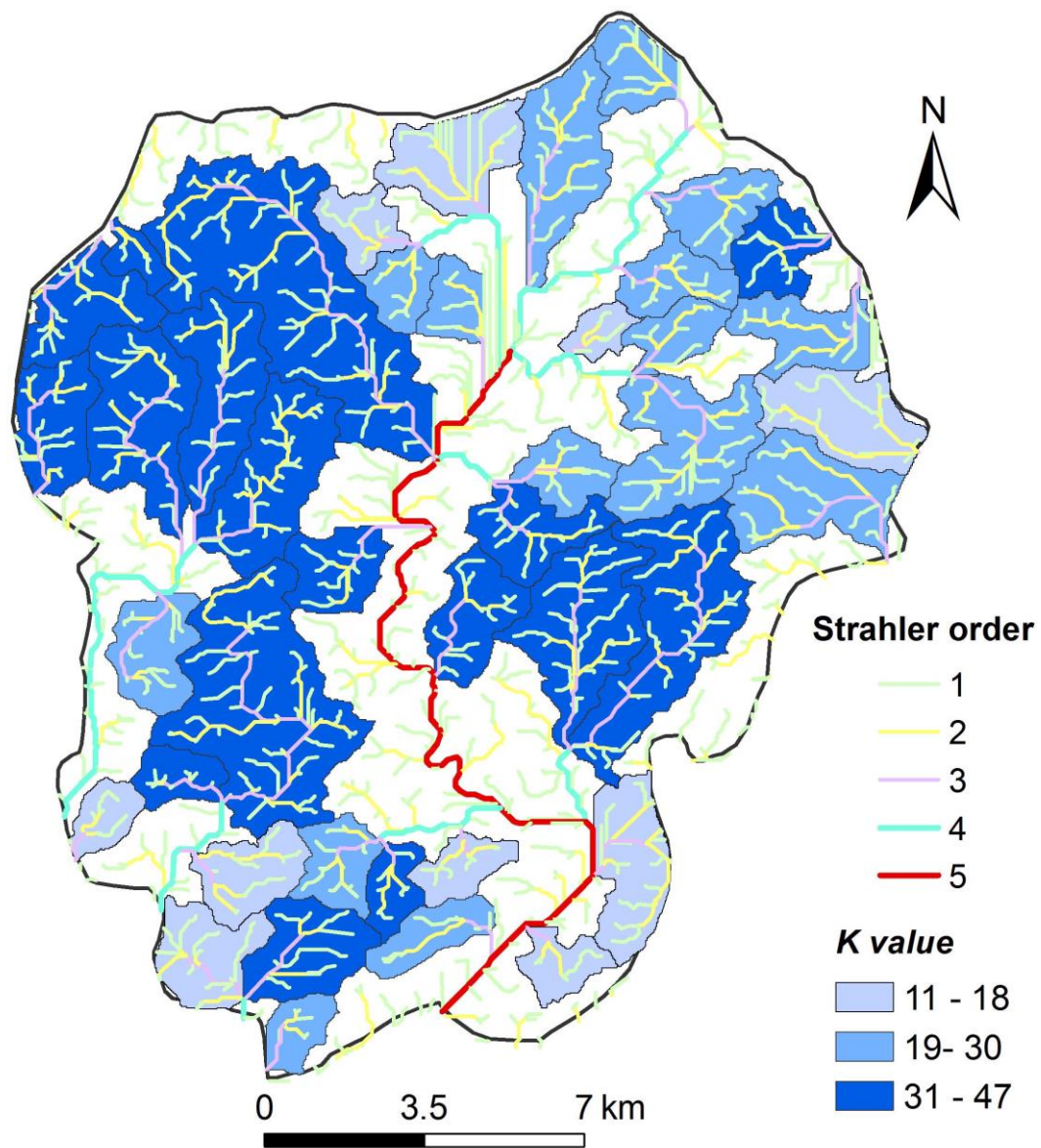


Figure 4-18. Spatial distribution of K for each watershed in Mt. Danxia.

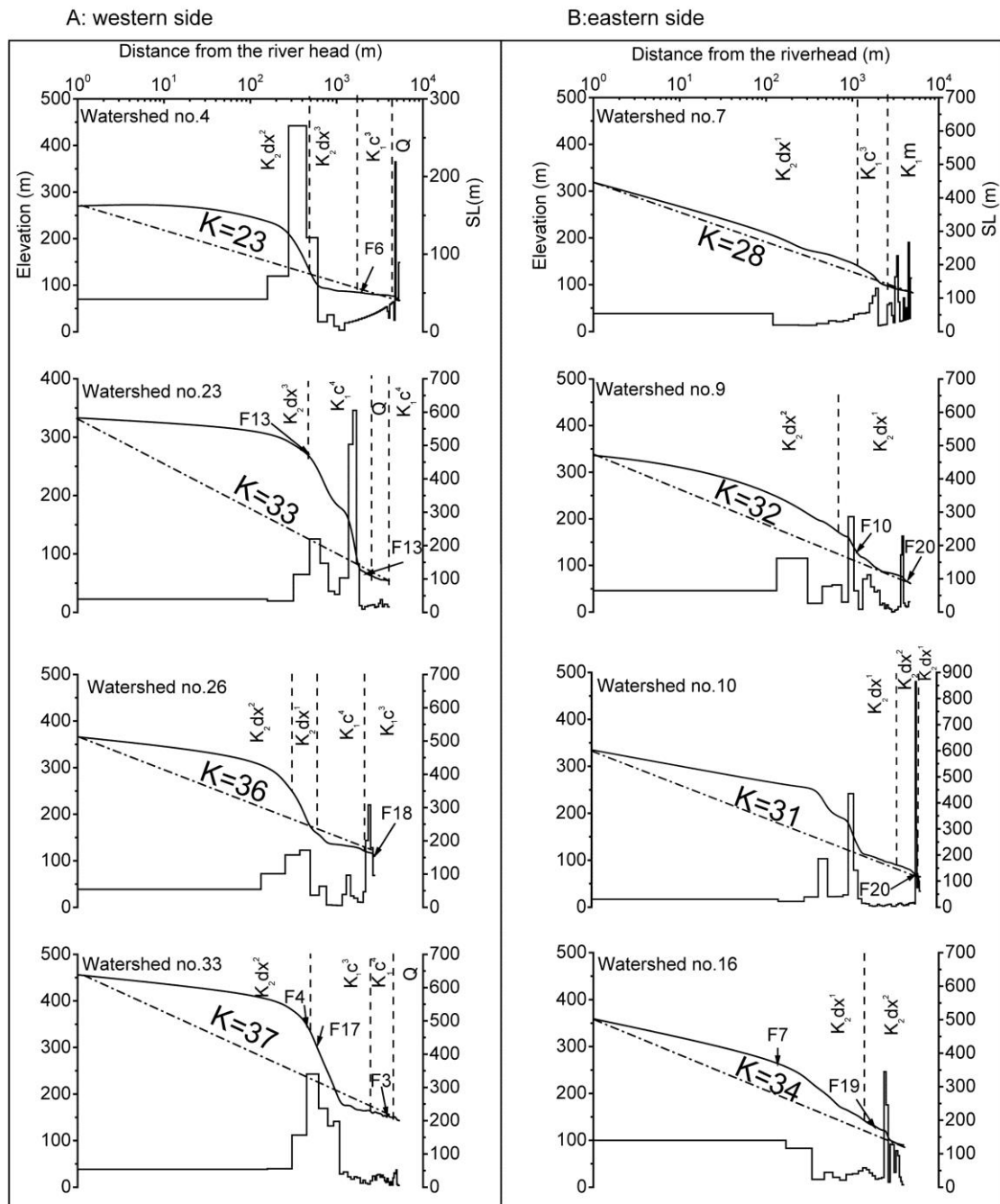


Figure 4-19. Examples of Hack profiles (semi-log plot of distance versus elevation along a river) in the western side (A) and the eastern side (B) with step SL curves and overall K values. The dashed line shows the equilibrium profile of each tributary. Fault numbers such as F6 correspond to those in Figure 2-6. Vertical dotted lines show rock boundaries; see Figure 2-6 for rock formation symbols.

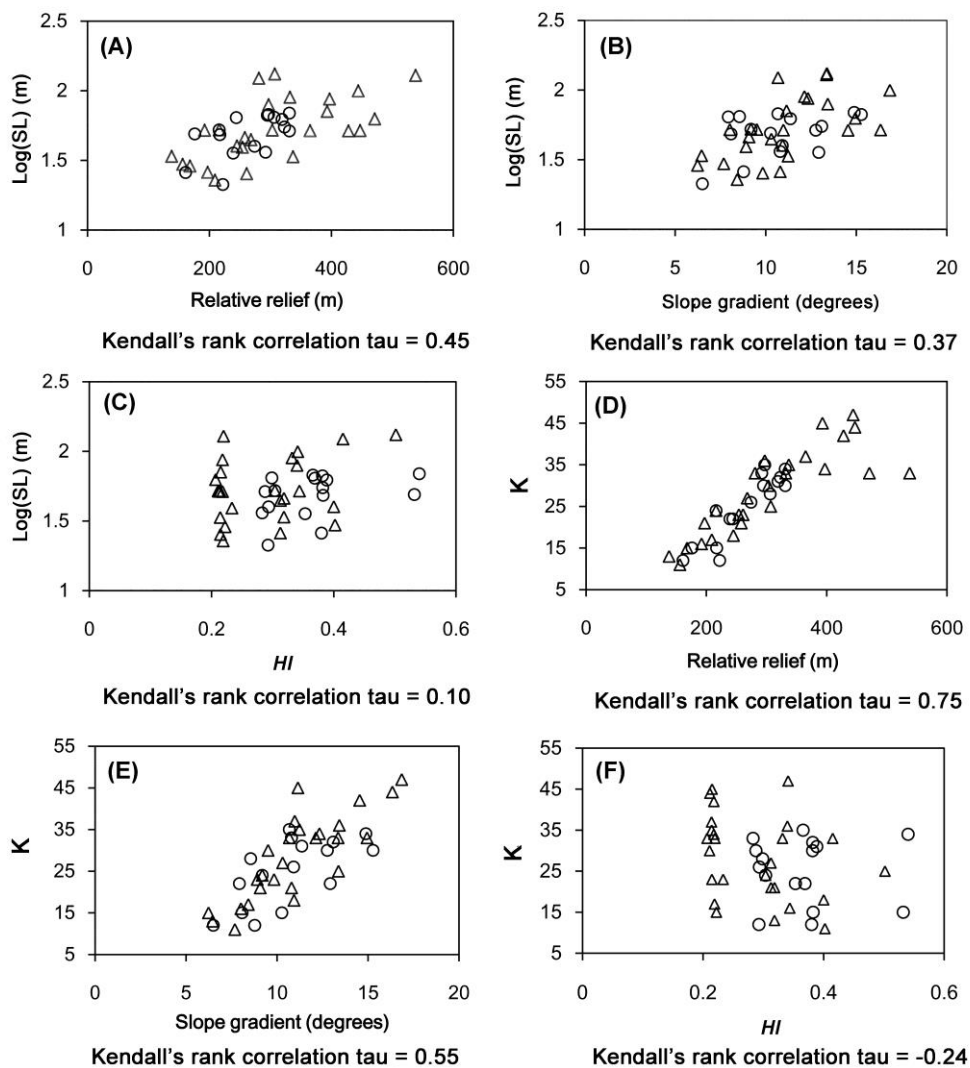


Figure 4-20. Relationships of SL and K with topographic indices for Mt. Danxia. (A) SL versus relative relief, (B) SL versus slope gradient, (C) SL versus HI , (D) K versus relative relief, (E) K versus slope gradient, (F) K versus HI . Triangles: western side; Circles: eastern side

The measured SL values for the watersheds in Mt. Longhu range from 0 to 760.1 m, with a mean of 80.8 m and a standard deviation of 123.7 m. The majority of the study reaches (78%) show SL smaller than 100 m. The values were grouped into four classes according to the size of the standard deviation: 0–19, 20–142, 143–266, and >266 m (Figure 4-21). The classes of SL >266 m can be regarded as anomalously high because they

only appear in 9% of all reaches. They are often found in the lowermost reaches in a watershed (Figure 4-21).

SL differs according to lithology. Figure 4-22 summarizes *SL* values for the major rock types observed along river reaches in Mt. Longhu: Quaternary (Qh), Upper Cretaceous (K_{2h}), Low Cretaceous (K_{1s}, K_{1z}, J_{3e}, J_{3d}), Upper Jurassic (J_{3w}, J_{3r}), Middle Jurassic (J_{2z}), Triassic (T_{3m}) to Precambrian (Tonian) (Qbwy) rocks. The order of the mean or modal *SL* values approximately corresponds to rock resistance, and the Kruskal-Wallis test has shown that the difference is statistically significant ($p < 0.001$).

The *K* values for Mt. Longhu are between 3 and 103 with a mean of 24.4. Figure 4-23 shows the distribution of *K* for each watershed. Watersheds with the higher *K* values occur exclusively in the uppermost area.

The relationships between the slope gradient, relative relief, *HI*, *SL* and *K* were also investigated (Figure 4-24). *SL* and *K* have significant linear correlations with relative relief and slope gradient (Figures 4-24A, B, D, E), but not with *HI* (Figures 4-24 6C, F).

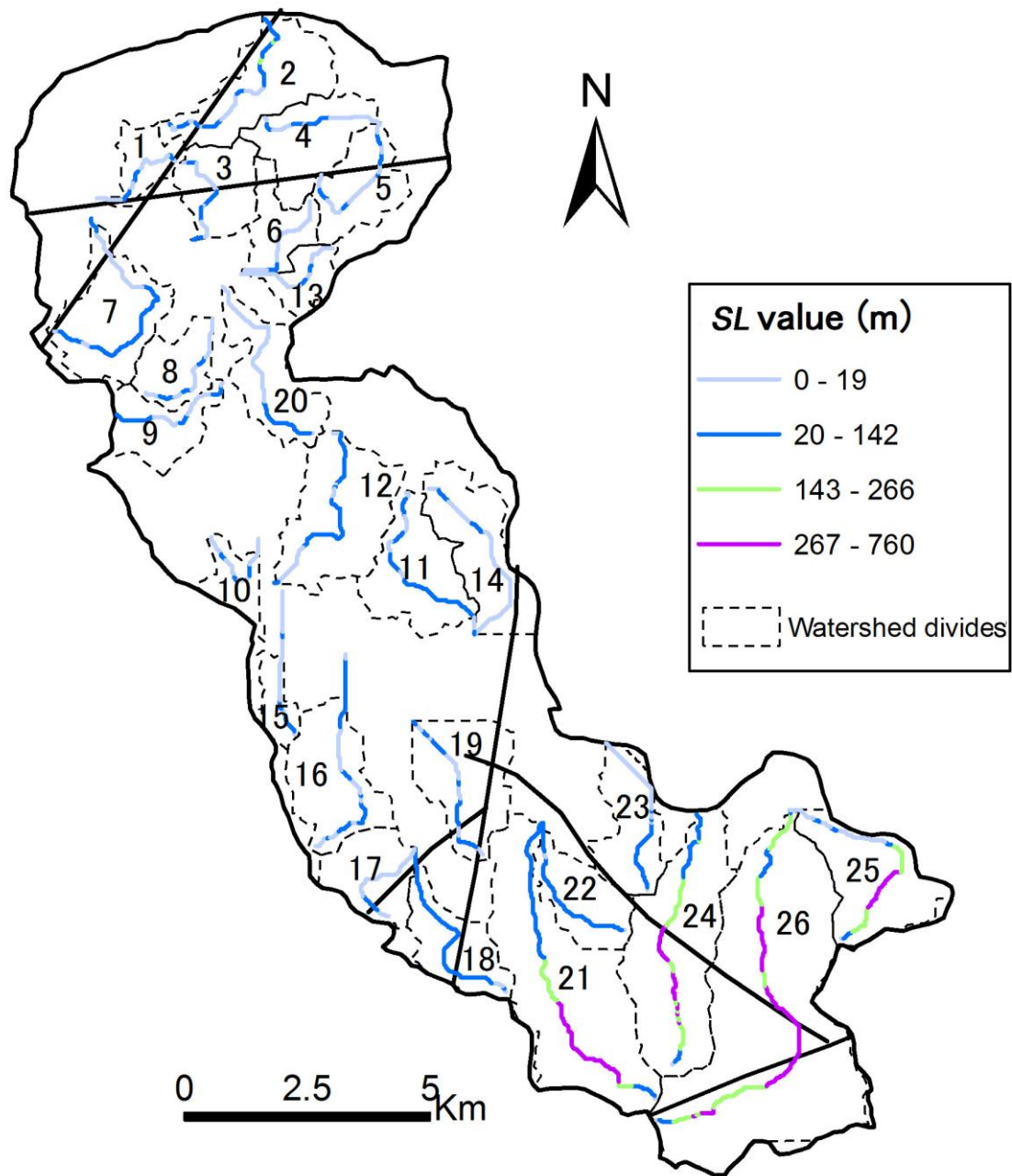


Figure 4-21. Distribution of *SL* along the main stream of each watershed in Mt. Longhu.

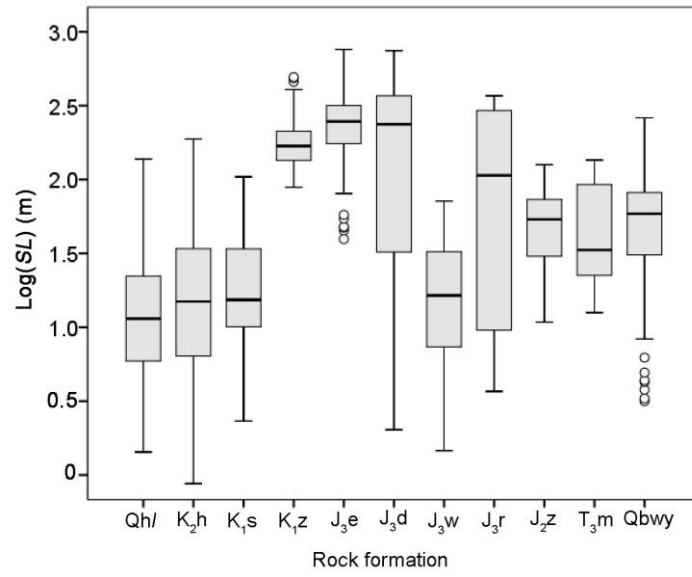


Figure 4-22. Box plots of logarithmic values of SL for the eleven major rock types in Mt. Longhu. The difference between the rock types is significant based on the Kruskal-Wallis test ($p < 0.001$).

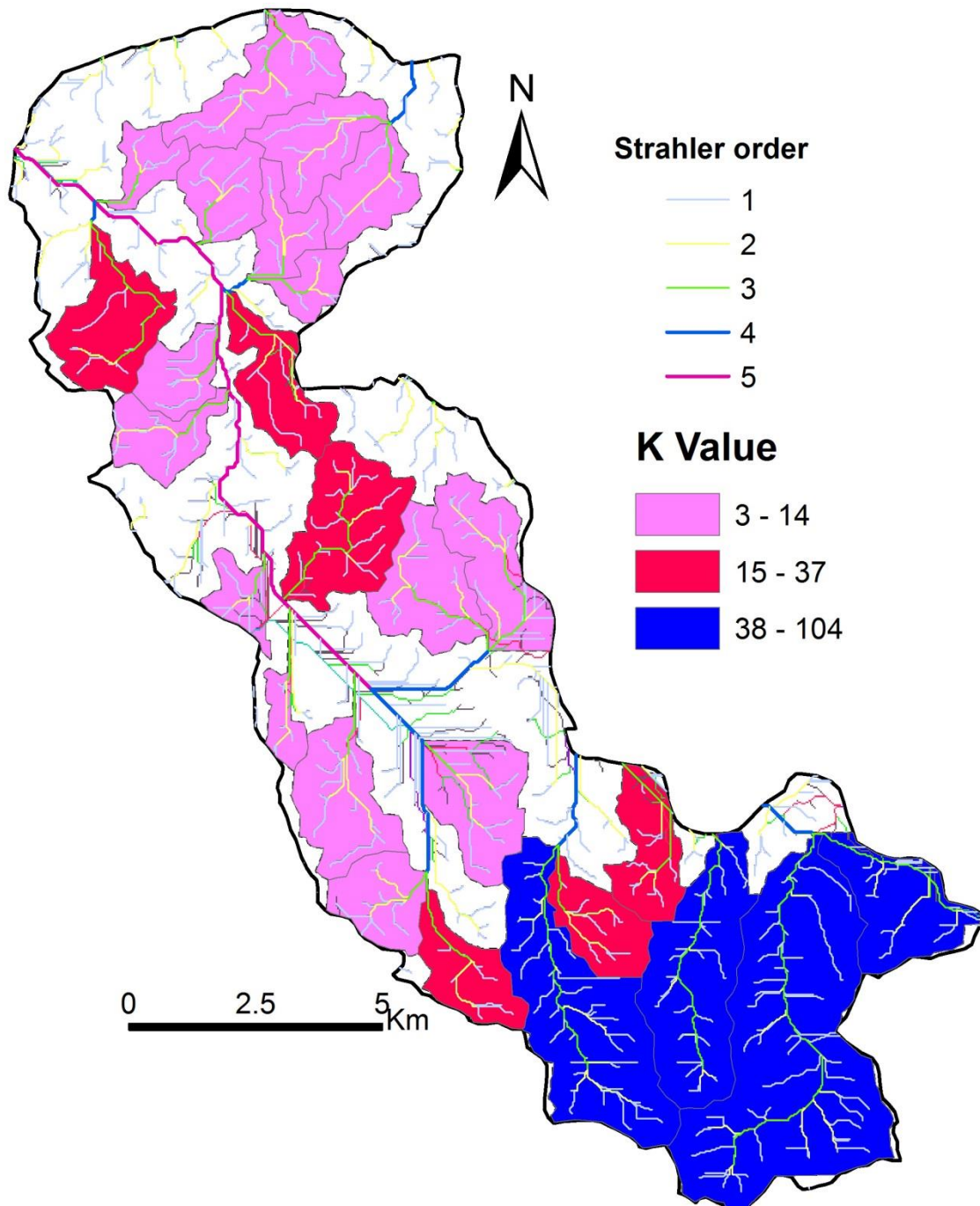


Figure 4-23. Spatial distribution of K of each watershed in Mt. Longhu.

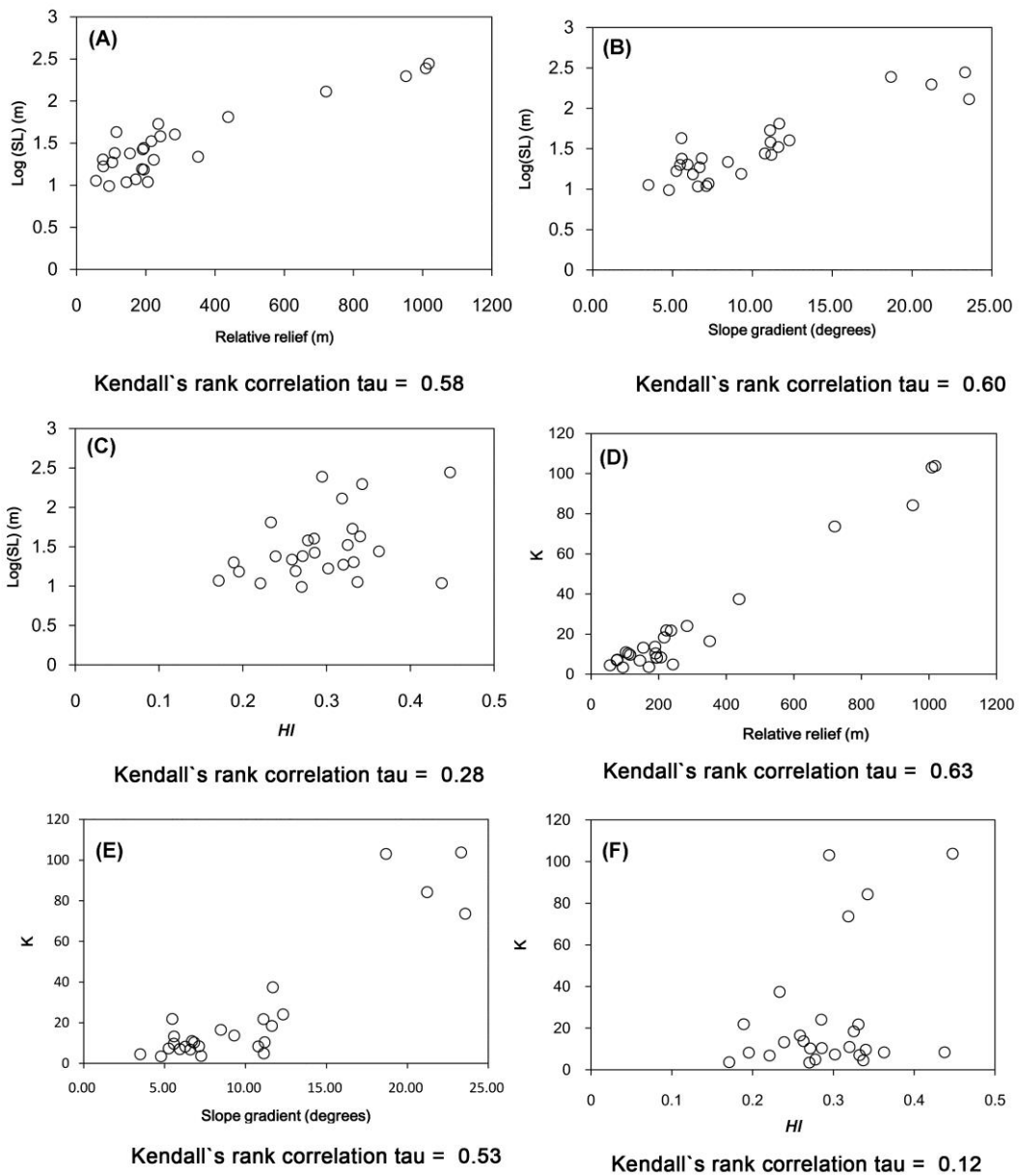


Figure 4-24. Relationships of *SL* and *K* with topographic indices for Mt. Longhu. (A) *SL* versus relative relief, (B) *SL* versus slope gradient, (C) *SL* versus *HI*, (D) *K* versus relative relief, (E) *K* versus slope gradient, (F) *K* versus *HI*.

4.2.2. Distribution and characteristics of knickzones and the anomalous points

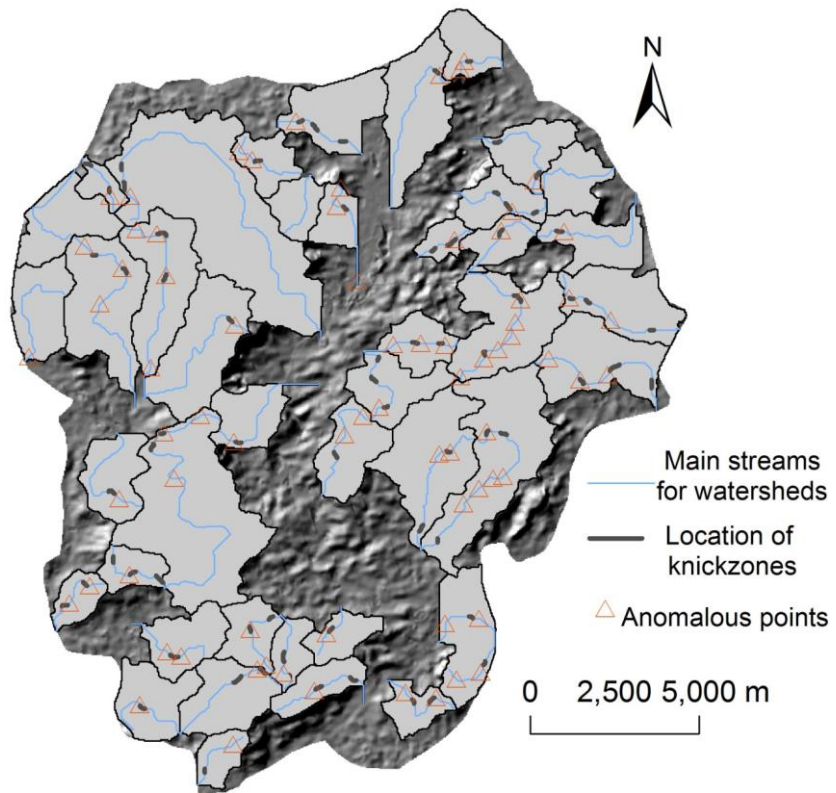
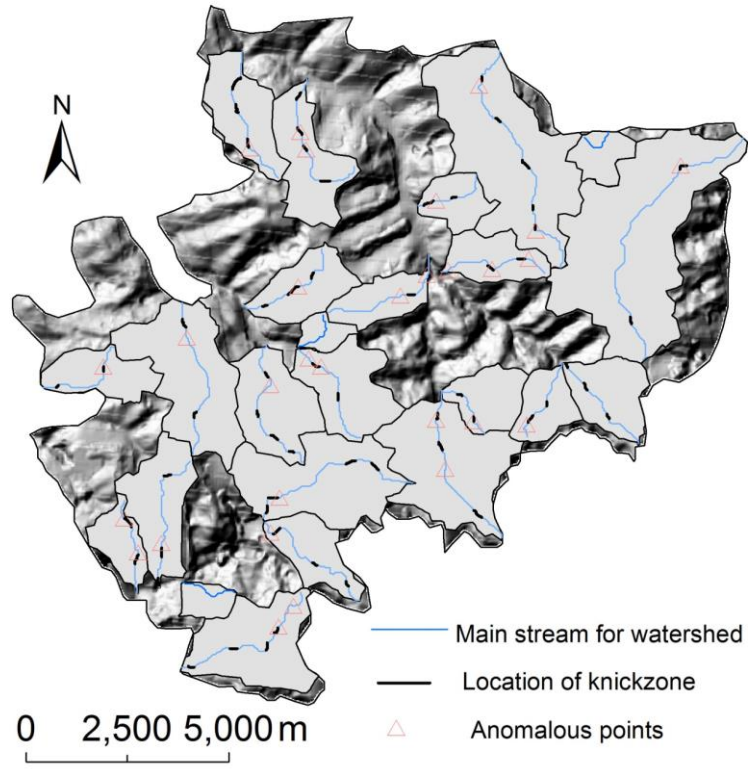
In the Chishui area, 56 knickzones were extracted, with the knickzone frequency and knickzone density of 0.67/km and 12.7%, respectively. In Mt. Danxia, 73 knickzones were extracted, with their frequency and density being 0.36/km and 5.6%. In Mt. Longhu, 45 knickzones were extracted with their frequency and knickzone density being 0.33/km and 6.1%, respectively.

Parameters that represent the shape of the knickzone: height, length, mean gradient and R_d were also calculated. Statistical values of these form parameters were summarized in Table 4-6. It is clear that knickzones in the Chishui area tend to be taller and steeper than those in the other two areas, whereas knickzone length does not differ significantly among the three areas.

Figure 4-25 shows the locations of knickzones and anomalous points. The location of ca. 70% of the identified anomalous points correspond to those of knickzones.

Table 4-6. General properties of knickzone forms in Chishui, Mt. Danxia and Mt. Longhu.

		Height (m)	Length (m)	Gradient (m/m)	R_d (m^{-1})
CHISHUI	Mean	74.9	184.4	0.412	2.10E-04
	Standard deviation	39.6	58.2	0.189	1.11E-04
	Maximum	215.0	360.0	1.100	5.03E-04
	Minimum	16.0	120.0	0.089	3.91E-05
DANXIA	Mean	25.9	162.7	0.164	1.02E-04
	Standard deviation	21.9	44.9	0.141	1.11E-04
	Maximum	99.0	300.0	0.700	7.29E-04
	Minimum	5.0	120.0	0.028	-6.82E-06
LONGHU	Mean	26.4	185.1	0.131	5.18E-05
	Standard deviation	28.8	43.9	0.123	1.92E-05
	Maximum	139.0	300.0	0.579	1.02E-04
	Minimum	5.0	120.0	0.028	2.16E-05



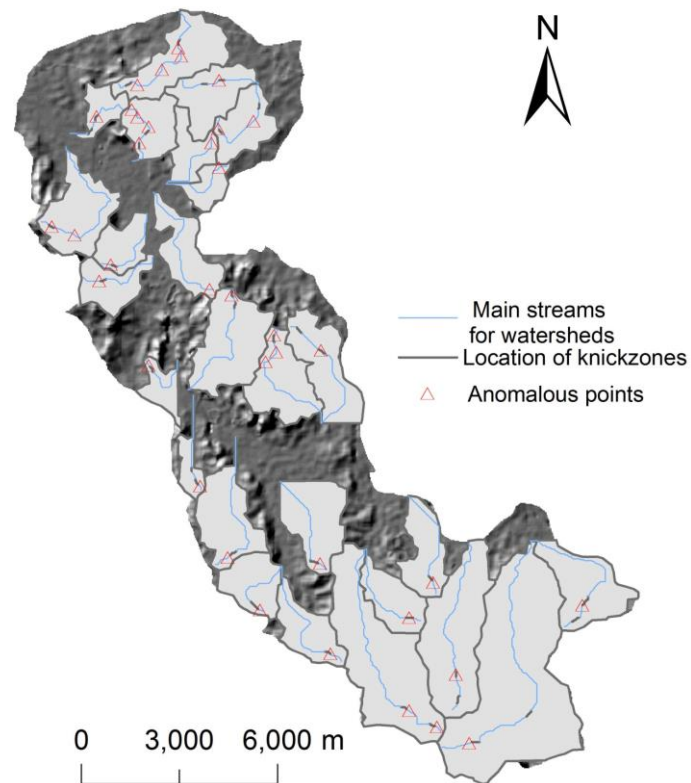


Figure 4-25. Spatial distribution of knickzones and anomalous points in each study area.

The height, length, gradient, and relative steepness of each knickzone were examined in relation to the upstream distance, normalized upstream distance, and drainage area (Figures 4-26 – 34). The results show that small knickzones can occur anywhere along the rivers, whereas large knickzones >80 m in height or >250 m in length, are concentrated in upper reaches. The knickzone gradient and R_d also tend to decrease with increasing upstream distance, normalized upstream distance, and drainage area.

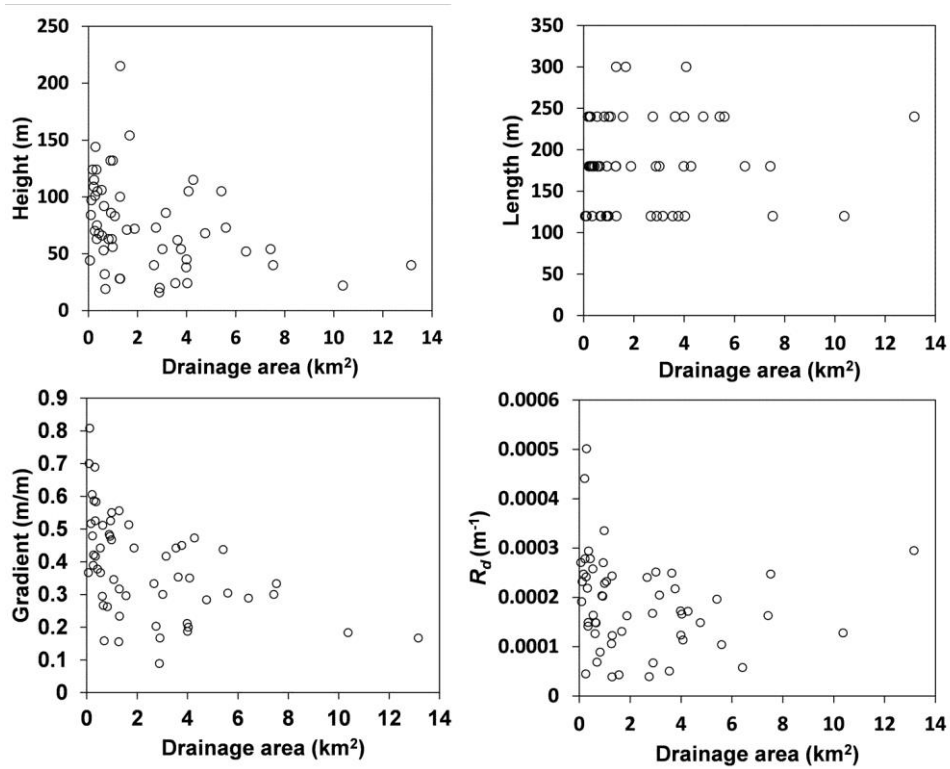


Figure 4-26. Relationships between form parameters of knickzones and drainage area in the Chishui area.

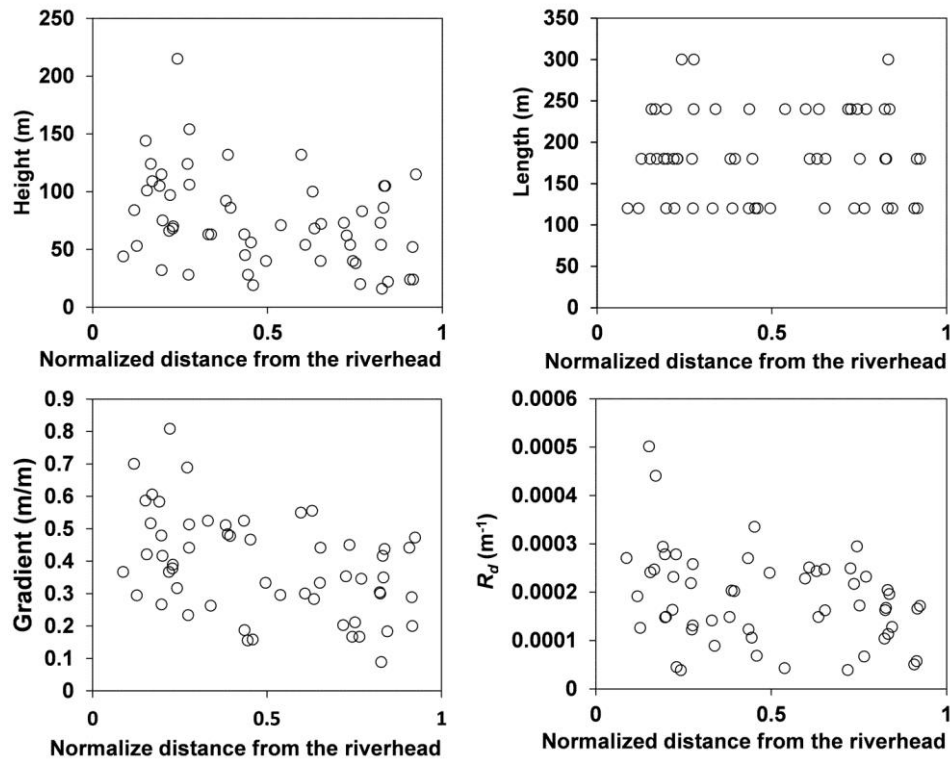


Figure 4-27. Relationships between form parameters of knickzones and normalized distance from the riverhead in the Chishui area.

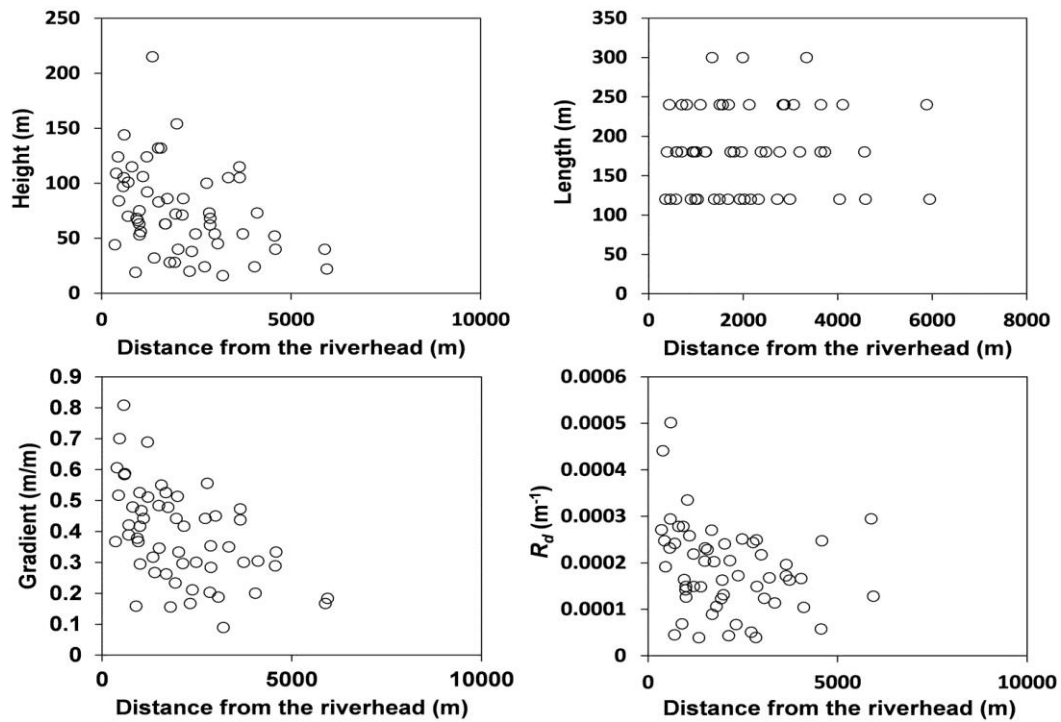


Figure 4-28. Relationships between form parameters of knickzones and distance from the riverhead in the Chishui area.

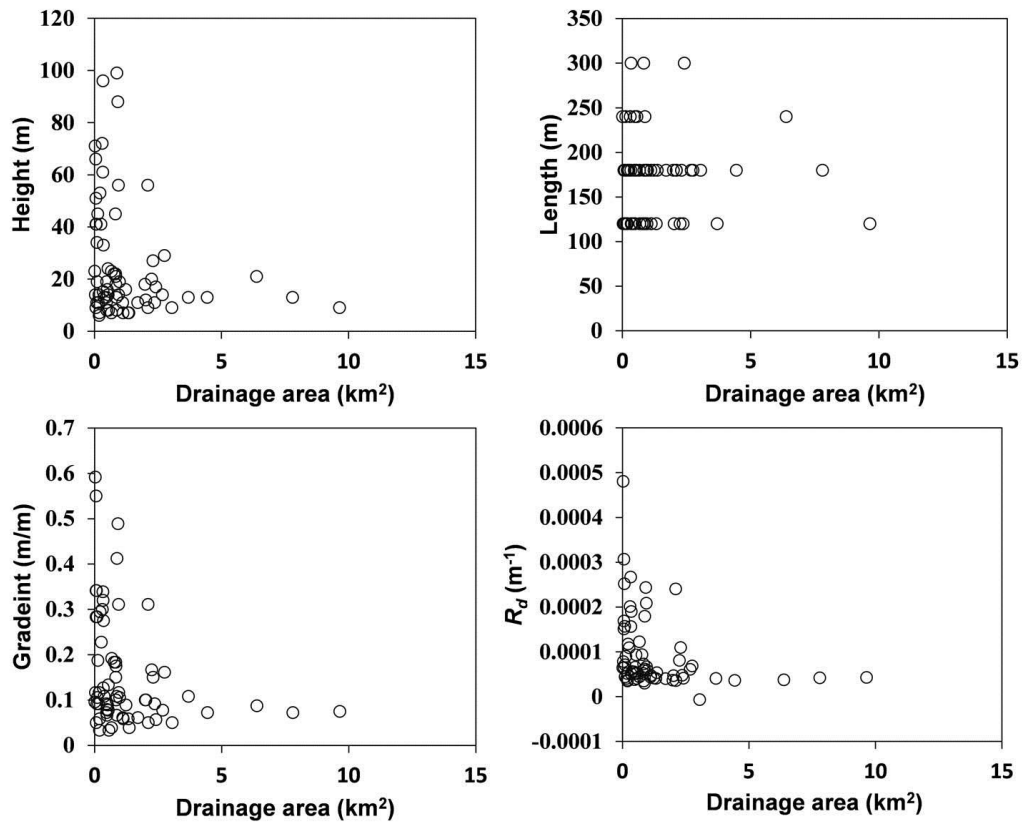


Figure 4-29. Relationships between form parameters of knickzones and drainage area in Mt. Danxia.

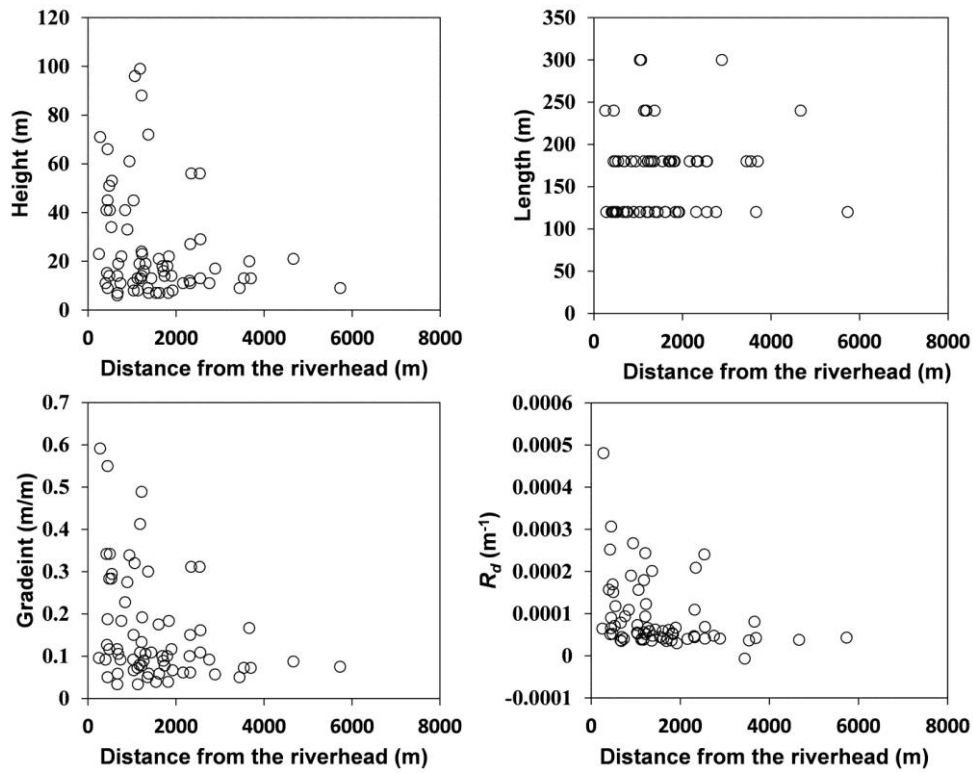


Figure 4-30. Relationships between form parameters of knickzones and distance from the riverhead in Mt. Danxia.

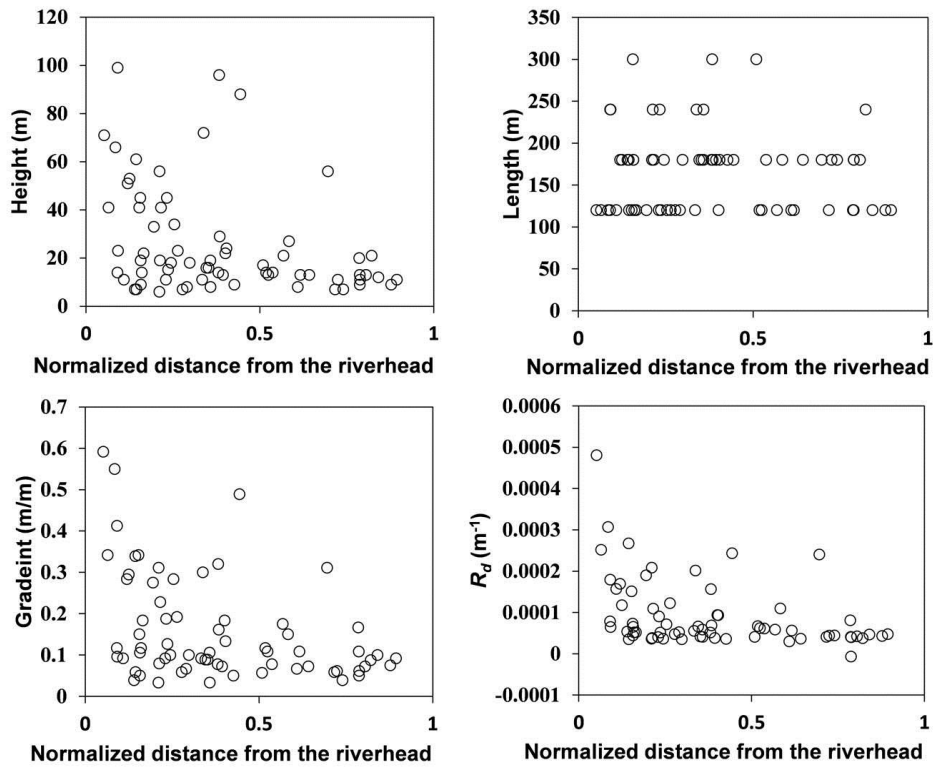


Figure 4-31. Relationships between form parameters of knickzones and normalized distance from the riverhead in Mt. Danxia.

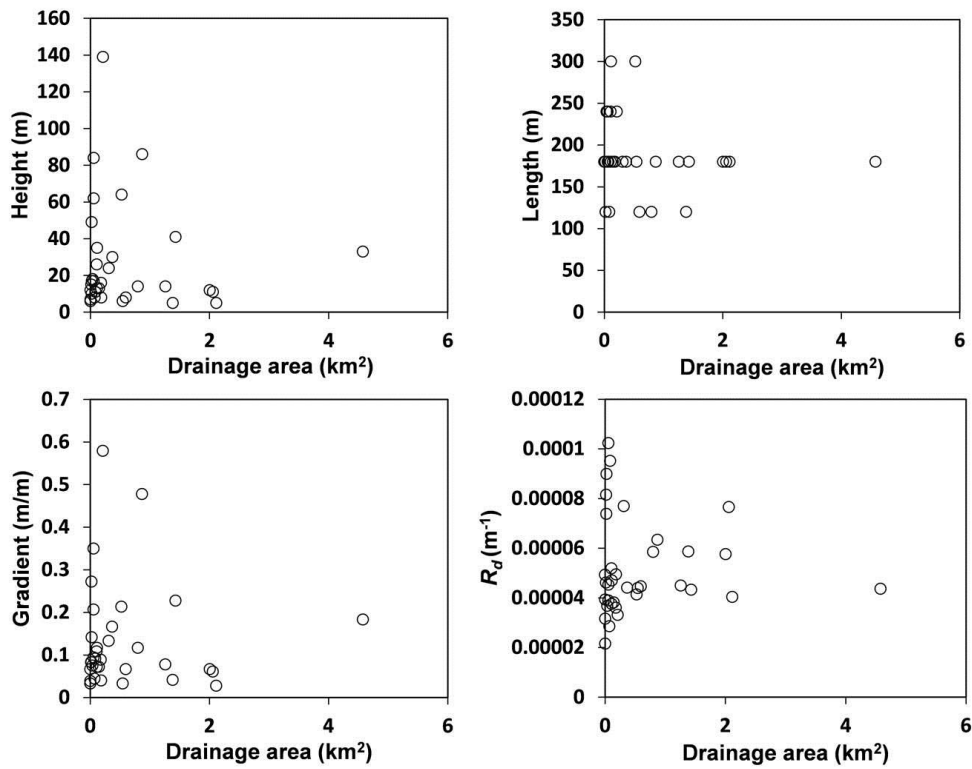


Figure 4-32. Relationships between form parameters of knickzones and drainage area in Mt. Longhu.

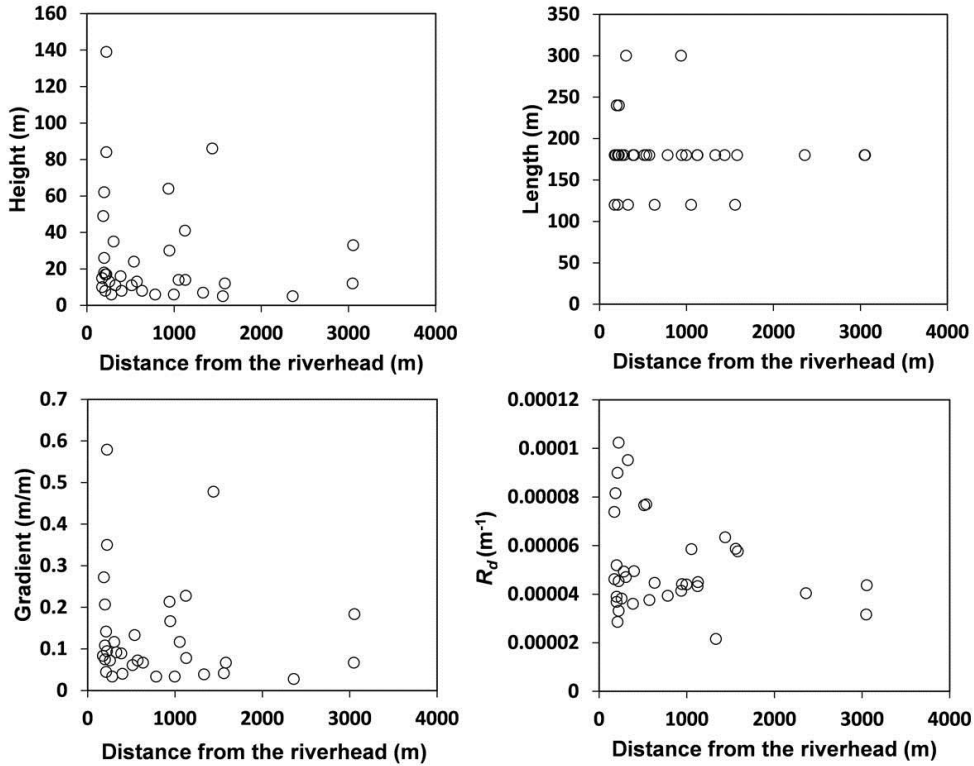


Figure 4-33. Relationships between form parameters of knickzones and distance from the riverhead in Mt. Longhu.

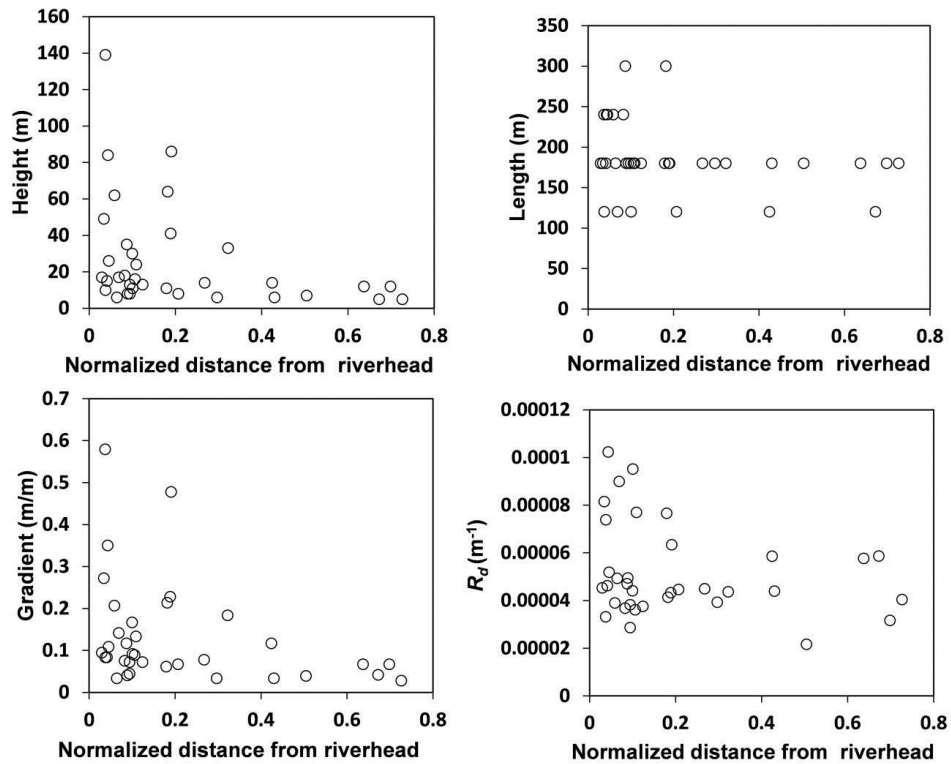


Figure 4-34. Relationships between form parameters of knickzones and normalized distance from the riverhead in Mt. Longhu.

The frequency, density and form parameters of knickzones were calculated for river segments of each stream order and averaged (Table 4-7). In Mt. Danxia and Mt. Longhu, knickzones are more common in the first- and second-order streams, and knickzone frequency decreases with increasing stream order. However, the opposite holds true for the Chishui area; knickzone frequency and density are lowest for the first-order streams. This difference is evident from the plots of Figures 4-25 to 4-34. In the Chishui area, knickzones are often found in downstream parts (>4 km² in drainage area), but in Mt. Danxia, knickzones in such locations are more limited, and in Mt. Longhu, almost no knickzones occur there.

Table 4-7. Knickzone characteristics according to stream order.

	Stream order	Knickzone frequency (km ⁻¹)	Knickzone density (%)	Height (m)	Length (m)	Gradient (m/m)	R_d (m ⁻¹)
CHISHUI	1	0.130	2.45	92.4	180.0	0.53	2.61E-04
	2	0.280	5.41	77.3	182.5	0.43	1.94E-04
	3	0.250	4.37	70.9	208.2	0.34	2.02E-04
DANXIA	1	0.141	2.23	34.2	158.4	0.23	1.57E-04
	2	0.135	2.23	23.7	166.0	0.13	7.71E-05
	3	0.096	1.69	21.5	176.5	0.12	6.80E-05
LONGHU	1	0.190	3.60	23.4	189.0	0.12	5.54E-05
	2	0.076	1.43	42.9	187.5	0.20	4.80E-05
	3	0.067	1.31	16.3	171.4	0.09	4.56E-05

The abundance and form parameters of the knickzone are calculated for each rock formation unit (Tables 4-8). In Mt. Danxia, the abundance of the knickzones is largest for the Danxia Formation and smallest for the Quaternary sediments. The average knickzone height and steepness (R_d) for the Danxia Formation are larger than those of other rock types, and about 59% of the tall knickzones are underlain by the Danxia Formation. In Mt. Longhu, the abundance of the knickzone are largest for the Hekou Formation (K₂h) and smallest for the Zhangping Formation (J₂z). The average knickzone height and steepness (R_d) are the largest for the Elinghu Formation (J₃e) and about 64% of the tall knickzones are underlain by volcanic rocks (J₃e).

Table 4-8. Knickpoint characteristics according to lithology.

	Lithology	Knickzone frequency (km ⁻¹)	Knickzone density (%)	Gradient (m/m)	R_d (m ⁻¹)	Height (m)	Length (m)
DANXIA	Danxia	0.20	3.59	0.169	1.17E-04	26.4	163.1
	Changba	0.14	2.61	0.176	9.52E-05	30.5	171.1
	Quaternary	0.03	0.47	0.065	4.11E-05	11.0	168.0
LONGHU	K ₂ h	0.15	2.57	0.064	4.87E-05	10.6	168.8
	K ₁ s	0.02	0.34	0.067	5.74E-05	12.0	180.0
	J ₃ e	0.08	1.60	0.287	5.21E-05	61.8	210.0
	J ₃ d	0.02	0.40	0.148	3.75E-05	39.0	210.0
	J ₃ w	0.03	0.40	0.114	7.05E-05	16.3	140.0
	J ₂ z	0.01	0.17	0.272	8.15E-05	49.0	180.0
	Qbwy	0.03	0.68	0.077	4.44E-05	20.3	240.0

4.3. Watershed transverse profiles

Relationships between the averaged shape parameters of the transverse profiles were investigated for each study area. Tables 4-9, 4-10 and 4-11 show the correlation coefficients of the relationships and their significance. The correlations were divided into four levels based on the p value: >99%, 99–95%, 95–90% and <90%. The following positive correlations are consistently strong: W and R , $Av\alpha$ and $SD\alpha$, KUH and $SK\alpha$ and $SK\alpha$ and $SKU\alpha$. For the other cases, the number of significant positive correlations increases in the following order: Chishui, Mt. Danxia, and Mt. Longhu. Particularly the correlations between six simple parameters related to profile dimensions (W and R), height (AVH and SDH) and slope ($Av\alpha$ and $SD\alpha$) increase.

Table 4-9. Correlation coefficients between average shape parameters of transverse profiles and their significance for the Chishui area.

	<i>W</i>	<i>R</i>	<i>AVH</i>	<i>SDH</i>	<i>SKH</i>	<i>KUH</i>	<i>AVα</i>	<i>SDα</i>	<i>SKα</i>	<i>KUα</i>
<i>W</i>										
<i>R</i>	0.5876									
<i>AVH</i>	0.3067	0.1025								
<i>SDH</i>	-0.128	-0.01	-0.626							
<i>SKH</i>	-0.215	-0.216	0.1303	-0.402						
<i>KUH</i>	0.3773	-6E-04	0.1139	0.0616	-0.462					
<i>AVα</i>	-0.311	0.3788	0.0672	-0.083	0.0556	-0.499				
<i>SDα</i>	-0.313	0.2773	-8E-04	0.0621	-0.156	-0.224	0.7617			
<i>SKα</i>	0.4172	-0.121	0.0311	0.0303	-0.03	0.5735	-0.861	-0.555		
<i>KUα</i>	0.1072	-0.018	0.0713	-0.14	0.2928	0.0101	-0.296	-0.415	0.485	

	<i>W</i>	<i>R</i>	<i>AVH</i>	<i>SDH</i>	<i>SKH</i>	<i>KUH</i>	<i>AVα</i>	<i>SDα</i>	<i>SKα</i>	<i>KUα</i>
<i>W</i>										
<i>R</i>	+++									
<i>AVH</i>	+									
<i>SDH</i>			---							
<i>SKH</i>				--						
<i>KUH</i>	+				--					
<i>AVα</i>	-	+				--				
<i>SDα</i>	-	+					+++			
<i>SKα</i>	++					+++	---	---		
<i>KUα</i>					+		-	--	++	

+++ positive correlation with more than 99% significance

++ positive correlation with 95% to 99% significance

+ positive correlation with 90% to 95% significance

--- negative correlation with more than 99% significance

-- negative correlation with 95% to 99% significance

- negative correlation with 90% to 95% significance

Table 4-10. Correlation coefficients between average shape parameters of transverse profiles and their significance for Mt. Danxia.

	<i>W</i>	<i>R</i>	<i>AVH</i>	<i>SDH</i>	<i>SKH</i>	<i>KUH</i>	<i>AVα</i>	<i>SDα</i>	<i>SKα</i>	<i>KUα</i>
<i>W</i>	-									
<i>R</i>	0.591	-								
<i>AVH</i>	-0.114	0.298	-							
<i>SDH</i>	0.365	0.863	0.519	-						
<i>SKH</i>	0.048	0.176	0.090	0.148	-					
<i>KUH</i>	0.153	-0.014	-0.308	-0.274	0.197	-				
<i>AVα</i>	-0.153	0.475	0.514	0.565	-0.159	-0.314	-			
<i>SDα</i>	-0.001	0.591	0.458	0.649	-0.016	-0.127	0.858	-		
<i>SKα</i>	0.317	0.124	-0.251	0.012	0.202	0.359	-0.269	0.192	-	
<i>KUα</i>	0.208	0.052	-0.320	-0.045	0.095	0.251	-0.143	0.187	0.881	-

	<i>W</i>	<i>R</i>	<i>AVH</i>	<i>SDH</i>	<i>SKH</i>	<i>KUH</i>	<i>AVα</i>	<i>SDα</i>	<i>SKα</i>	<i>KUα</i>
<i>W</i>										
<i>R</i>	+++									
<i>AVH</i>		+								
<i>SDH</i>	+	+++	++							
<i>SKH</i>										
<i>KUH</i>										
<i>AVα</i>		++	++	+++		-				
<i>SDα</i>		+++	++	+++			+++			
<i>SKα</i>	+					++				
<i>KUα</i>			-			++			+++	

+++ positive correlation with more than 99% significance

++ positive correlation with 95% to 99% significance

+ positive correlation with 90% to 95% significance

--- negative correlation with more than 99% significance

-- negative correlation with 95% to 99% significance

- negative correlation with 90% to 95% significance

Table 4-11. Correlation coefficient between average shape parameters of transverse profiles for Mt. Longhu.

	<i>W</i>	<i>R</i>	<i>AVH</i>	<i>SDH</i>	<i>SKH</i>	<i>KUH</i>	<i>AVα</i>	<i>SDα</i>	<i>SKα</i>	<i>KUα</i>
<i>W</i>										
<i>R</i>	0.5931									
<i>AVH</i>	0.5007	0.9496								
<i>SDH</i>	0.603	0.9839	0.9542							
<i>SKH</i>	0.0469	-0.256	-0.353	-0.303						
<i>KUH</i>	0.0698	-0.381	-0.454	-0.41	0.8521					
<i>AVα</i>	0.4719	0.944	0.8915	0.9341	-0.33	-0.494				
<i>SDα</i>	0.5824	0.8674	0.7527	0.8461	-0.145	-0.314	0.9076			
<i>SKα</i>	0.2208	-0.38	-0.473	-0.401	0.6397	0.6875	-0.493	-0.235		
<i>KUα</i>	0.2534	-0.335	-0.403	-0.348	0.5293	0.6379	-0.437	-0.22	0.9393	

	<i>W</i>	<i>R</i>	<i>AVH</i>	<i>SDH</i>	<i>SKH</i>	<i>KUH</i>	<i>AVα</i>	<i>SDα</i>	<i>SKα</i>	<i>KUα</i>
<i>W</i>										
<i>R</i>	+++									
<i>AVH</i>	+++	+++								
<i>SDH</i>	+++	+++	+++							
<i>SKH</i>										
<i>KUH</i>			-	-	+++					
<i>AVα</i>	++	+++	+++	+++			--			
<i>SDα</i>	+++	+++	+++	+++				+++		
<i>SKα</i>			--		+++	+++	--			
<i>KUα</i>					++	+++	--		+++	

+++ positive correlation with more than 99% significance

++ positive correlation with 95% to 99% significance

+ positive correlation with 90% to 95% significance

--- negative correlation with more than 99% significance

-- negative correlation with 95% to 99% significance

- negative correlation with 90% to 95% significance

4.4. Relations between longitudinal, transverse and overall watershed characteristics

The relationships between the representative shape parameters of longitudinal/transverse profiles and watersheds were examined. The parameters are those regarding to transverse profiles (W , R , $AV\alpha$ and AVH), longitudinal profiles (β , B , SL and K), and watersheds (average slope = γ and HI). The correlation coefficients and their significance based on the p value are shown in Table 4-12.

It is clear that the number of positive correlations increases in the following order: Chishui, Mt. Danxia, and Mt. Longhu. The following positive correlations are always strong: B and SL , B and K , γ and $AV\alpha$, W and R (as already indicated), and SL and K . In the case of Chishui, most other correlations are insignificant but a few strong negative correlations are observed. In Mt. Danxia, negative correlations disappeared and more positive correlations occurred. In Mt. Longhu, almost all correlations are statistically significant and always positive.

Table 4-12. Average value of longitudinal/transverse profile for the whole watershed based on the types of slope angle - drainage density.

	CHISHUI	DANXIA	LONGHU	CHISHUI	DANXIA	LONGHU
$\beta \sim B$	0.171	0.316	0.640			+++
$\beta \sim \gamma$	0.185	0.306	0.867			+++
$\beta \sim HI$	0.094	-0.130	0.199			
$\beta \sim AV\alpha$	0.227	0.234	0.768			+++
$\beta \sim W$	-0.684	-0.235	0.483	---		++
$\beta \sim R$	-0.428	0.077	0.791	--		+++
$\beta \sim AVH$	-0.295	0.401	0.893		++	+++
$\beta \sim SL$	-0.370	0.215	0.867	-		+++
$\beta \sim K$	-0.143	0.579	0.944		+++	+++
$B \sim \gamma$	-0.289	0.412	0.654		++	+++
$B \sim HI$	0.135	-0.020	0.174			
$B \sim AV\alpha$	-0.246	0.099	0.575			+++
$B \sim W$	-0.268	0.419	0.437		++	++
$B \sim R$	-0.158	0.454	0.662		++	+++
$B \sim AVH$	-0.651	-0.010	0.719	---		+++
$B \sim SL$	0.622	0.616	0.792	+++	+++	+++
$B \sim K$	0.718	0.609	0.742	+++	+++	+++
$\gamma \sim HI$	-0.150	0.195	0.387			
$\gamma \sim AV\alpha$	0.844	0.646	0.962	+++	+++	+++
$\gamma \sim W$	-0.137	0.230	0.545			+++
$\gamma \sim R$	0.438	0.604	0.928	++	+++	+++
$\gamma \sim AVH$	0.0870	0.607	0.939		+++	+++
$\gamma \sim SL$	-0.360	0.512	0.871	-	+++	+++
$\gamma \sim K$	-0.221	0.714	0.897	-	+++	+++
$HI \sim AV\alpha$	0.131	0.337	0.381		+	+
$HI \sim W$	0.087	-0.207	0.459			++
$HI \sim R$	-0.033	-0.083	0.460			++
$HI \sim AVH$	0.000	0.240	0.410			++
$HI \sim SL$	0.273	0.409	0.416		++	++
$HI \sim K$	-0.014	-0.183	0.341			
$AV\alpha \sim W$	-0.266	-0.151	0.481			++
$AV\alpha \sim R$	0.420	0.476	0.906	++	++	+++
$AV\alpha \sim AVH$	0.057	0.515	0.894		++	+++
$AV\alpha \sim SL$	-0.247	0.286	0.804			+++
$AV\alpha \sim K$	-0.143	0.338	0.813			+++
$W \sim R$	0.588	0.591	0.715	+++	+++	+++
$W \sim AVH$	0.319	-0.114	0.650			+++
$W \sim SL$	0.203	0.171	0.675			+++
$W \sim K$	0.055	0.265	0.621			+++
$R \sim AVH$	0.107	0.298	0.967			+++
$R \sim SL$	0.110	0.271	0.925			+++
$R \sim K$	0.159	0.480	0.903		++	+++
$AVH \sim SL$	-0.345	0.409	0.969	--	++	+++
$AVH \sim K$	-0.511	0.562	0.970	---	+++	+++
$SL \sim K$	0.782	0.519	0.975	+++	+++	+++

+++ positive correlation with more than 99% significance

++ positive correlation with 95% to 99% significance

+ positive correlation with 90% to 95% significance

--- negative correlation with more than 99% significance

-- negative correlation with 95% to 99% significance

- negative correlation with 90% to 95% significance

CHAPTER 5 DISCUSSION

5.1. Evolutionary stages of Danxia landforms

The evolutionary stages of Danxia landforms in the three study areas have been regarded as follows: Chishui – youth or early, Mt. Danxia – mature, and Mt. Longhu – old (Luo, 1999; Xiong et al., 2009; Jiang et al., 2009; Huang, 2010; Kusky et al, 2010; Guo et al., 2011; Li et al., 2013; Peng, et al., 2013). The identification of these stages were based on 1) the general Davisian scheme (Davis, 1899) which is essentially qualitative, and 2) visual observations and interpretation of landform characteristics in the field or via the use of topographic maps and aerial/satellite images. The evolutionary stages of Danxia landforms in some other areas have also been determined in such a way (Peng, 2000, 2001; Huang, 2002; Zhu et al., 2009; Jiang et al., 2010). However, as far as the author knows, no studies have investigated detailed morphometric characteristics of Danxia landforms to determine their evolutionary stages or discuss whether the previously inferred stages are appropriate.

From various geomorphometric analyses conducted in this study, it is possible to quantitatively and objectively compare the geomorphological characteristics of the three study areas. The results of analyses show distinct differences in landform characteristics related to the evolutionary stages of landforms. *HI* has often been used to determine such stages. According to Strahler (1952), *HI* values larger than 0.6 correspond to the youthful stage, those between 0.35 and 0.6 to the equilibrium (mature) stage, and those less than 0.35 to the monadnock (old) stage. The mean values of *HI* for Chishui, Mt. Danxia and Mt. Longhu are 0.56, 0.32, and 0.29, respectively (Table 4-1). If the *HI* criterion proposed by Strahler (1952) is strictly applied, the Chishui area corresponds not to the youth stage but

the mature stage, and Mt. Danxia corresponds not to the mature stage but the old stage. However, the ranges by Strahler (1952) should be considered only approximate because they are inferred without investigating many examples in the world. In addition, not only the mean but also the range of *HI* in each area (Table 4-1) should be taken into account. In the Chishui area, some watersheds have *HI* higher than 0.6, whereas such high *HI* values are not found in the other two areas. In addition, both the minimum and maximum *HI* values for Mt. Danxia are larger than those for Mt. Longhu. Therefore, it can be said that the Chishui area belongs to the (late) youth stage; Mt. Danxia to the (late) mature stage; and Mt. Longhu to the old stage. Consequently, it is safe to say that the previously inferred geomorphic stages are confirmed. However, based on the *HI* values, the stages of Mt. Danxia and Mt. Longhu do not look significantly different.

Some other morphometric parameters also indicate general geomorphological differences among the three areas in relation to landform evolution. First, the Chishui area is characterized by steeper topography compared with the other two areas. The mean values of slope-related parameters, mean slope (γ), β , $SL K$, and $Av\alpha$ are all largest in the Chishui area (Table 4-1). The two relief-related parameters, the relative relief and R , also have the highest mean values in the Chishui area (Table 4-1). The values of these parameters for Mt. Danxia are those for Mt. Longhu are more similar, but the former are consistently larger than the latter except for the relative relief (Table 4-1). These indicate that, with the progress of the evolutionary stage from youth to old, erosion led to more subdued topography. According to the Davisian scheme, topographic slope is considered to be largest in the mature stage, characterized by deep V-shaped valleys. However, in the case of the study areas, development of deep gorges in the Chishui area has led to much steeper topography than in Mt. Danxia with the mature stage. Danxia landforms are named after Mt. Danxia and hence it has often been thought as the most typical area of Danxia landforms.

At the same time, Danxia landforms are often defined as landforms with steep side walls and relatively flat-topped ridges (Huang, 1982, 2010; Peng, 2000; Qi et al., 2005; Ouyang et al., 2009). Although such landforms can be observed in some places of Mt. Danxia, the Chishui area contains more of such topography, and can be regarded as a more typical case of Danxia landforms.

The inferred development of the geomorphic stage due to erosion is confirmed by the results of stream network analyses. The mean drainage density increases in the following order: Chishui, Mt. Danxia and Mt. Longhu (Table 4-1), which agrees with more eroded topography in the latter stage. The frequency of the four types of the drainage density–slope angle relationship shows more complex situation in the Chishui area, where all the four types occur with relatively similar frequencies. In the other two areas, by contrast, only one type (Type 4) is dominant. Type 4 represents negative correlations between drainage density and slope, which are characteristics where diffusive processes including landslides are dominant (e.g., Oguchi, 1997; Tailing and Sowter, 1999). In the areas of Danxia landforms, channelization is an important process forming topography along rivers and streams such as gorges, but slopes on valley-sides and ridges are mainly shaped by diffusive processes such as toppling, rock falls, and gradual rock weathering. Therefore, the dominance of Type 4 in the latter stages seems to reflect the occurrence of more eroded landforms.

The higher topographic complexity in the Chishui area is also confirmed by the distribution and form of knickzones. As written in Section 4.2.2, the density and height of knickzones in the Chishui area are much higher than in the other areas. Particularly the longitudinal profiles in downstream areas with drainage areas larger than 4 km² are much more complex with distinct knickzones in the Chishui area, whereas such knickzones in downstream areas are limited in the other two areas.

Although many morphometric parameters for Mt. Danxia and Mt. Longhu show relatively small differences, Table 4-12 has revealed that the correlations of the parameters show a marked difference; there are much more significant correlations for Mt. Longhu compared to Mt. Danxia. This observation points to more harmonized and thus more advanced landforms in Mt. Longhu, where topographic slope, relief, height and dimensions are more strongly related after significant landform shaping due to erosion. One distinct character is the significant correlation between β and γ , which indicates that the watershed slope is affected by the longitudinal slope. This correlation does not occur in the other two areas, although the significant correlation between $Av\alpha$ and γ is common to all the three areas. In other words, during the earlier stages of erosion of Danxia landforms, transverse profiles play a major role in determining the watershed slope, whereas in the old stage after the valley side slopes are more subdued, the relative importance of the longitudinal slope increases.

The above discussion may provide a guideline to determine evolutionary stages of landforms. Although some select parameters like *HI* and drainage density tend to be used to evaluate general landform characteristics and evolution stages, there may be some other aspects which cannot be detected by these parameters but are related to landform evolution. The present study suggests that the correlations of various morphometric parameters effectively indicate such relatively minor topographic differences associated with the advance of the landform evolutionary stage.

5.2. Effect of geology

The morphometric analyses conducted in this study have also revealed the effect of bedrock geology mainly in Mt. Danxia and Mt. Longhu, where different formations of bedrock are distributed. The inferred aspects of rock control, in terms of stream orientation, hypsometry, and river longitudinal profiles, are discussed below.

5.2.1. Stream network orientation

Previous studies indicate that stream flow orientation is controlled by geological structure of bedrock (e.g. Ciotoli et al., 2003; Guarnieri et al., 2005). Among the three studied areas, Mt. Danxia shows the clearest correlations between the orientations of streams and those of faults. As noted in Section 4.1.2, the orientations of the higher order streams tend to correspond to those of the major faults, whereas the lower order streams additionally follow the directions of minor faults (Figures 2-4 and 4-2). Huang (2010) pointed out the correlation between the N–S flowing Jinjiang River and the orientation of F6 (Renhua fault), and this study indicates such correlations are commonly found over the Mt. Danxia, even on smaller scales. In addition, the large and small rivers are found to behave differently. The large rivers tend to follow only the major structures like F6, while the small rivers flow more flexibly.

In the Chishui area, stream orientations are more clearly controlled by overall topographic gradient of the area – from southeast to northwest (Figure 4-1). The lack of distinct faults in the area (Figure 2-3) seems to facilitate this topographic control. However, according to Luo (1999), two joint systems exist in this area (30° – 40° and 310° – 320° in orientation) which may also be responsible for the dominance of the NW stream orientation in the high order streams. Figure 4-1 indicates that flow directions are more varied for

lower order streams, which is common to Mt. Danxia and confirms the higher flexibility of low-order streams.

Although several faults take place in Mt. Longhu, unlike Mt. Danxia, the orientations of the faults are not concentrated toward some particular directions (Figure 2-9). Instead, the dominant effect of the overall topographic gradient toward the north is evident, although the 1st order streams evidently show more flexibility (Figure 4-3).

It should be noted that in Mt. Danxia, not only the abundance of faults but also the lower gradient of the trunk stream may facilitate the control by faults on stream orientations. Figures 2-1, 2-4 and 2-7 illustrate that in Mt. Danxia, the gradient of trunk stream is smaller than the other two areas. In summary, whether the distribution of faults or overall topographic gradient exerts control on stream orientations depends on the abundance of faults and the level of overall topographic gradient.

5.2.2. Hypsometrical integral and curves

Several researchers have suggested that the hypsometric integral corresponds to not only evolutionary stages but also lithological resistance (Lifton and Chase, 1992; Hurtrez and Lucazeau, 1999; Walcott and Summerfield, 2008). This issue is addressed for Mt. Danxia and Mt. Longhu having different bedrock types in each area.

In Mt. Danxia, the eastern and western sides are characterized by different bedrock lithology, and the western side has higher *HI* values (Table 4-5). The eastern side is mostly underlain by the Danxia Formation, whereas that of the western side consists of a combination of the Changba and Danxia Formations (Figure 2-6). On the western side, the Danxia Formation often exhibits steeper escarpments because it is more resistant to erosion than the Changba Formation (Huang, 2010; Peng, 2000). Zhu et al. (2010) also suggest that

the Changba Formation is more susceptible to freeze-thaw action than the Danxia Formation, which may have been an important erosion process during glacial periods. Therefore, the more resistant Danxia Formation seems to account for the less eroded topography of the eastern side, characterized by higher *HI* values. This is confirmed by the statistical test to compare *HI* values for the two formations regardless of watershed location (Figure 4-10).

The correlation between watershed hypsometry and the rock types can be presented more quantitatively. As noted in Section 4.1.5, the watersheds in Mt. Danxia are grouped into three classes based on *HI* and the shape of hypsometric curves. Class 1 with low *HI* occupies 28.6% of the watersheds underlain mainly by the Changba Formation, in contrast to 16.6% underlain mainly by the Danxia formation. For Class 2 with intermediate *HI*, the ratios are 16.7% and 21.5%, respectively; for Class 3 with high *HI*, the ratios are 4.7% and 11.9%, respectively. In other words, the relative abundance of the watersheds underlain mainly by the Changba Formation tends to decrease with increasing *HI*. It can also be noted that the distribution of the Class 3 watersheds (Figure 4-9) tends to correspond to less dissected topography underlain by the uppermost member of the Danxia Formation (K_2dx^3 in Figure 2-6). This observation suggests that the markedly resistant member of the Danxia Formation acts as a cap rock, preventing deep erosion (see the right side of Figure 2-6C). Therefore, we conclude that differences in watershed hypsometry within Mt. Danxia strongly reflect the bedrock's resistance to erosion. This agrees with the findings of Walcott and Summerfield (2007), who found a strong correlation between *HI* and bedrock resistance in the passive margin of southeast Africa. The study areas including Mt. Danxia are also located in a passive margin with no records of recent intense seismic and tectonic activities. Even in the long term, the low relative heights of the Middle Pleistocene river terraces (<50 m) in Mt. Danxia indicate limited tectonic uplift. The effect of lithology on

landforms seems to be more distinct in passive margins compared with tectonically active areas.

It should be noted, however, that the effects of tectonics on the topography of Mt. Danxia cannot be ruled out completely. Although the watersheds in the western side are characterized by more advanced erosion in terms of hypsometry, the mean watershed elevation tends to be higher on the western side (~160 m a.s.l.) than the eastern side (~130 m a.s.l.). This phenomenon may be caused by the relative uplift of the western side due to the slow but long-term activity of the F6 under NE–SW tectonic compression (Zhang and Ji, 1995; Zhang and Wang, 2007).

In Mt. Longhu, differences in *HI* according to geology are also statistically confirmed (Figure 4-12). Zhu et al. (2009) and Kusky (2010) pointed out that in the southern side of Mt. Longhu, the volcanic Elinghu Formation (J_3e) exhibits steeper escarpments because it is more resistant to erosion. This observation corresponds to the highest values of *HI* for the Elinghu Formation (Figure 4-12), which seems to account for the less eroded topography of the easternmost part of Mt. Longhu.

5.2.3. ***SL* and Hack profiles**

SL has been used to evaluate possible effects of tectonic activity and rock resistance on topography (Keller and Pinter, 1996). In Mt. Danxia, *SL* differs according to lithology. Figure 4-17 summarizes *SL* values for the three major rock types along river reaches in Mt. Danxia: the Danxia and Changba Formations, and the Quaternary sediments. Although the range of data is large, the order of mean or modal *SL* values corresponds to the level of rock resistance, and the Kruskal-Wallis test has shown that the difference is statistically significant ($p < 0.001$). Consequently, not only drainage watershed topography, as represented by hypsometry, but also channel forms are affected by lithology.

The difference in the average SL between the western and eastern sides may be also related to more heterogeneous lithology in the western side. Visual comparison of Figures 2-4 and 4-16 indicates that SL tends to be higher at the boundary of the Danxia and Changba Formations, because the local slope gradient tends to be high due to the deeper incision in the lower, more erodible, Changba Formation. The effect of lithology on SL is also supported by the Hack profiles. On the western side, the Hack profiles tend to show a markedly convex shape (Figure 4-19A), which seems to reflect the transition from the more resistant Danxia Formation to the less resistant Changba Formation. However, most major rivers in the eastern side show less convex Hack profiles (Figure 4-19B), reflecting the homogeneity of the bedrock. The average K value for the western side (28.3) is slightly higher than that for the eastern side (25.0), suggesting that the lithological contrasts in the western side led to somewhat steeper reaches. These results agree with Duvall et al. (2004) who indicated streams flowing from resistant to less resistant bedrock exhibit highly concave profiles and increased gradients along their lower reaches. VanLaningham et al. (2006) also noted that rivers on more resistant rocks have lower longitudinal concavity.

In addition, some locally high SL values correspond to faults, rather than rock boundaries, e.g., Watersheds 4 (F6), 23 (F13), 26 (F18), and 33 (F4 and F17) of the western side (Figures 2-4 and 4-19A). As shown in Figure 4-16, waterfall-type knickpoints are observed in watersheds 20 and 42 (Huang, 2010). These knickpoints are also located close to the faults, and correspond with locally high SL values, as indicated elsewhere (Brookfield, 1998; Štěpančíková et al., 2008). The influence of the faults on SL is also shown by the buffer analysis: 48% of anomalously high SL values are located within the buffer zones along the major faults. The distribution of faults is much denser in the western side (Figure 2-6), which may account for the relatively higher SL values in this region.

However, some anomalously high SL values correspond to neither rock boundaries nor

the major faults e.g. Watersheds 9, 10, and 16 in the eastern sector (Figure 4-19B). The Hack profiles also sometimes show local concavity within a single rock type, as for Watershed 10 (Figure 4-19B). Further studies are needed to inquire into the causes of such anomalies.

In Mt. Longhu, the resistant J_{3e} Formation (Zhu et al., 2009; Kusky, 2010) tend to have the highest SL values, whereas the least resistant Quaternary sediments have the lowest SL values (Figure 4-22). This agrees with the lithologic control on HI . However, the effects of lithology need to be investigated in detail in future, because information in rock resistance is unavailable for some of the lithology types shown in Figure 4-22.

5.2.4. **Knickzone generation and distribution**

In Mt. Danxia and Mt. Longhu, the effects of rock properties on the form of knickzones can be inferred. More knickzones are found in the typical red terrestrial sedimentary rocks such as the Danxia Formation in Mt. Danxia and the Hekou Formation (K_{2h}) in Mt. Longhu (Table 4-9). As noted in Section 4.2.2, tall knickzones tend to be concentrated in areas underlain by the Danxia Formation and the volcanic Elinghu Formation (J_{3e}). Although these observations seem to reflect rock control on knickzone formation, all the results are not consistent with the other cases of rock control. For example, the Hekou Formation (K_{2h}) in Mt. Longhu is characterized by abundant knickzones but SL values for the formation are not high (Figure 4-22), in contrast to the Elinghu Formation (J_{3e}). As noted above, further research is needed about the details of rock control, particularly in Mt. Longhu.

5.3. Watersheds in the Chishui area

In Chishui, geology is homogeneous at least at the formation level. However, the watersheds there are characterized by the relatively even occurrences of the four different types of drainage density–slope angle relationship (Figure 4-7). As noted, the Types 3 and 4 watersheds tend to be located in the northeastern and central areas at the upper reaches of the main stream, whereas the Types 1 and 2 watersheds tend to occur in the lower parts. Visual comparison of Figures 4-7, 4-8 and 4-14 shows that Types 1 and 2 are characterized by higher values of the hypsometric integral and K , as compared with Types 3 and 4. In other words, Types 1 and 2 represent steeper topography in the downstream direction and the earlier stage of landform development. Such differences seem to reflect differing stages of channel development corresponding to relative watershed location: watersheds in the lower areas have been affected more by deeper incision of the trunk stream.

The above inference indicates that the Types 3 and 4 watersheds in the Chishui area have experienced less erosion than the Types 1 and 2 watersheds. This is in contrast to the extensive occurrence of Type 4 watersheds in Mt. Danxia and Mt. Longhu, where much more advanced erosion is inferred. In other words, the Type 4 watersheds in the Chishui area differ essentially from those in the other two areas. Although both of them have some similarities in terms of topographic characteristics, those in the Chishui area will develop toward the other types such as Types 1 and 2 in future with the progress of erosion. In contrast, the Types 1 and 2 watersheds in the Chishui area will develop into Type 4 like those observed in the other two areas. The case of the Chishui area indicates the importance of relative location in determining topographic characteristics of Danxia landforms at the early stage.

5.4. Evaluation of morphometric parameters for efficient research

This paper utilizes a large number of morphometric parameters for performing extensive terrain analyses. However, it is not always easy to take such a time-consuming approach. Although the results of this paper indicate that the use of various parameters provides useful results, some of the parameters tend to be correlated with each other. Therefore, it is important to indicate the most useful parameters for future efficient research.

The relationships between the relative relief, the mean basin slope (γ), HI , SL and K for each of the three study areas (Figures 4-15, 4-20, 4-24) show that the relative relief, K , and SL always have high correlations. Concerning γ , K , and SL , their positive correlations are strong for Mt. Danxia and Mt. Longhu, but very weak or insignificant in the Chishui area. In contrast, HI does not correlate well with SL and K in all the three cases. Such discussion is also possible from Table 4-14. Even in Mt. Longhu, where most combinations of morphometric parameters exhibit positive correlations, four combinations, $\beta \sim HI$, $\beta \sim \gamma$, $\gamma \sim HI$, and $HI \sim K$ do not show significant correlations. The Hypsometric curve is standardized in terms of both relief and area to permit comparisons of drainage basins with different sizes (Rosenblatt and Pinet, 1994; Hurtrez et al., 1999). In contrast, most other geomorphometric parameters of drainage basins are often related to relief and/or area. Thus, HI is a highly independent parameter and should be included for performing effective morphometric analyses of watersheds. For the other parameters, whether they are required or not may depend on the evolutionary stages of landforms to be investigated – more parameters are needed for landforms in earlier stages. Still, some parameters such as the relative relief, K and S are highly correlated so the use of all of them may be unnecessary.

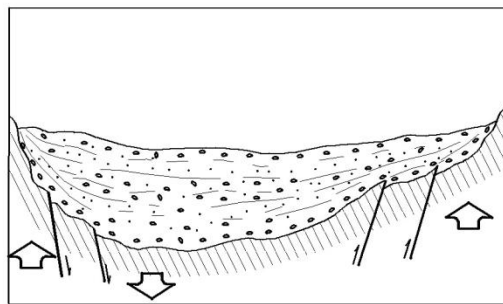
The detection of knickzones is highly tedious although it may give important information about the characteristics of river longitudinal profiles. The results of this study indicate that knickzones correspond well to the anomalous points which can be much more easily identified from the data of river longitudinal profiles. Therefore, the detection of anomalous points and the visual inspection of their topography using a DEM or a topographic map could be used as a quicker method of knickzone detection.

5.5. Comparison with a previous model of Danxia landform evolution

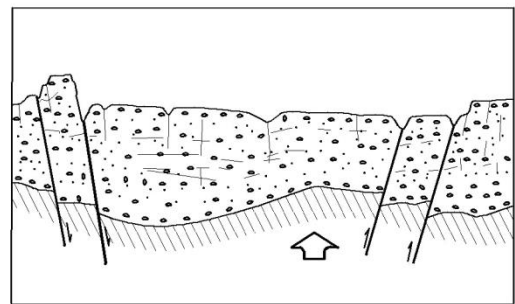
As noted, existing studies on Danxia landforms are numerous in China but they tend to be qualitative and speculative. A representative study by Peng (2001) includes an illustrated model of the evolution process of Danxia landforms (Figure 5-1). The areas studied correspond to the later four figures: C to F.

Comparison of the three figures with the result of this study indicates that Figure 5-1(C and D) corresponds to the Chishui area, and Figure 5-1F to Mt. Longhu without strong discrepancies. However, Figure 5-1E does not represent well the results from Mt. Danxia, although the figure represents the late mature stage of landform evolution, and Mt. Danxia is often regarded as the typical case of the stage. One problem is that the mean topographic slope and relative relief of the section of Figure 5-1E does not differ significantly from that of Figure 5-1D, although Mt. Danxia has more gentler topography than the Chishui area. In addition, the observed increase in drainage density with the progress of erosion is not well illustrated; rather, the final stage in Figure 5F appears to have lower drainage density. Another problem common to all illustrations is uniform lithology. The present study has shown that the differences in bedrock lithology play a

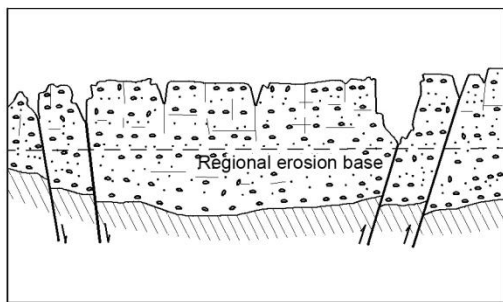
certain role in determining the characteristics of Danxia landforms. Based on the obtained results, I propose an improved model with more detailed topographic characteristics and effects of geology (Figure 5-2). Interbedded rocks with soft and hard layers induced differential weathering and dilapidation which played a role in the formation of different types of Danxia landforms.



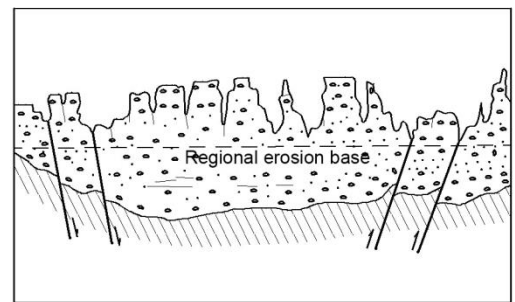
A. The basin was initially formed in Upper Cretaceous Epoch



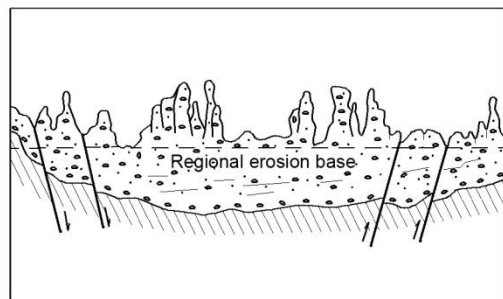
B. Then the basin was faulted because of elevation movement.



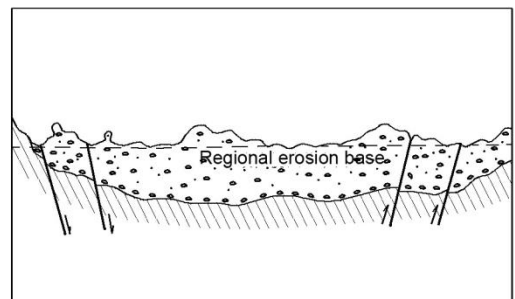
C. In the juvenile stage (strongly cut down by water; there are narrow gorges and continuous original surface or planation surface is kept on the mountaintop.



D. In the early mature stage (mountaintop is gradually segregative; mesas, hoodoo columns, Danxia peak clusters and narrow gorges develop.)

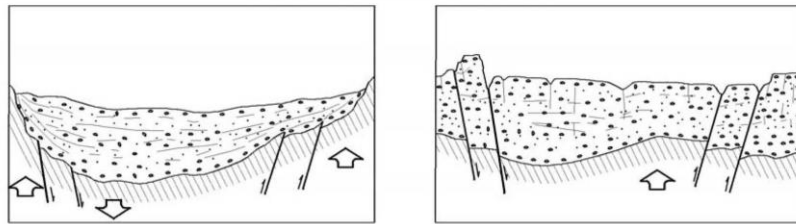


E. In the late mature stage (trunk valley is close to the erosion base; hoodoos develop near the valley and Danxia peak clusters develop far away from the valley.



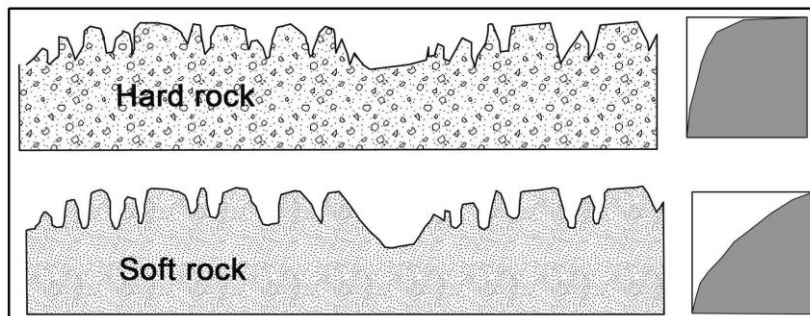
F. In the old stage (Trunk valley and major branches reach to the erosion base; valley plain, red hills, stone towers and kopjes occur with intervals)

Figure 5-1. Peng's (2001) model of evolution of Danxia landforms.

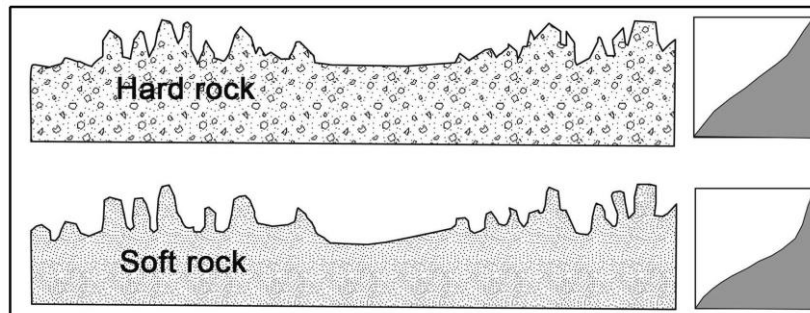


(a) A basin was initially formed in the Upper Cretaceous

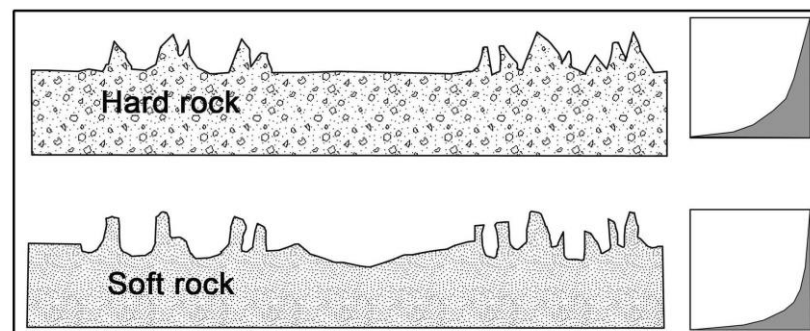
(b) Then the basin was faulted because of tectonic stress



(c) In the young stage, narrow and steep valleys with steep cliff walls formed as a result of river downcutting. Streams tend to have high gradients. Convex hypsometric curves indicate slightly eroded terrain with low drainage density and high hypsometric integrals. In areas with softer bedrock, slightly convex long profiles with less convex hypsometric curves, and wide and deep valleys develop.



(d) In the mature stage, wide and gentle valleys develop. Streams tend to have moderate gradients. Rocks are eroded quickly by running water. S-shaped hypsometric curves indicate moderately eroded terrain with moderate hypsometric integrals and drainage density. In areas with softer bedrock, slightly concave long profiles with more concave hypsometric curves, and wide and deep valleys develop.



(e) In the old stage, valleys are characterized by greater width and low relief. Stream tends to have low gradients. Concave hypsometric curves indicate that much of the rocks have already been eroded away, leading to low hypsometric integrals and high drainage density. In areas with softer bedrock, slightly concave long profiles with more concave hypsometric curves, and wide and deep valley develop.

Figure 5-2. Improved model of evolution of Danxia landforms.

CHAPTER 6 CONCLUSIONS

Research on Danxia landforms in China so far has focused on the definition, classification, qualitative description and discussion about the origin of Cretaceous strata. Most of such research is speculative because of the lack of support from quantitative data and their numerical and statistical analyses. This study has examined the characteristics of Danxia landforms using morphometric parameters in relation to general watershed form, stream-net structure, stream longitudinal profiles, valley transverse profiles extracted from DEMs and digital geological maps. Although lithological influence on the development of Danxia landforms has often been suggested, it has not been confirmed by quantitative analyses of topography. Evolution of landforms can be inferred from morphometry, i.e., quantitative measurements of geomorphic properties. For example, drainage networks and river longitudinal profiles are widely used as indicators of geomorphological evolution in relation to environmental factors.

The main aims of this study were to investigate quantitative topographic characteristics of Danxia landforms at different erosional stages, and relationships between topography and bedrock geology including bedrock structure and lithology. Three areas in subtropical areas in China, the Chishui area, Mt. Danxia and Mt. Longhu, were selected because they are typical examples of Danxia landforms, included in the World Heritage sites, and have different stages of geomorphic evolution: youth – Chishui, mature – Mt. Danxia and old – Mt. Longhu.

Watersheds and stream-nets within each study area were delineated using the threshold contributing area method. Then the various shape parameters including mean slope, relative relief, and the hypsometric integral were obtained for each watershed and their correlations were investigated. Longitudinal and transverse profiles of each watershed

were also collected from the DEM. For the transverse profiles, shape parameters such as width, relief, height, slope as well as their standard deviation, skewness and kurtosis were acquired. For the longitudinal profile, the stream length gradient (*SL*) index, the Hack profile, and a power function fitted to the profile were derived. Relationships between the longitudinal, transverse and overall watershed characteristics were also investigated using representative shape parameters. Parameters related to stream-net structure including drainage density, stream orders, the bifurcation ratio, the stream length ratio and stream orientation were also obtained. Knickzones along streams were also identified by using the changing rate of the stream gradient at different spatial scales. Then the relationships between the morphometric properties and those between topography and geology were investigated.

The results of various geomorphometric analyses show distinct differences in landform characteristics among the three areas related to the evolutionary stages of landforms. Based on *HI* values, previously inferred geomorphic stages were confirmed. Other parameters related to slope and relief and drainage density were also found to change consistently with the evolutionary stage. Correlations between morphometric parameters also effectively indicate relatively minor topographic differences among the three areas associated with the advance of the landform evolutionary stage.

Regarding stream orientation, watersheds in Mt. Danxia show the clearest correlations between the orientations of streams and those of faults. In the Chishui area and Mt. Longhu, stream orientations are more clearly controlled by overall topographic gradient of each area. Such differences are related to the density of faults and the overall gradient of the area along the trunk stream.

Differences in the hypsometric curves and *HI* values for the western and eastern sides of Mt. Danxia and high *HI* values in Mt. Longhu result from lithological differences. The

more resistant rock accounts for the less eroded topography characterized by higher *HI* values. *SL* also differs according to rock units and some locally high *SL* values correspond to faults, rather than rock boundaries according to the analysis of the Hack profiles.

Knickzones are more common in the first and second-order streams in Mt. Danxia and Mt. Longhu; however, in the Chishui area, knickzones are often found in downstream parts (>4 km² in drainage area), reflecting younger and less organized topography. More knickzones are found in the typical red terrestrial sedimentary rocks such as the Danxia Formation in Mt. Danxia and the Hekou Formation in Mt. Longhu, indicating rock control on knickzone formation.

In the Chishui area, difference in the drainage density–slope angle relationship seems to reflect differing stages of channel development corresponding to relative watershed location. The younger evolutionary stage and more homogeneous lithology in the area facilitated the influence of the relative location. The watersheds with the drainage density–slope angle relationships of Types 3 and 4 tend to be located in the northeastern and central parts in the Chishui area, at the upper reaches of the main stream. In contrast, watersheds with the Types 1 and 2 relationships tend to occur in the lower parts with earlier stage of development. Only Type 4 of the drainage density–slope angle relationship is dominant in Mt. Danxia and Mt. Longhu. The Type 4 watersheds in Mt. Danxia and Mt. Longhu were found to represent much more advanced stages of erosion compared to the Type 4 watersheds in the Chishui area.

The relationships between the representative shape parameters of longitudinal/transverse profiles and watersheds were also examined. The number of positive correlations increases in the following order: Chishui, Mt. Danxia, and Mt. Longhu. With the advance of erosion, topography of Danxia landforms tends to have stronger correlations between various relief, slope, height and dimensional parameters, reflecting

the formation of more organized topography in the later stages.

The analyses using a large number of morphometric parameters conducted in this research permitted the detailed evaluation on the independence and effectiveness of each parameter. For example, *HI* was found to be independent of other parameters for any stages of landform evolution so future studies using a lesser number of parameters should include *HI*.

The results of this study were compared with a previous model of the evolution of Danxia landforms. Some characteristics of landforms, such as the differences in slope and relief among the areas with different evolutionary stages and change in drainage density, are not well represented in the previous model. In addition, the effects of geological differences within an area need to be included in such a model. So I proposed a new model based on the hypsometric curve shape and cross section correspond to lithological resistance.

Compared to previous studies on Danxia landforms, this paper conducted more quantitative and more detailed analyses using a large number of morphometric parameters and geology data. However, because of such an intensive approach, only three representative areas of Danxia landforms could be investigated. Additional studies on Danxia landforms in other areas with various evolutionary stages are required. Furthermore, more detail analyses on the effects of the geology are necessary. Future studies are recommended to use higher-resolution spatial data and some field survey approaches to understand the detailed characteristics of the Danxia landforms and bedrock geology. Although this paper focuses on relatively close subtropical areas and hence the effects of climate factors were not discussed, the issue needs to be addressed in future by selecting Danxia landforms in climatically different areas.

ACKNOWLEDGEMENTS

I would first and foremost like to thank my supervisor, Dr. Takashi OGUCHI for his undying enthusiasm and support throughout the last five years. He gave me useful suggestions which always resulted in improved research. I would also like to thank Dr. Yuichi S. HAYAKAWA at the Center for Spatial Information Science, The University of Tokyo for his technical support with data analysis. He also provided supportive advices to me. Members of the laboratory of Dr. OGUCHI also deserve my sincerest thanks for their warm friendship and assistance without which I could not complete my thesis. I would also like to thank Dr. Hua PENG in Sun Yat-Sen University, China, for his tremendous help with data collection and assistance.

REFERENCES

- Abrahams, A. D., 1984. Channel networks: A geomorphological perspective. *Water Resources Research* 20(2), 161-188.
- Ansan, V., Mangold, N., 2006. New observations of Warrego Valles, Mars: evidence for precipitation and surface runoff. *Planetary and Space Science* 54, 219–242.
- Arp, C., Whitman, M., Jones, B., Kemnitz, R., Grosse, G., Urban, F., 2012. Drainage Network Structure and Hydrologic Behavior of Three Lake-Rich Watersheds on the Arctic Coastal Plain, Alaska. *Arctic, Antarctic, and Alpine Research* 44, 385-398.
- Azor, A., Keller, E.A., Yeats, R.S., 2002. Geomorphic indicators of active fold growth: South Mountain-Oak Ridge anticline, Ventura Basin, southern California. *Geological Society of America Bulletin* 114, 745–753.
- Bali, R., Agarwal, K.K., Ali, S.N., Rastogi, S.K., Krishna, K., 2012. Drainage morphometry of Himalayan Glacio-fluvial basin, India: hydrologic and neotectonic implications. *Environmental Earth Sciences*, 66(4), 1163-1174.
- Barnes, J.B., Pelletier, J.D., 2006. Latitudinal variation of denudation in the evolution of the Bolivian Andes. *American Journal of Science* 306, 1-31.
- Baumgartner, P., 1987. Age and genesis of Tethyan Jurassic radiolarites. *Eclogae Geologicae Helvetiae* 80, 831-879.
- Bishop, P., 1986. Horizontal stability of the Australian continental drainage divide in south central New South Wales during the Cainozoic. *Australian Journal of Earth Sciences* 33(3), 295-307.
- Bishop, P., Hoey, T.B., Jansen, J.D., Artza, I.L., 2005. Knickpoint recession rates and catchment area: the case of uplifted rivers in Eastern Scotland. *Earth Surface Processes and Landforms* 30, 767–778.

- Bloomfield, J., Bricker, S., Newell, A., 2011. Some relationships between lithology, basin form and hydrology: a case study from the Thames basin, UK. *Hydrological Processes* 25, 2518-2530.
- Brocklehurst, S.H., Whipple, K.X., 2002. Glacial erosion and relief production in the Eastern Sierra Nevada, California. *Geomorphology* 42, 1-24.
- Brookfield, M.E., 1998. The evolution of the great river systems of southern Asia during the Cenozoic India-Asia collision: Rivers draining southward. *Geomorphology* 22, 285-312.
- Bull, W.B., McFadden, L.D., 1977. Tectonic geomorphology north and south of the Garlock fault, California. D.O. Doehring (Ed.), *Geomorphology in Arid Regions*. Proc. 8th Annual Geomorphology Symp. State Univ. of New York at Binghamton, 115-137.
- Burbank, D.W., Anderson, W., 2001. *Tectonic Geomorphology*.
- Burbank, D.W., Leland, J., Fielding, E., Anderson, R.S., Brozovic, N., Reid, M.R., Duncan, C., 1996. Bedrock incision, rock uplift and threshold hillslopes in the northwestern Himalayas. *Nature* 379, 505-510.
- Burnett, A.W., Schumm, S.A., 1983. Alluvial river response to neotectonic deformation in Louisiana and Mississippi. *Science* 222, 49-50.
- Chen, A., 2005. Discuss several issues on Danxia landform. theory and practice of geotourism. The 11th Collection on Geo-Tourism. Chinese Forestry Press, Beijing, pp. 1 - 10 (in Chinese).
- Chen, G., 1935. Red rock series in Guangdong. *Quarterly Journal of Science of National Sun Yat-sen University* 6(4), 783-784.
- Chen, G., 1935. Red rock systems of Guangdong Province. *The Science Quarterly of The National Sun Yat-sen University* 6(4), 1 - 30 (in Chinese).
- Chen, Y.C., Sung, Q., Cheng, K.Y., 2003. Along strike variations in morphometric feature in the Western Foothills of Taiwan: tectonic implications based on stream-gradient and hypsometric analysis. *Geomorphology* 56, 109-137.
- Cheng, K.Y., Hung, J.H., Chang, H.C., Tsai, H., Sung, Q.C., 2012. Scale independence of basin

- hypsometry and steady state topography. *Geomorphology* 171, 1-11.
- Cheng, S., Cheng, Z., Hua P., 2010. Anti-pressure experimental study on rocks in level cave of Jinshiyan of Danxiashan in Guangdong Province. *Journal of Anhui Normal University: Natural Science* 33(2), 170-174.
- Chorley, G., 1957. Climate and morphometry. *Journal of Geology* 65, 628-638.
- Chorley, R.J., Schumm, S.A., Sugdden, D.E., 1984. *Geomorphology*. Methuen, 605p.
- Ciotoli, G., Della Seta, M., Del Monte, M., Fredi, P., Lombardi, S., Lupia Palmieri, E., Pugliese, F., 2003. Morphological and geochemical evidence of neotectonics in the volcanic area of Monti Vulsini (Latium, Italy). *Quaternary International* 101–102, 103–113.
- Clark, J.M., Chapman, P.J., Adamson, J.K., 2005. Influence of drought induced acidification on the mobility of dissolved organic carbon in peat soils. *Global Change Biology* 11, 791–809.
- Clark, M.L., Clark, D.B., Roberts, D.A., 2004. Small-footprint lidar estimation of sub-canopy elevation and tree height in a tropical rain forest landscape. *Remote Sensing of Environment* 91, 68–89.
- Crosby, B.T., Whipple, K.X., 2006. Knickpoint initiation and distribution within fluvial networks: 236 waterfalls in the Waipaoa River, North Island, New Zealand. *Geomorphology* 82(1), 16-38.
- Crosta, G.B., Frattini, P., 2004. Controls on modern alluvial fan processes in the central Alps, northern Italy. *Earth Surface Processes and Landforms* 29, 267–293.
- Davis, J.C., Sampson, R.J., 2002. *Statistics and data analysis in geology*.
- Davis, W. M., 1899. The Geographical Cycle. *Geographical Journal* 14, 481-504.
- DeGraff, J.V., Romesburg, H.C., 1981. Subsidence crack closure; rate, magnitude, and sequence. *International Association of Engineering Geology Bulletin* 23.

- Delcaillau, B., Deffontaines, B., Floissac, L., Angelier, J., Deramond, J., Souquet, P., Lee, J.F., 1998. Morphotectonic evidence from lateral propagation of an active frontal fold; Pakuashan anticline, foothills of Taiwan. *Geomorphology* 24(4), 263-290.
- Duvall, A., Kirby, E., Burbank, D., 2004. Tectonic and lithologic controls on bedrock channel profiles and processes in coastal California. *Journal of Geophysical Research: Earth Surface* (2003–2012), 109(F3).
- Edward, A.K., Nicholas, P., 2002. Active tectonics: earthquakes, uplift, and landscape.
- El Hamdouni, R., Irigaray, C., Fernández, T., Chacón, J., Keller, E.A., 2008. Assessment of relative active tectonics, southwest border of the Sierra Nevada (southern Spain). *Geomorphology* 96(1–2), 150–173.
- Eliet, P.P., Gawthorpe, R.L., 1995. Drainage development and sediment supply within rifts, examples from the Sperchios basin, central Greece. *Journal of the Geological Society* 152(5), 883-893.
- Esper Angillieri, M.Y., 2008. Morphometric analysis of Colangüil river basin and flash flood hazard, San Juan, Argentina. *Environmental Geology* 55, 107-111.
- Eschmeyer, W.N., Ferraris, C.J., Hoang, M.D., 1998. Catalog of fishes. California Academy of Sciences, San Francisco.
- Ferraris, F., Firpo, M., Pazzaglia, F.J., 2012. DEM analyses and morphotectonic interpretation: The Plio-Quaternary evolution of the eastern Ligurian Alps, Italy. *Geomorphology* 149, 27-40.
- Finnegan, N.J., Roe, G., Montgomery, D.R., Hallet, B., 2005. Controls on the channel width of rivers: Implications for modeling fluvial incision of bedrock. *Geology* 33, 229-232.
- Flint, J.J., 1974. Stream gradient as a function of order, magnitude, and discharge. *Water Resources Research* 10, 969-973.
- Fried, A.W., Smith, N., 1992. Timescales and the role of inheritance in long-term landscape evolution, northern New England, Australia. *Earth Surface Processes and Landforms* 17,

375–385.

Gardiner, J., 1990. River catchment planning for land drainage, flood defence and the environment.

Water and Environment Journal 4, 442-450.

Giannoni, F., Roth, G., Rudari, R. 2005. A procedure for drainage network identification from geomorphology and its application to the prediction of the hydrologic response. Advances in

Water Resources 28(6), 567-581.

Goldrick, G., Bishop, P., 1995. Differentiating the roles of lithology and uplift in the steepening of bedrock river long profiles: An example from southeastern Australia. Journal of Geology 103,

227-231.

Goldrick, G., Bishop, P., 2007. Regional analysis of bedrock stream long profiles: evaluation of Hack's SL form, and formulation and assessment of an alternative (the DS form). Earth Surface

Processes and Landforms 32, 649–671.

Graf, W.L., 1970. The geomorphology of the glacial valley cross section. Arctic and Alpine Research, 303-312.

Gratton D.J., Howarth P.J., Marceau D.J., 1990. Combining DEM parameters with Landsat MSS and TM imagery in a GIS for mountain glacier characterization. IEEE Transactions on

Geoscience and Remote Sensing 28, 766-769.

Gregory, K.J., Gardiner, V., 1975. Drainage density and climate. Zeitschrift fur Geomorphologie 19, 287-298.

Gregory, K.J., Walling, D.E., 1973. Drainage Basin Form and Process. Edward Arnold, London, 456p.

Guarnieri, P., Di Stefano, A., Carbone, S., Lentini, F., Del Ben, A., 2005. A multidisciplinary approach to the reconstruction of the Quaternary evolution of the Messina Strait (with

Geological Map of the Messina Strait 1:25.000 scale) G. Pasquarè, C. Venturini (Eds.),

- Mapping Geology in Italy, APAT, Roma, 45–50.
- Guo, F.S., Jiang, Y.B., Hu, Z.H., Liu, L.Q., Li, H., 2011. Evolution and Genesis System Features of Danxia Lanform in Longhushan World Geopark. *Journal of Mountain Science* 29, 195-201.
- Guo, F.S., Zhou, Z.M., Kong, Y.R., 2004. Danxia landform genesis and scenic feature on Longhu Mountain, Jiangxi Province. *Areas of outstanding natural beauty: a discussion paper*, 437-439 (In Chinese).
- Gupta, V.K., Mesa, O.J., 1988. Runoff generation and hydrologic response via channel network geomorphology—Recent progress and open problems. *Journal of Hydrology* 102, 3-28.
- Hack, J.T., 1957. Studies of longitudinal stream profiles in Virginia and Maryland. U.S. Geological Survey Professional Paper 294B, 45-97.
- Hack, J.T., 1973. Stream-profile analysis and stream-gradient index. *Journal of Research of the U.S. Geological Survey* 1, 421-429.
- Hack, J.T., 1975. Dynamic equilibrium and landscape evolution. In: Melhorn, W.N., Flemal, R.C. (eds.), *Theories of Landform Development*. State University of New York Publications in Geomorphology, Binghamton, 87-102.
- Hack, J.T., 1982. *Physiographic divisions and differential uplift in the Piedmont and Blue Ridge*. US Government Printing Office.
- Hadley, R.F., Schumm, S.A., 1961. Sediment sources and drainage-basin characteristics in upper Cheyenne River basin. U.S. Geological Survey Water Supply Paper 1531, 137-196.
- Hancock, G.R., Evans, K.G. 2006. Channel head location and characteristics using digital elevation models. *Earth Surface Processes and Landforms* 31(7), 809-824.
- Hancock, G.R., Willgoose, G.R., 2001. The use of a landscape simulator in the validation of the Siberia catchment evolution model: declining equilibrium landforms. *Water Resources Research* 37, 1981–1992.

- Hao, Y.C., Sun, G.Y., 1986. China Cretaceous. China Stratigraphy 12. Beijing: Geology Press. (in Chinese).
- Harkins, N.W., Anastasio, D.J., Pazzaglia, F.J., 2005. Tectonic geomorphology of the Red Rock fault, insights into segmentation and landscape evolution of a developing range front normal fault. *Journal of structural geology* 27(11), 1925-1939.
- Hayakawa, Y.S., Oguchi, T., 2006. DEM-based identification of fluvial knickzones and its application to Japanese mountain rivers. *Geomorphology* 78(1), 90-106.
- Hayakawa, Y.S., Oguchi, T., 2009. GIS analysis of fluvial knickzone distribution in Japanese mountain watersheds. *Geomorphology* 111(1), 27-37.
- Hooke, R.L., 1972. Geomorphic evidence for late-Wisconsin and Holocene tectonic deformation, Death Valley, California. *Geological Society of America Bulletin* 83, 2073-2098.
- Horton, R.E., 1932. Drainage basin characteristics. *Transactions American Geophysical Union* 13, 350-361.
- Horton, R.E., 1945. Erosional development of streams and their drainage basins; hydrophysical approach to quantitative morphology. *Bulletin of the Geological Society of America* 56, 275-370.
- Hovius, N., 2000. Macroscale process systems of mountain belt erosion. *Geomorphology and global tectonics*, 77-105.
- Howard, A.D., 1967. Drainage basin analysis in geologic interpretation. *American Association of Petroleum Geologists Bulletin* 51, 2246-2259.
- Howard, A.D., 1990. Role of hypsometry and planform in basin hydrologic response. *Hydrological Processes* 4, 373-385.
- Howard, A.D., 1994. A detachment limited model of drainage basin evolution. *Water Resources Research* 30, 2261-2285.
- Howard, K. A., 1971. Paleozoic metasediments in the northern Ruby Mountains,

- Nevada. Geological Society of America Bulletin 82(1), 259-264.
- Huang, J., 1982. A kind of basic mode of slope development of Danxia landform. Tropical Geomorphology 3(2), 107–134 (in Chinese).
- Huang, J., 1992. Research report on Danxia Landform in China. Tropical Geomorphology (Supplement), 1–36 (in Chinese).
- Huang, J., 1999. Distributions of Danxia landform in China. Economic Geography 19 (Supplement), 31-35 (in Chinese).
- Huang, J., 2002. A preliminary study on the Danxia landforms in Taining country, Fujian province, China. Tropical Geomorphology 22 (Supplement), 176-198 (in Chinese).
- Huang J., 2004. Quantitative survey of several important issues concerning with the formation of the Danxia landforms. Tropical Geography 24(2), 123-126 (in Chinese).
- Huang, J., 2010. Danxiashan Landform. Beijing: Science Press 2010 (in Chinese).
- Huang, J., Chen, Z.J., Huang, K.G., 1992. The definition and classification of Danxia landform. Tropical Geomorphology (Supplement), 37-39 (in Chinese).
- Huang, J., Chen, Z.J., 2003. The discussion on the definition and classification to Danxia landform. Econ Geogr 23 (Supplement), 6-11.
- Huang, J., Liu, S.R., Gao, Q.Z., 2006. Study on the fluvial terraces of the Wujiang River and quantitative dating of the Jinjiling mount, northern Guangdong province. Economic Geography 26, 1-7 (in Chinese).
- Huang, X., Niemann, J.D., 2006. Modelling the potential impacts of groundwater hydrology on long - term drainage basin evolution. Earth Surface Processes and Landforms 31(14), 1802-1823.
- Hupp, C.R., 1986. The headward extent of fluvial landforms and associated vegetation on Massanutten Mountain, Virginia. Earth Surface Processes and Landforms 11, 545-555.
- Hurtrez, J.E., Lucazeau, F., 1999. Lithological control on relief and hypsometry in the Hérault drainage basin, Comptes Rendues Académie des Sciences de la terre et des planètes. Earth

and Planetary Sciences 328(10), 687–694 (in France).

Hurtrez, J.E., Sol, C., Lucazeau, F., 1999. Effect of drainage area on hypsometry from an analysis of small-scale drainage basins in the Siwalik Hills (central Nepal). *Earth Surface Processes and Landforms* 24, 799 - 808

Istanbulluoglu, E., Bras, R.L., 2005. Vegetation-modulated landscape evolution: effects of vegetation on landscape processes, drainage density, and topography. *J. Geophys. Res.* 10, 1–19.

Jaboyedoff, M., Couture, R., Locat, P., 2009. Structural analysis of Turtle Mountain (Alberta) using digital elevation model: toward a progressive failure. *Geomorphology* 103, 5-16.

Jenson, S.K., Domingue, J.O., 1988. Extracting topographic structure from digital elevation data for geographic information system analysis. *Photogrammetric engineering and remote sensing* 54(11), 1593-1600.

Jiang, F.W., Guo, F.S., Jiang Y.B., Hu, Z.H., 2011. Cause of formation and protection for landscape rockfall of Danxia landform in Longhushan. *Journal of Mountain Science* 29(2), 202-209 (in Chinese).

Jiang, Y.B., Guo, F.S., Hu, Z.H., 2009. A study on the features of Danxia land form in longhushan world geopark and comparing with others in China. *Journal of mountain science* 27(3), 353-360 (in Chinese).

Jiang, Y.B., Guo, F.S., Hu, Z.H., Liu, L.Q., Wu, Z.C., 2010. A Study on the Features of Danxia Landform and Its Landscape Types in Xinjiang Basin. *Journal of Mountain Science* 28, 505-512.

Jie, O.Y., Cheng, Z., Hua, P., 2011. Experimental research on vulnerability of Danxia rocks to resistance against acid erosion in Langshan, Hunan Province. *Advances in Earth Science* 26(9), 965-970.

Jones-Cecil, M., Askew, B.L., McGRATH, M.B., 1988. Analysis of stream-profile data and inferred

- tectonic activity. US Government Printing Office, Eastern Ozark Mountains region.
- Judson, S., Andrews, G.W., 1955. Pattern and form of some valleys in the Driftless Area, Wisconsin. *Journal of Geology* 63, 328-336.
- Keller, E.A., Pinter, N., 1996. *Active Tectonics*. Prentice Hall, Upper Saddle River, NJ.
- Keller, E.A., Pinter, N., 2002. *Active tectonics: Earthquakes, uplift, and landscape* (second edition). Englewood Cliffs, New Jersey, Prentice Hall, 362p.
- Keller, E.A., Rockwell, T. K., 1984. Tectonic Geomorphology, Quaternary Chronology, and Paleoseismicity. *Developments and Applications of Geomorphology*, 203-239.
- Keller, G., 1986. Stepwise mass extinctions and impact events: Late Eocene to Early Oligocene. *Marine Micropaleontology* 10(4), 267-293.
- Kirby, E., Whipple, K.X., Patterns of exhumation and rock uplift along the eastern margin of the Tibetan Plateau inferred from thermochronology and bedrock river incision. *Eos Trans. AGU* 81(48), Fall Meet. Suppl., Abstract T52F-03.
- Kirby, E., Whipple, K.X., Tang, W., Zhiliang, C., 2003. Distribution of active rock uplift along the eastern margin of the Tibetan Plateau: Inferences from bedrock channel longitudinal profiles. *J. Geophys. Res.* 108(B4), 2217.
- Korup, O., Schmidt, J., McSavenecy, M.J., 2005. Regional relief characteristics and denudation pattern of the western Southern Alps, New Zealand. *Geomorphology* 71, 402–423.
- Koukouvelas, I.K., 1998. The Egeion fault, earthquake-related and long-term deformation, Gulf of Corinth, Greece. *J. Geodynamics* 26(2-4), 501-513.
- Krishnamurty, J., 1996. An approach to demarcate groundwater potential zones through remote sensing and a geographic information system. *International Journal of Remote Sensing* 10, 1876-1884.
- Kühni, A., Pfiffner, O., 2001. The relief of the Swiss Alps and adjacent areas and its relation to lithology and structure: topographic analysis from a 250-m DEM. *Geomorphology* 41,

285-307.

- Kusky, T.M., Ye, M.H., Wang, J.P., Wang, L., 2010. Geological Evolution of Longhushan World Geopark in Relation to Global Tectonics. *Journal of Earth Science* 21, 1-18.
- Labus, M., Bochen, J., 2012. Sandstone degradation: an experimental study of accelerated weathering. *Environmental Earth Sciences* 67, 2027-2042.
- Langbein, W.B., 1947. Topographic characteristics of drainage basins. U.S. Geological Survey Professional Paper 968C, 125-157.
- Lavé, J., Avouac, J.P., 2001. Fluvial incision and tectonic uplift across the Himalayas of central Nepal. *J. Geophys. Res.* 106, 26,561–26,591.
- Leeder, M.R., Seger, M.J., Stark, C.P., 1991. Sedimentation and tectonic geomorphology adjacent to major active and inactive normal faults, southern Greece. *Journal of the Geological Society* 148(2), 331-343.
- Li, Y.H., Dingwall, P.R., Wang, H.Y., Zhou, L.Y., 2009. The evolution of Langshan Danxia landform of Hunan Province, China and its global significance. First international symposium on Danxia landform 179-187 (in Chinese).
- Li, X., He, Q.C., Dong, Y., Cao, H.J., Wang, Z.J., Duan, X.M., 2013. An Analysis of Characteristics and Evolution of Danxia Landform in the South of Chishui County. *Guizhou Academic Geographica Sinica* 34(4), 501-508 (in Chinese).
- Li, Z.W., Guo, F.S., Sun, L., Zhang, W.X., 2012. Relations between Danxia Landform and Taoist Culture in Longhushan Mountain. *Tropical geography* 32, 647-651
- Lifton, N.A., Chase, C.G., 1992. Tectonic, climatic and lithologic influences on landscape fractal dimension and hypsometry: implications for landscape evolution in the San Gabriel Mountains, California. *Geomorphology* 5, 77–114.
- Lin, Z., Oguchi, T., 2004. Drainage density, slope angle, and relative basin position in Japanese bare lands from high-resolution DEMs. *Geomorphology* 63, 159–173.

- Lin, Z., Oguchi, T., 2006. DEM analysis on longitudinal and transverse profiles of steep mountainous watersheds. *Geomorphology* 78, 77–89.
- Lin, Z., Oguchi, T., 2009. Longitudinal and transverse profiles of hilly and mountainous watersheds in Japan. *Geomorphology* 111, 17–26.
- Liu, X.R., Liu, R.H., 2003. The discussion on idea question of Danxia landform. *Economic Geography* 23 (Supplement), 12-18.
- Luo, B.S., 1993. The development of Danxia landform in Jinjiling District and its relationship to unloading effect. *Journal of Guangdong Institute of Technology* 10(1), 83-90.
- Luo, D.C., 1999. Study on certain problems of Danxia geomorphology. *Economic Geography* 19 (Supplement), 15-18.
- Luo, W., 1998. Hypsometric analysis with a geographic information system. *Computers & Geosciences* 24, 815-821.
- Luo, W., 2000. Quantifying groundwater - sapping landforms with a hypsometric technique. *Journal of Geophysical Research: Planets (1991–2012)* 105(E1), 1685-1694.
- Luo, W., 2002. Hypsometric analysis of Margaritifer Sinus and origin of valley networks. *J. Geophys. Res.* 107(E10), 5071.
- Luoto, M., 2007. New insights into factors controlling drainage density in subarctic landscapes. *Arct. Antarct. Alp. Res* 39(1), 117–126.
- Lv, S.W., Li, X., 2012. Danxia Landform Type and Development Mode of Jiangxi Longhu Mountain Geological Park. *Advances in Geosciences* 2, 74-80.
- Mackin, J. H., 1948. Concept of the graded river. *Geological Society of America Bulletin* 59(5), 463-512.
- Maidment, D.R., 2002. *ArcHydro: GIS for Water Resources*. ESRI Press, Redlands.
- Magesh, N.S., Chandrasekar, N., Soundranayagam, J.P., 2011. Morphometric evaluation of Papanasam and Manimuthar watersheds, parts of Western Ghats, Tirunelveli district, Tamil

- Nadu, India: a GIS approach. *Environmental Earth Sciences* 64(2), 373-381.
- Mark, D.M., 1984. Automated detection of drainage networks from digital elevation models. *Cartographica* 21(2-3), 168-178.
- Maroukian, H., Gaki-Papanastassiou, K., Karymbalis, E., Vouvalidis, K., Pavlopoulos, K., Papanastassiou, D., Albanakis, K., 2008. Morphotectonic control on drainage network evolution in the Perachora Peninsula, Greece. *Geomorphology* 102, 81-92.
- Martz, L.W., Garbrecht, J., 1992. Numerical definition of drainage network and subcatchment areas from digital elevation models. *Computers and Geosciences* 18(6), 747-761.
- Masek, J.G., Isacks, B.L., Gubbels, T.L., Fielding, E.J., 1994. Erosion and tectonics at the margins of continental plateaus. *Journal of Geophysical Research* 99, 13941-13956.
- McAllister, M., 1999. A watershed algorithm for triangulated terrains. InCCCG.
- McCulloh, R.P., 2003. The stream net as an indicator of cryptic systematic fracturing in Louisiana. *Southeastern Geology* 42, 1-17.
- McKeown, F.A., Jones-Cecil, M., Askew, B.L., McGrath, M.B., 1988. Analysis of stream-profile data and inferred tectonic activity, Eastern Ozark Mountains Region. United States Geological Survey Bulletin 1807, 39p.
- Melton, M.A., 1958. Correlation structure of morphometric properties of drainage systems and their controlling agents. *Journal of Geology* 66, 442-460.
- Melton, M.A., 1957. An analysis of the relations among elements of climate, surface properties, and geomorphology. Dept. Geol. Columbia Univ. Tech. Rep. 11, Proj. NR 389-042, Off. of Nav. Res., New York.
- Merritts, D., Ellis, M., 1994. Introduction to special section on tectonics and topography. *Journal of Geophysical Research* 99, 12135-12141.
- Merritts, D., Vincent, K.R., 1989. Geomorphic response of coastal streams to low, intermediate, and high rates of uplift, Mendocino triple junction region, northern California. *Geological*

- Society of America Bulletin 101, 1373– 1388.
- Merritts, D., Vincent, K.R., Wohl, E.E., 1994. Long river profiles, tectonism, and eustasy: a guide to interpreting fluvial terraces. *J. Geophys Res.* 99, 14031–14050.
- Mino, Y., 1942. *Basis Theories of Geomorphology*. Kokon-Shoin, Tokyo, 517p (in Japanese).
- Moglen, G.E., Bras, R.L., 1995. The effect of spatial heterogeneities on geomorphic expression in a model of basin evolution. *Water Resour. Res.* 31, 2613–2624.
- Moglen G.E., Eltahir, E.A., Bras, R.L., 1998. On the sensitivity of drainage density to climate change. *Water Resources Research* 34, 855-862.
- Montgomery, D.R., Balco, G., Willet, S.D., 2001. Climate, tectonics, and the morphology of the Andes. *Geology* 29, 579–582.
- Montgomery, D.R., Dietrich, W.E., 1988. Where do channels begin? *Nature* 336, 232-234.
- Montgomery, D.R., Dietrich, W.E., 1989. Source areas, drainage density, and channel initiation. *Water Resources Research* 25, 1907–1918.
- Montgomery, D.R., Dietrich, W.E., 1992. Channel initiation and the problem of landscape scale. *Science* 255, 826– 830.
- Morisawa, M.E., 1959. *Relation of Morphometric Properties to Runoff in the Little Mill Creek, Ohio Drainage Basin*. Columbia University, Dept. of Geol., Technical Report 17, office of Naval Research, Project NR 389-042.
- Nag, S. K., Chakraborty, S., 2003. Influence of rock types and structures in the development of drainage network in hard rock area. *Journal of the Indian Society of Remote Sensing* 31(1), 25-35.
- O'Callaghan, J.F., Mark, D.M., 1984. The extraction of drainage networks from digital elevation data. *Computer vision, graphics, and image processing* 28(3), 323-344.
- Oguchi, T., 1997. Drainage Density and Relative Relief in Humid Steep Mountains with Frequent Slope Failure. *Earth surface processes and landforms* 22(2), 107.

- Ohmori, H., 1993. Changes in the hypsometric curve through mountain building resulting from concurrent tectonics and denudation. *Geomorphology* 8, 263–277.
- Ouyang, J., Zhu C., Peng, H., Hu, Z.N., Yu, J.B., Wang, H.Y., LV, W., Xu, L.S., 2009. Experimental research on vulnerability of Danxia rocks to resistance against acid erosion in Langshan, Hunan Province. *Advances in earth science* 26(9), 965-970 (in Chinese).
- Ouyang, J., Zhu, C., Peng, H., 2013. Exploring the Development Mechanisms of Danxia Landforms in the World Nature Heritage Sites of China Danxia. *Advances in earth science* 3, 18-21 (in Chinese).
- Ouyang, J., Zhu, C., Peng, H., Yu, J., Li, L., Zhou, R., Zhang, G., Zhu, G., Li, Z., Zhong, Y., 2009. Types and spatial combinations of Danxia landform of Fangyan in Zhejiang Province. *Journal of Geographical Sciences* 19, 631-640.
- Peng, H., 1992. The natural geomorphology research in Danxiashan. *Tropical Geography* 12, 66-76.
- Peng, H., 2000. *Danxia Geomorphology of China and its Progress in Research Work*. Guangzhou: Sun Yat-Sen University Press (in Chinese).
- Peng, H., 2001. Danxia geomorphology of China: a review. *Chinese Science Bulletin* 46 (Supplement), 38–44.
- Peng, H., 2002. The research on classification system of danxia landform 22, 28-35.
- Peng, H., Pan, Z.X., Yan, L.B., Scott, S., 2013. A review of the research on red beds and Danxia landform. *Acat Geographica Sinica* 68(9), 1170-1181 (in Chinese).
- Peng, H., Wu Z., 2003. A preliminary study on the characteristics and the distribution of red beds. *Acta Sci Nat Univ Sunyatseni* 42, 109-113 (in Chinese).
- Pérez-Peña, J., Azañón, J., Booth-Rea, G., Azor, A., Delgado, J., 2009. Differentiating geology and tectonics using a spatial autocorrelation technique for the hypsometric integral. *Journal of Geophysical Research: Earth Surface* (2003–2012), 114.
- Pérez-Peña, J.V., Azor, A., Azañón, J.M., Keller, E.A., 2010. Active tectonics in the Sierra Nevada

- (Betic Cordillera, SE Spain): Insights from geomorphic indexes and drainage pattern analysis. *Geomorphology* 119, 74-87.
- Pike, R.J., Wilson, S.E., 1971. Elevation-relief ratio, hypsometric integral and geomorphic area-altitude analysis. *Geological Society of America Bulletin* 82, 1079-1084.
- Press, F., Siever, P., 1998. *Understanding Earth*. W.H. Freeman and Company, New York.
- Qi, D.L., Yu, R., Zhang R.S., 2005. On the spatial pattern of Danxia Landform in China. *Acta Geographica Sinica* 60(1), 41–52.
- Ramírez-Herrera, M.T., 1998. Geomorphic assessment of active tectonics in the Acambay Graben, Mexican volcanic belt. *Earth Surface Processes and Landforms* 23, 317–332.
- Ren, F., 2009. *Formation Model of Danxia Landform in the Longhushan Geopark, China*. Beijing: China University of Geosciences Press (In Chinese).
- Rice, S.P., Church, M., 2001. Longitudinal profiles in simple alluvial systems. *Water Resources Research* 37, 417–426.
- Robinson, D., Williams, R., 1976. Aspects of the geomorphology of the sandstone cliffs of the central Weald: Report of an excursion to West Hoathly and Groombridge Saturday, 5 October 1974. *Proceedings of the Geologists' Association* 87, 93-99.
- Rosenblatt, P., Pinet, P.C., 1994. Comparative hypsometric analysis of earth and venus. *Geophysical Research Letters* 21, 465 - 468.
- Rodríguez-Iturbe, I., Valdés, J.B., 1979. The geomorphologic structure of hydrologic response. *Water Resources Research* 15, 1409-1420.
- Roe, G.H., Montgomery, D.R., Hallet, B., 2002. Effects of orographic precipitation variations on the concavity of steady-state river profiles. *Geology* 30, 143-146.
- Sameena, M., Krishnamurthy, J., Jayaraman, V., Ranganna, G., 2009. Evaluation of drainage networks developed in hard rock terrain. *Geocarto International* 24, 397-420.
- Schumm, S.A., 1956. Evolution of drainage systems and slopes in badlands at Perth Amboy, New

- Jersey. Geological Society of America Bulletin 67, 597-646.
- Schumm, S.A., 1986. Alluvial river response to active tectonics. *Active tectonics*, 80-94.
- Seeber, L., Gornitz, V., 1983. River profiles along the Himalayan arc as indicators of active tectonics. *Tectonophysics* 92, 335-367.
- Seidl, M.A., Dietrich, W.E., 1992. The problem of channel erosion into bedrock, in Schmidt, K.H., and de Ploey, J., eds. *Functional geomorphology: Catena*, suppl. 23, 101-124.
- Seong, Y.B., Owen, L.A., Yi, C., Finkel, R.C., Schoenbohm, L., 2008. Geomorphology of anomalously high glaciated mountains at the northwestern end of Tibet: Muztag Ata and Kongur Shan. *Geomorphology* 103, 227-250.
- Sepinski, T.F., Coradetti, S., 2004. Comparing morphologies of drainage basins on Mars and Earth using integral-geometry and neural maps. *Geophysical Research Letters* 31(15).
- Sharp, M., Richards, K., Willis, I., Arnold, N., Nienow, P., Lawson, W., Tison, J.L., 1993. Geometry, bed topography and drainage system structure of the Haut Glacier d'Arolla, Switzerland. *Earth Surface Processes and Landforms* 18, 557-571.
- Shimano, Y., 1992. Characteristics of the stream network composition of the drainage basin in Japanese islands. *Environ. Geol. Water Sci.* 20(1), 5-14.
- Shu, L.S., Zhou, X.M., Deng, P., Wang, B., Jiang, S.Y., Yu, J.H., 2009. Mesozoic tectonic evolution of the Southeast China Block: New insights from basin analysis. *J Asian Earth Sci.* 34(3), 376-391.
- Silva, J.B., Pereira, M.F., Chichorro, M., 2003. Upper Paleozoic basins development under orogen-parallel sinistral transcurrent regime in the SW Iberian Massif (Portugal). In: *Proc VI Congresso Nacional de Geologia*, Lisboa.
- Singh, V., Tandon, S.K., 2008. The Pinjaur dun (intermontane longitudinal valley) and associated active mountain fronts, NW Himalaya: tectonic geomorphology and morphotectonic evolution. *Geomorphology*, 102, 376-394.

- Sinha, S.K., Parker, G., 1996. Causes of concavity in longitudinal profiles of rivers. *Water Resources Research*, 32, 1417-1428.
- Sklar, L.S., Dietrich, W.E., 1998. River longitudinal profiles and bedrock incision models: stream power and the influence of sediment supply. In *Rivers Over Rock: Fluvial Processes in Bedrock Channels*. American Geophysical Union Geophysical Monograph Series 107, Tinkler K, Wohl E E (eds), 237–260.
- Sklar, L.S., Dietrich, W.E., 2004. A mechanistic model for river incision into bedrock by saltating bedload. *Water Resources Research* 40, W06301.
- Sklar, L.S., Dietrich, W.E., 2006. The role of sediment in controlling bedrock channel slope: implications of the saltation–abrasion incision model. *Geomorphology* 82, 58–83.
- Sklar, L.S., Dietrich, W.E., 2008. Implications of the saltation–abrasion bedrock incision model for steady-state river longitudinal profile relief and concavity. *Earth Surface Processes and Landforms* 33, 1129–1151.
- Smith, K.G., 1958. Erosional processes and landforms in Badlands National Monument, South Dakota. *Geological Society of America Bulletin* 69, 975– 1008.
- Snow, R.S., Slingerland, R.L., 1987. Mathematical modeling of graded river profiles. *Journal of Geology* 95, 15-33.
- Snyder, N.P., Whipple, K.X., Tucker, G.E., Merritts, D.J., 2000. Landscape response to tectonic forcing: Digital elevation model analysis of stream profiles in the Mendocino triple junction region, northern California. *Geological Society of America Bulletin* 112, 1250-1263.
- Snyder, N.P., Whipple, K.X., Tucker, G.E., Merritts, D.J., 2003. Channel response to tectonic forcing: Analysis of stream morphology and hydrology in the Mendocino triple junction region, northern California. *Geomorphology* 53, 97-127.
- Sorriso-Valvo, M., Antronico, L., Le Pera, E., 1998. Controls on modern fan morphology in Calabria, Southern Italy. *Geomorphology* 24, 169–187.

- Stark, C.P., 2006. A self-regulating model of bedrock river channel geometry. *Geophys. Res. Lett.* 32, L04402.
- Štěpančíková, P., Stemberk, J., Vilímek, V., Košťák, B., 2008. Neotectonic development of drainage networks in the East Sudeten Mountains and monitoring of recent fault displacements (Czech Republic). Special Issue on: Impact of Active Tectonics and Uplift on Fluvial Landscapes and River Valley Development *Geomorphology* 102, 68–80.
- Stock, J.D., Montgomery, D.R., 1999. Geologic constraints on bedrock river incision using the stream power law. *Journal of Geophysical Research* 104, 4983-4993.
- Strahler, A.N., 1952. Hypsometric (area-altitude) analysis of erosional topography. *Bulletin of the Geological Society of America* 63, 1117-1142.
- Strahler, A.N., 1964. Quantitative geomorphology of drainage basins and channel networks. In: Chow, V.T. (ed.), *Handbook of Applied Hydrology*. McGraw-Hill, New York, section 4-II.
- Tailing, P., Sowter, M.J., 1999. Drainage density on progressively tilted surfaces with different gradients, Wheeler Ridge, California. *Earth Surface Processes and Landforms* 24, 809– 824.
- Tarolli, P., Dalla Fontana, G., 2009. Hillslope-to-valley transition morphology: New opportunities from high resolution DTMs. *Geomorphology* 113(1), 47-56.
- Toy, T.J., Hadley, R.F., 1987. *Geomorphology and Reclamation of Disturbed Lands*. Academic Press, Orlando, 480p.
- Troiani, F., Della Seta, M., 2008. The use of the Stream Length-Gradient Index in morphotectonic analysis of small catchments: a case study from central Italy. *Geomorphology* 102, 159–168.
- Tucker, G.E., Catani, F., Rinaldo, A., Bras, R.L., 2001. Statistical analysis of drainage density from digital terrain data. *Geomorphology* 36(3), 187-202.
- Turowski, J.M., Lague, D., Hovius, N., 2007. The cover effect in bedrock abrasion: A new derivation and its implications for the modeling of bedrock channel morphology. *J. Geophys. Res.* 112, F04006.

- VanLaningham, S., Duncan, R.A., Piasias, N.G., 2006. Erosion by rivers and transport pathways in the ocean: A provenance tool using ^{40}Ar - ^{39}Ar incremental heating on fine-grained sediment. *J. Geophys. Res.*, 111.
- Vijith, H., Satheesh, R., 2006. GIS based morphometric analysis of two major upland sub-watersheds of Meenachil river in Kerala. *Journal of the Indian Society of Remote Sensing* 34(2), 181-185.
- Vogt, J.V., Colombo, R., Bertolo, F., 2003. Deriving drainage networks and catchment boundaries: a new methodology combining digital elevation data and environmental characteristics. *Geomorphology* 53(3), 281-298.
- Vojtko, R., Benová, A., Bóna, J., Hók, J., 2012. Neotectonic evolution of the northern Laborec drainage basin (northeastern part of Slovakia). *Geomorphology* 138, 276-294.
- Walcott, R.C., Summerfield, M.A., 2007. Scale dependence of hypsometric integrals: an analysis of southeast African basins. *Geomorphology* 96, 174-186.
- Weissel, J.K., Seidl, M.A., 1998. Inland propagation of erosional escarpments and river profile evolution across the southeast Australian passive continental margin: in Tinkler, K.J., and Wohl, E.E., eds., *Rivers over rock: Fluvial processes in bedrock channels*. American Geophysical Union Geophysical Monograph 107, 189-206.
- Wells, S.G., Bullard, T.F., Menges, C.M., Drake, P.G., Karas, P.A., Kelson, K.I., Ritter, J.B., Wesling, J.R., 2012. Regional variations in tectonic geomorphology along a segmented convergent plate boundary pacific coast of Costa Rica. *Geomorphology* 1, 239-265.
- Weng, L., Chen, Y., 2012. *Agriculture & Technology* 3, 23-26 (in Chinese).
- Whipple, K.X., Tucker, G.E., 1999. Dynamics of the stream-power river incision model: Implications for height limits of mountain ranges, landscape response timescales, and research needs. *Journal of Geophysical Research: Solid Earth* (1978–2012) 104(B8), 17661-17674.

- Whittaker, A.C., Cowie, P.A., Attal, M., Tucker, G.E., Roberts, G.P., 2007a. Bedrock channel adjustment to tectonic forcing: Implications for predicting river incision rates. *Geology* 35, 103–106.
- Willgoose, G., Hancock, G., 1998. Revisiting the hypsometric curve as an indicator of form and process in transport-limited catchment. *Earth Surf. Processes Landforms* 23, 611–623.
- Willis, I.C., Fitzsimmons, C.D., Melvold, K., Andreassen, L.M., Giesen, R.H., 2012. Structure, morphology and water flux of a subglacial drainage system, Midtdalsbreen, Norway. *Hydrological Processes* 26, 3810-3829.
- Wobus, C.W., Kean, J.W., Tucker, G.E., Anderson, R.S., 2008. Modeling the evolution of channel shape: Balancing computational efficiency with hydraulic fidelity. *J. Geophys. Res.* 113, F02004.
- Wobus, C.W., Tucker, G.E., Anderson, R.S., 2006b. Self-formed bedrock channels. *Geophysical Research Letters* 33, L18408.
- Wu, Z.C., Peng, H., 2005, A study on Danxia landform classification in Guangdong. *Tropical geography* 25(4), 301-306 (in Chinese).
- Xiong, K.N., Chris, W., Peng, J., Zhou, Z.F., Chen, H., Rong, L., Xiao, S.Z., Du, F.J., 2009. Researches on the feature of Chishui Danxia and its World Natural Heritage Values. First International Symposium on Danxia Landform, 102-112.
- Yatsu, E., 1950. On relief energy of the Chichibu Mountains, Japan. *Transactions Otsuka Geographical Association* 6, 323– 330 (in Japanese).
- Zeng, Z., Huang, S., 1978. Red bed in southeastern China. *Journal of South China Normal University (Natural Science)* 2, 43–57 (in Chinese).
- Zhu, C., Peng, H., Li, Z., Zhang, G., Li, L., Yu, J., Xu, L., 2009. Age and genesis of the Danxia landform on Jianglang Mountain, Zhejiang Province. *Journal of Geographical Sciences* 19(5), 615-630.

Zimpfer, G.L., 1982. Hydrology and Geomorphology of an Experimental Drainage Basin.

Unpublished Ph.D dissertation, Colorado State University.

Zuchiewicz, W., 1998. Quaternary tectonics of the Outer West Carpathians, Poland. *Tectonophysics*

297, 121–132.